

Pertanika Journal of  
**SCIENCE &  
TECHNOLOGY**

VOLUME 15 NO. 1 • JANUARY 2007

A scientific journal published by Universiti Putra Malaysia Press

## About the Journal

Pertanika is an international peer-reviewed journal devoted to the publication of original papers, and it serves as a forum for practical approaches to improving quality in issues pertaining to tropical agriculture and its related fields. Pertanika Journal of Tropical Agricultural Science began publication in 1978. In 1992, a decision was made to streamline Pertanika into three journals to meet the need for specialised journals in areas of study aligned with the interdisciplinary strengths of the university. The revamped, Pertanika Journal of Science and Technology (JST) is now focusing on research in science and engineering, and its related fields. Other Pertanika series include Pertanika Journal of Tropical Agricultural Science (JTAS); and Pertanika Journal of Social Sciences and Humanities (JSSH).

JST is published in English and it is open to authors around the world regardless of the nationality. It is currently published two times a year i.e. in **January and July**.

## Goal of Pertanika

Our goal is to bring the highest quality research to the widest possible audience.

## Quality

We aim for excellence, sustained by a responsible and professional approach to journal publishing.

## Future vision

We are continuously improving access to our journal archives, content, and research services. We have the drive to realise exciting new horizons that will benefit not only the academic community, but society itself.

We also have views on the future of our journals. The emergence of the online medium as the predominant vehicle for the 'consumption' and distribution of much academic research will be the ultimate instrument in the dissemination of the research news to our scientists and readers.

## Aims and scope

Pertanika Journal of Science and Technology aims to provide a forum for high quality research related to science and engineering research. Areas relevant to the scope of the journal include: *bioinformatics, bioscience, biotechnology and bio-molecular sciences, chemistry, computer science, ecology, engineering, engineering design, environmental control and management, mathematics and statistics, medicine and health sciences, nanotechnology, physics, safety and emergency management*, and related fields of study.

JST accepts submission of mainly four types: original articles, short communications, reviews, and proposals for special issues.

## Editorial Statement

Pertanika is the official journal of Universiti Putra Malaysia. The abbreviation for Pertanika Journal of Science & Technology is *Pertanika J. Sci. Technol.*

### Editor-in-Chief

Sudhanshu Shekhar Jamuar (Professor Dr.)  
Electrical and Electronic Engineering, Engineering

### Editorial Board

Nor Aripin Shamaan (Professor Dr.) Biochemistry, Biotechnology and Biomolecular Sciences	Mohd Adzir Mahdi (A/ Professor Dr.) Computer & Communication System, Engineering
Raja Noor Zailiha Raja Abd. Rahman (Professor Dr.) Microbiology, Biotechnology and Biomolecular Sciences	Mohd Saleh Jaafar (A/ Professor Dr.) Civil Engineering, Engineering
Mohamed Othman (A/ Professor Dr.) Communication Technology & Network, Computer Science and Information Technology	Farida Jamal (Professor Dr.) Medical Microbiology & Parasitology, Medicine and Health Sciences
Desa Ahmad (Professor Dr.) Biological and Agricultural Engineering, Engineering	Ahmad Makmum Abdullah (A/ Professor Dr.) Environmental Sciences, Environmental Studies
Fakhrul-Razi Ahmadun (A/ Professor Dr.) Chemical and Environmental Engineering, Engineering	Abdul Halim Shaari (Professor Dr.) Physics, Science
Megat Mohamad Hamdan b. Megat Ahmad (A/ Professor Dr.) Mechanical and Manufacturing Engineering, Engineering	Yap Chee Kong (Dr.) Biology, Science

### Executive Editor

Nayan Deep S. Kanwal (Dr.)  
Environmental issues- landscape plant modelling applications  
Research Management Centre (RMC)

### International Advisory Board

S.C. Dutta Roy (Professor Dr.) Indian Institute of Technology (IIT) Delhi, New Delhi, India	Yi Li (Professor Dr.) Chinese Academy of Sciences, Beijing
Usman Chatib Warsa (Professor Dr.) Universitas Indonesia, Jakarta, Indonesia	Peter J. Heggs (Professor Dr.) The University of Manchester, U.K.
Graham Megson (Professor Dr.) The University of Reading, U.K.	Said S.E.H. Elnashaie (Professor Dr.) Queen's University, USA
Rod Smith (Professor Dr.) University of Southern Queensland, Australia	Malin Premaratne (Dr.) Monash University, Australia
Shinsuke Fujiwara (Professor Dr.) Kwansei Gakuin University, Japan	Peter G. Alderson (Dr.) The University of Nottingham Malaysia Campus
Ferda Mavituna (Professor Dr.) The University of Manchester, U.K.	Mohammed Ismail Elnaggar (Professor Dr.) Ohio State University, USA

### Editorial Office

Pertanika, Research Management Centre (RMC), 4th Floor, Administration Building  
Universiti Putra Malaysia, 43400 Serdang, Selangor, Malaysia  
Tel: +603 8946 6185, 8946 6192 • Fax: +603 8947 2075  
E-mail: ndeeps@admin.upm.edu.my  
www.rmc.upm.edu.my/pertanika

### Publisher

The UPM Press  
Universiti Putra Malaysia  
43400 UPM, Serdang, Selangor, Malaysia  
Tel: +603 8946 8855, 8946 8854 • Fax: +603 8941 6172  
penerbit@putra.upm.edu.my  
URL: http://penerbit.upm.edu.my

**ARCHIVE COPY**  
*(Please Do Not Remove)*

**PERTANIKA EDITORIAL OFFICE**  
Research Management Centre (RMC)  
1st Floor, IDEA Tower II  
UPM-MTDC, Technology Centre  
Universiti Putra Malaysia  
43400 Serdang, Selangor, Malaysia  
Tel: +603 8947 1622, 8947 1619, 8947 1616

**Pertanika Journal of SCIENCE & TECHNOLOGY**  
**VOLUME 15 NO. 1 • (JANUARY 2007)**

Predicting Freezing Time for Keropok Lekor - <i>M. Nordin Ibrahim, Sergei Y. Spotar &amp; No Amaiza Mohd. Amin</i>	1
Performance Evaluation of a Terrain-Accommodating Oil Palm Loose Fruit Collector - <i>Rimfiel B. Janius &amp; Abadanjumi Eskandar</i>	15
Array Beampattern Using Goal - <i>Farrukh Nagi &amp; Wong Hung Way</i>	25
Assessment of Public Exposure to Electromagnetic Fields by Overhead Power Transmission Lines: A Case Study - <i>Law Puong Ling, Awangku Abdul Rahman, Azhaili Baharun &amp; Ngu Lock Hei</i>	35
Antraquinones and Xanthoness from <i>Cratoxylum glaucum</i> (Guttiferae) - <i>G.C.L. Ee, A.S.M. Kua &amp; M. Rahmani</i>	43
Determining the Optimum Process Mean Based on Manufacturing Cost and Quality Loss - <i>Chung-Ho Chen</i>	49
A Method of Estimating the $p$ -adic Sizes of Common Zeros of Partial Derivative Polynomials Associated with a Seventh Degree Form - <i>Siti Hasana Sapar, Kamel Ariffin Mohd Atan &amp; Mohamad Rushdan Md Said</i>	61
Xanthoness and Xanthone Derivatives from <i>Garcinia nitida</i> - <i>G.C.L. Ee, C.K. Lim, Y. H. Taufiq-Yap, M.A Sukari &amp; M. Rahmani</i>	77

## Predicting Freezing Time for Keropok Lekor

M. Nordin Ibrahim, Sergei Y. Spotar & Nor Amaiza Mohd. Amin

Department of Process & Food Engineering, Faculty of Engineering,  
Universiti Putra Malaysia, 43400 UPM, Serdang, Selangor, Malaysia

Received: 17 March 2003

### ABSTRAK

Proses penyejukan *keropok lekor* dikaji secara eksperimen dan simulasi berangka pemindahan haba tidak mantap. Perubahan suhu di tengah sampel *keropok lekor* semasa proses penyejukan di dalam peti sejuk tiupan angin telah diperolehi. Model kaedah berangka yang dibina melibatkan penyelesaian persamaan Fourier untuk silinder fana dan sfera berasaskan nilai entalpi berubah. Pekali pemindahan haba ditentukan melalui kaedah perubahan sifat terma aluminium yang mempunyai dimensi sama seperti sampel *keropok lekor* yang dikaji. Kandungan air, protein kasar, lemak, karbohidrat dan abu ditentukan untuk menilai perubahan sifat terma *keropok lekor* mengikut suhu. Sifat terma iaitu konduktiviti terma, entalpi dan takat beku ditentukan dengan menggunakan pertalian kandungan. Masa penyejukan diperolehi daripada kiraan dan eksperimen menunjukkan perbandingan yang baik di antara mereka, untuk setiap sampel *keropok lekor* berbentuk silinder dan sfera. Bagi sampel *keropok lekor* bergaris pusat 20 mm berbentuk silinder dan sfera, masa penyejukan kepada suhu sejuk beku - 20°C ialah masing-masing 20 min dan 15 min.

### ABSTRACT

The freezing process of *keropok lekor* (fish sausage) has been studied experimentally and by numerical simulation of unsteady heat transfer. Core temperature history of *keropok lekor* samples placed in the air-blast freezer were registered. The developed numerical model utilizes the solution of the Fourier equation of heat transfer for an infinite cylinder and for a sphere with variable product enthalpy. Heat transfer coefficient was determined from the thermal history of aluminum cylinder with dimensions similar to experimental *keropok lekor*. The contents of water, crude protein, fat, carbohydrate and ash were determined to evaluate variations of *keropok lekor* thermal properties with temperature. These thermal properties, i.e. thermal conductivity, enthalpy freezing point, were obtained by using composition correlations. Calculated and experimental freezing times are in good agreement with each other, for each of the cylindrical and spherical *keropok lekor* samples. For 20 mm diameter cylindrical and spherical *keropok lekor* samples, the freezing time to achieve a frozen temperature of - 20°C were 20 min and 15 min, respectively.

**Keywords:** *Keropok lekor*, freezing time, thermal properties

### INTRODUCTION

Most commercial freezing operations of foodstuff are done by using air blast freezer because of its relatively low capital cost and high throughput. Also, it is simple to use and highly flexible since food of different shapes and sizes can be frozen. Embong (1988) found that the shelf life of *keropok lekor* could be extended to more than 7 weeks when packed and frozen in air blast freezer. Chan and Pan (1995) used air blast freezer for

freezing tilapia to determine its freezing point and freezing rate. Chevalier *et al.* (2000) investigated on the freezing rate and ice crystal formation in a cylindrical model food (gelatin) by using air blast freezing and brine freezing techniques. Agnelli and Macheroni (2001) developed a simulation model for implementing cryo-mechanical freezing on foodstuff.

The main objective of this paper is to present the application of modeling technique for investigating the freezing process of common local food product, *keropok lekor* (fish sausage) which in its processed state consists of a mixture of fish meat, starches, salts, monosodium glutamate and sugar. The emphasis is to investigate the freezing process of *keropok lekor* by mathematical modeling to enable numerical simulation of the freezing process be carried out. Freezing of *keropok lekor* was conducted using air blast freezer; this experimental data and some published data were used for validating the modeling and simulation approach. The ultimate output would be the temperature history during freezing which enable us to predict the freezing time of the product.

### BASIC EQUATIONS AND ASSUMPTIONS FOR MATHEMATICAL MODELLING

As a physical phenomenon with phase change, the food freezing process is characterized by the generation and development of the freezing front which involves a considerable amount of latent heat being absorbed within this front. Two physical models for freezing are commonly in use namely, the continuously varying  $k(T)$  and  $H(T)$  model, and the unique phase change front model (Cleland, 1990). The former approach is being applied here for investigating the *keropok lekor* freezing process. This involves solving numerically the heat conduction equations given below:

for a cylinder

$$\rho(T) \frac{\partial H(T)}{\partial t} = \frac{1}{r} \frac{\partial}{\partial r} \left[ k(T) r \frac{\partial T}{\partial r} \right] \quad (1)$$

and for a sphere

$$\rho(T) \frac{\partial H(T)}{\partial t} = \frac{1}{r^2} \frac{\partial}{\partial r} \left[ k(T) r^2 \frac{\partial T}{\partial r} \right] \quad (2)$$

with the following initial and boundary conditions:

$$T = T_0 \text{ for } t = 0; \quad h(T_s)(T_\infty - T_s) = k(T) \left( \frac{\partial T}{\partial r} \right)_{r=R} \quad (3)$$

where convective heat transfer coefficient ( $h$ ) is a function of the surface temperature ( $T_s$ ) and  $H(T)$ ,  $k(T)$  are temperature dependent product enthalpy and thermal conductivity respectively.

Equations (1, 2) were solved numerically using finite difference approach, with the enthalpy as unknown variable on a fixed grid. Consequently, calculated value of enthalpy allowed the determination of the temperature in each point of the grid. As time

increment added, this temperature value is used for enthalpy calculation corresponding to the new time step. The number of  $N = 40$  evenly distributed radial grid points was established as adequate for obtaining a good precision. The discretisation gave the following expressions for the enthalpy values:

For a Cylinder  
surface ( $n=N$ ):

$$H_N^{t+1} = H_N^t + \frac{2\Delta t}{\rho(T_N^t)(\Delta r)^2 \left(2N - \frac{1}{2}\right)} \left( hN\Delta r (T_b - T_N^t) \right) - k \left( \frac{T_N^t - T_{N-1}^t}{2} \right) (N-1) (T_N^t - T_{N-1}^t) \quad (4)$$

interior ( $n=N-1...1$ ):

$$H_n^{t+1} = H_n^t + \frac{\Delta t}{\rho(T_n^t)n(\Delta r)^2} \left( k \left( \frac{T_{n+1}^t + T_n^t}{2} \right) (T_{n+1}^t - T_n^t) \left( n + \frac{1}{2} \right) \right) - k \left( \frac{T_n^t + T_{n-1}^t}{2} \right) (T_n^t - T_{n-1}^t) \left( n - \frac{1}{2} \right) \quad (5)$$

center ( $n=0$ ):

$$H_0^{t+1} = H_0^t + \frac{4\Delta t \left( k \left( \frac{T_1^t + T_0^t}{2} \right) (T_1^t - T_0^t) \right)}{\rho(T_0^t)(\Delta r)^2} \quad (6)$$

For a Sphere  
surface ( $n=N$ ):

$$H_N^{t+1} = H_N^t + \frac{\Delta t}{\rho(T_N^t)(\Delta r)^2 \left( \frac{N^2}{2} - \frac{N}{4} - \frac{1}{24} \right)} \left( hN^2\Delta r (T_b - T_N^t) \right) - k \left( \frac{T_N^t - T_{N-1}^t}{2} \right) \left( N - \frac{1}{2} \right)^2 (T_N^t - T_{N-1}^t) \quad (7)$$

interior ( $n=N-1...1$ ):

$$H_n^{t+1} = H_n^t + \frac{\Delta t}{\rho(T_n^t) \left( N^2 + \frac{1}{2} \right) (\Delta r)^2} \left( k \left( \frac{T_{n+1}^t + T_n^t}{2} \right) (T_{n+1}^t - T_n^t) \left( n + \frac{1}{2} \right)^2 \right) \tag{8}$$

$$- k \left( \frac{T_n^t + T_{n-1}^t}{2} \right) (T_n^t - T_{n-1}^t) \left( n - \frac{1}{2} \right)^2$$

center ( $n=0$ ):

$$H_0^{t+1} = H_0^t + \frac{6\Delta t \left( k \left( \frac{T_1^t + T_0^t}{2} \right) (T_1^t - T_0^t) \right)}{\rho(T_0^t) (\Delta r)^2} \tag{9}$$

At the beginning of freezing, the heat capacity of the nearest to the surface layer of the  $\Delta r/2$  thickness is assumed negligible giving the 'initial' surface temperature

$$T_N^0 = \frac{\Delta r N h T_b + k \left( \frac{T_N^0 - T_{N-1}^0}{2} \right) \left( N - \frac{1}{2} \right) T_{N-1}^0}{k \left( \frac{T_N^0 - T_{N-1}^0}{2} \right) \left( N - \frac{1}{2} \right) + \Delta r N h} \tag{10}$$

Solution of the Equations (1,2) as given by Equations (6,9) requires the approximation of thermal properties of the product as temperature changes. This is achieved by firstly, determining *keropok lekor* compositions experimentally by proximate analysis; and next approximating the properties by utilizing appropriate correlations based upon product compositions. The selected correlations for the product physical properties as a function of temperature are listed below (Kenneth *et al.*, 1997):

Freezing (melting) point as a function of water content  $X_w$ :

$$T_f = \frac{1 - X_w}{0.06908 - 0.439 X_w} \tag{11}$$

ice fraction: for  $T \geq T_f$ ,  $X_i = 0$ ; for  $T < T_f$ ,  $X_i = (X_w - X_b) \left[ 1 - \frac{T_f}{T} \right]$  (12)

density:  $\rho(T) = \left[ \frac{X_w(T)}{\rho_w} + \frac{X_i(T)}{\rho_i} + \frac{X_f}{\rho_f} + \frac{X_p}{\rho_p} + \frac{X_c k_c}{\rho_c} + \frac{X_s k_s}{\rho_s} \right]$  (13)

thermal conductivity:

$$k(T) = \rho(T) \left[ \frac{X_I(T)k_I}{\rho_I} + \frac{X_W(T)k_W}{\rho_W} + \frac{X_F k_F}{\rho_F} + \frac{X_P k_P}{\rho_P} + \frac{X_C k_C}{\rho_C} + \frac{X_S k_S}{\rho_S} \right] \quad (14)$$

heat capacity:

$$\text{for } T \geq T_f, c_u = X_W c_W + X_F c_F + X_P c_P + X_I c_I;$$

$$\text{for } T < T_f, c(T) = cu - (XW - XB) \cdot \left[ \frac{\lambda_I T_f}{T^2} + (c_W - c_I) \right] \quad (15)$$

enthalpy:

$$\text{for } T > T_f, H(T) = cu(T - T_f);$$

$$\text{for } T \leq T_f, H(T) = (X_F c_F + X_P c_P + X_C)(T - T_f) + (X_W(T) c_W + X_I(T) c_I (T - T_f) - \lambda_I X_I(T)) \quad (16)$$

Numerical simulation of the freezing process was carried out based on the modeling approach described above so that the calculated result could be compared with experimental result. The approximations of physical properties of *keropok lekor* using the above correlations (11) - (16) and the numerical simulation of the freezing process were implemented by the application of Mathcad 2000 software package, following the algorithm as shown in Fig. 1.

### EXPERIMENTAL PROCEDURE

Proximate analysis was carried out in order to establish the composition of commercially produced *keropok lekor* used in this study. The homogeneous *keropok lekor* dough were analysed in triplicate samples for water, crude protein, fat, carbohydrates and ash (solids) contents according to Pearson (1976). The moisture content was determined by oven method, fat by Soxhlet apparatus, and the dried sample from fat was used to determine the ash content. Nitrogen content was analysed by Kjeldahl method, using 0.15 g of sample; protein content was then obtained by multiplying the nitrogen content by 6.25.

Based on the standard lumped thermal capacity method, the heat transfer coefficient (h) was determined experimentally from the thermal history of an aluminium body, with the shape and dimension similar to the treated *keropok lekor* sample. The value of h has been obtained from the slope of a plot of  $\ln T$  versus  $t$  of the following equation:

$$\ln T^* = \ln \frac{T - T_b}{T_0 - T_b} = - \frac{hA}{mc_{Al}} t \quad (17)$$

In the freezing process, *keropok lekor* sausages were frozen in the air-blast freezer (ARMPFIELD FT36-C) with freezing air temperature of -30°C. The product core (centre-line) temperature evolution with time was measured by using a data acquisition system (KRESSTLER DATATAKER DT50) with T-type thermocouple. Thermocouple wires were assembled along centre-line to prevent inaccuracy due to radial heat flux.

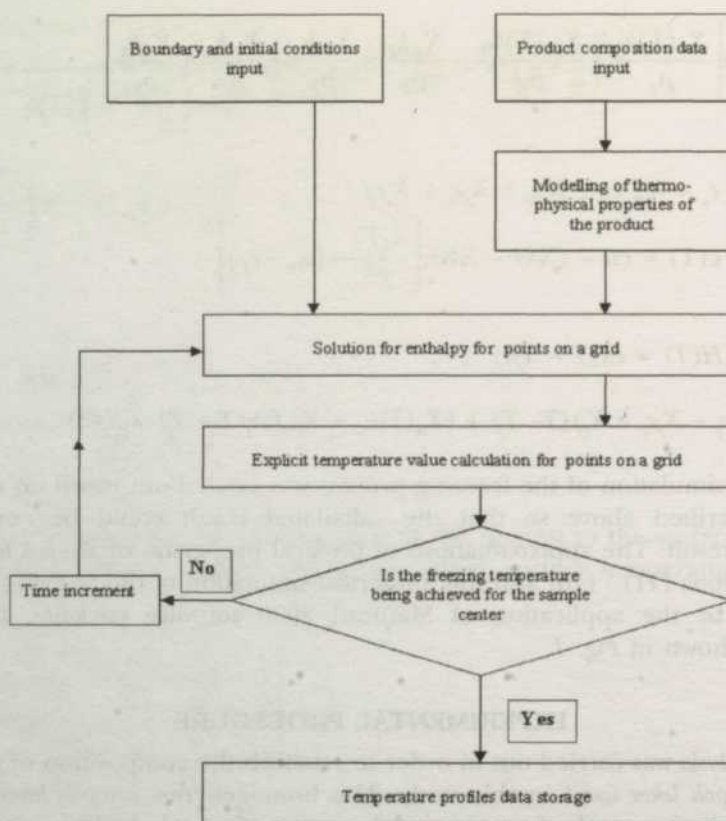


Fig. 1: Modelling algorithm

## RESULTS AND DISCUSSIONS

### Proximate Analysis

Proximate analysis showed that the *keropok lekor* (fish sausage) used in this study contained about 55.0% water, 8.5% crude protein (conversion factor for *keropok lekor*,  $N \times 6.25$ ), 0.5% fat, 31.5% carbohydrate and 4.5% ash as shown in Table 1. However, the composition depends on the ratio of fish meat to flour, type of fish and other additional flavors, which can vary according to individual producer's choice. The rather high percentage of fat in the published data (Table 1) is attributed to the addition of groundnut oil during processing.

### Heat Transfer Coefficient

From the slope of a plot of Equation (17) as shown in Fig. 2, the value of heat transfer coefficient ( $h$ ) was approximately  $80 \text{ W/m}^2 \text{ }^\circ\text{C}$ .

### Thermal Properties

Utilizing the composition data obtained in Table 1, the thermo-physical properties variations with temperature were determined by using the correlations as given in Equation (11) through (16). This theoretical simulation of the thermal physical properties was implemented in a Mathcad software package. The typical changes in thermal

TABLE 1  
Basic composition of *keropok lekor*

Composition (percentage)	Determined value (present paper)	Published data (Ibrahim, Ishak, 1980)
Water content	55.00	53.00
Fat	0.50	13.00
Crude protein	8.50	8.50
Carbohydrate	31.50	23.50
Ash	4.50	2.00

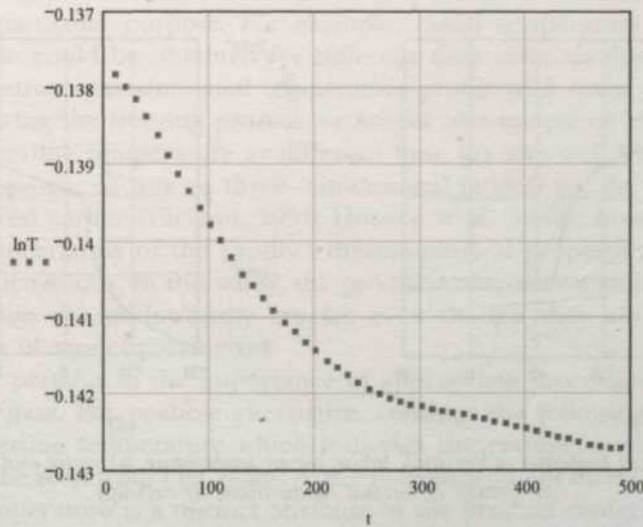


Fig. 2: Plot of  $\ln T$  versus  $t$  for heat transfer coefficient ( $h$ ) determination

properties with temperature are plotted in Fig. 3, from which the values of the thermo-physical properties of *keropok lekor* can be determined for any desired temperature. Water starts to change phase into ice after the freezing point ( $-2.6^{\circ}\text{C}$ ). The density is  $1110 \text{ kgm}^{-3}$  and the thermal conductivity is  $0.45 \text{ W (m }^{\circ}\text{C)}^{-1}$  and  $1.34 \text{ W (m }^{\circ}\text{C)}^{-1}$  for the fresh and frozen state, respectively. The enthalpy curve for *keropok lekor* presents a melting point of  $-2.6^{\circ}\text{C}$  with the latent heat of  $180 \text{ kJ kg}^{-1}$ .

*Comparison of Simulated and Experimental Result*

(i) For Gelatin Sample

The results of numerical simulation developed in this study were compared to the experimental data of Macchi (1995) for cylinders of gelatin with 70% water content. Gelatin was chosen as a model foodstuff in order to eliminate the heterogeneous characteristic of most foods. From the thermal point of view, it is representative of different kinds of foods. The functionality of enthalpy ( $H$ ) with temperature and other properties of gelatin necessary for modeling the entire freezing process were also obtained from Macchi (1995). The enthalpy curve for gelatin shows a melting point of  $-13.9^{\circ}\text{C}$  for a cooling rate of  $0.1\text{K min}^{-1}$ . The latent heat is  $160\text{kJ kg}^{-1}$  and the thermal

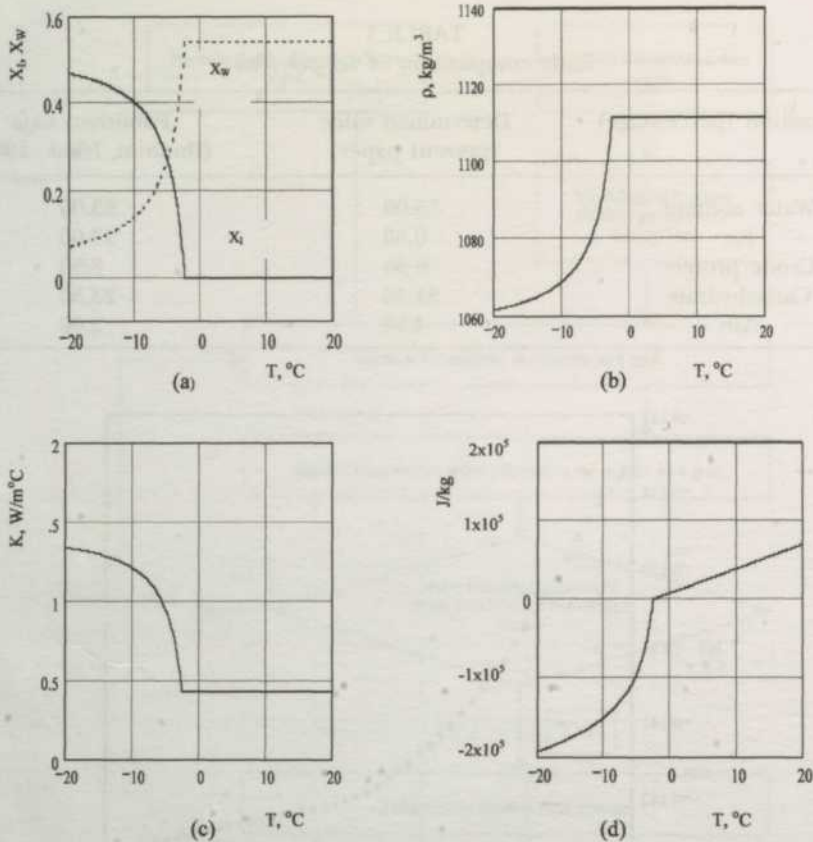


Fig. 3: Physical properties of keropok lekor versus temperature. a) water and ice fraction; b) density; c) thermal conductivity; d) enthalpy

conductivity is 0.55 W (mK)<sup>-1</sup> and 0.95 W (mK)<sup>-1</sup> for the fresh and frozen gel, respectively, and density is 1200 kg m<sup>-3</sup>. The calculated and experimental temperature profiles during freezing in the mechanical freezer are presented in Fig. 4. The profiles are at two different positions of the cylinder i.e. at the center and at the surface of the sample. It can be noted that the calculated temperature profiles are very close to the experimental temperature history of the gelatin cylinder. So, the simulation model represents satisfactorily the thermal process of the model foodstuff.

(ii) For *Keropok Lekor* Samples

Fig. 5 presents the experimental and calculated results for freezing of *keropok lekor* samples in the mechanical freezer. The standard geometrical shapes of *keropok lekor* samples (cylindrical and spherical) were utilized for this purpose. In general, calculated and experimental temperature profiles match each other reasonably well for both geometrical shapes. This enables the prediction of freezing time based on the model. It can be seen that the 30 mm diameter cylindrical sample require about 20 minutes to be completely frozen to the freezing point of -2.6°C, followed by another 10 minutes to achieve a frozen temperature of -20°C. The 20 mm diameter cylindrical sample required 15 minutes to be completely frozen to -2.6°C, followed by another 5 minutes to achieve a frozen temperature of -20°C. The 20 mm diameter spherical sample require a little less than

10 minutes to be completely frozen to  $-2.6^{\circ}\text{C}$ , followed by another 5 minutes to achieve a frozen temperature of  $-20^{\circ}\text{C}$ .

Even though there is some inconsistency below the freezing temperature, this is believed to be attributed to ambiguity of approximations for enthalpy, conductivity and other parameters rather than from other reasons. Although the measurement has been carried out with only one thermocouple located at the thermal center (the slowest cooling point) of the *keropok lekor* sample, the agreement of the calculated temperature profile with the experimental temperature profile for *keropok lekor* is observed to be satisfactory. As such it can be concluded that the temperature time profiles obtained from the simulation model for freezing *keropok lekor* with regular geometrical shapes (cylinder and sphere) are acceptable.

The model being reliable, some necessary further details on the freezing process can be obtained for particular purpose. For example, radial temperature profiles for the *keropok lekor* sample could be obtained for different time intervals during the freezing process. Fig. 6 illustrates the simulated temperature profile with radial positions at four different times during the freezing process for *keropok lekor* sample of 15mm radius. The experimental centerline temperature at different time fits very well with the simulated result. The development of two- or three- dimensional models for the freezing process has been considered earlier (Cleland, 1991; Hossain *et al.*, 1992); however, it seems in many cases that uncertainty of the product thermo-physical properties mainly controls the accuracy of calculations. In this study, the product composition analysis and relevant correlation selection are undoubtedly crucial; even though they are time- and cost-consuming factors of model parameters.

Another point pertains to the importance of appropriate processing and analysis of the experimental data. For possible alternative, consider the following presentation of the product centerline temperature which indicates the completeness of the freezing process. As it can be seen from Figs. 4 and 5, the plateau segment directly associated with freezing point temperature is a distinct attribute of the product centerline temperature history. This dominant peculiarity motivates the presentation of original data for the specific products in terms of dimensionless temperature versus dimensionless time; these modified variables taking the form as;

$$\text{Dimensionless temperature: } \bar{T} = \frac{T - T_f}{T_0 - T_b} \quad (18)$$

$$\text{Dimensionless time: } \bar{t} = \frac{\sqrt{\lambda}}{R} t \quad (19)$$

In fact the dimensionless time parameter (Equation 19) is built from Biot number by substituting  $\sqrt{\lambda}$  for  $\alpha/R$ , while the temperature in the form of Equation (18) is attached to the freezing point. For simplicity,  $T_f = 0^{\circ}\text{C}$  can be used for high water content product. With this approach, processed data for *keropok lekor* samples with different diameters are plotted in Fig. 7. It is observed that the points tend to converge to a single curve which is supposed to be the generalized centre-line temperature history for the given product. On this basis, the curve could be obtained from low cost experiment with small size sample and the relevant forecast for the product size in use could be done.

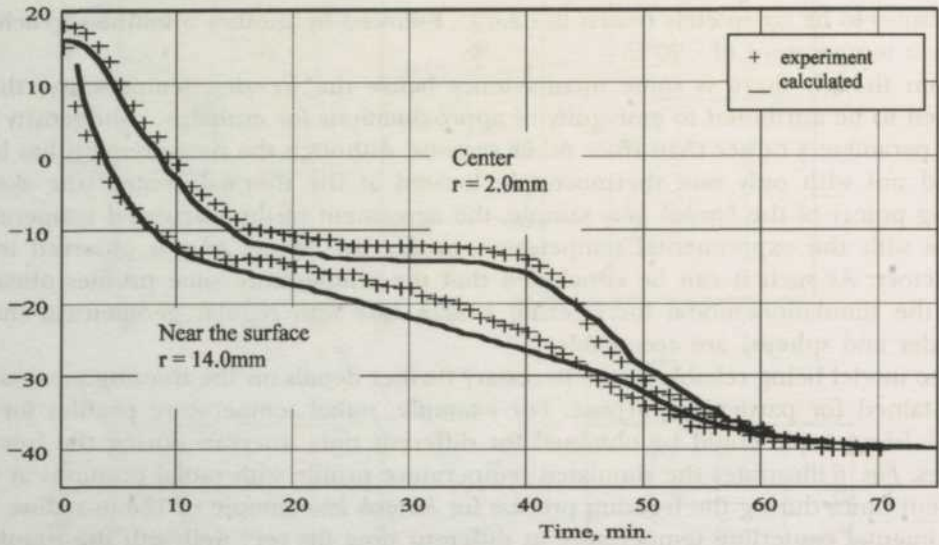


Fig. 4: Experimental (Macchi 1995) and calculated temperature profiles for gelatin cylinders ( $D=30\text{mm}$ ,  $L=100\text{mm}$ ) at different radius frozen in the mechanical freezer ( $T_{air}=-40^{\circ}\text{C}$ )

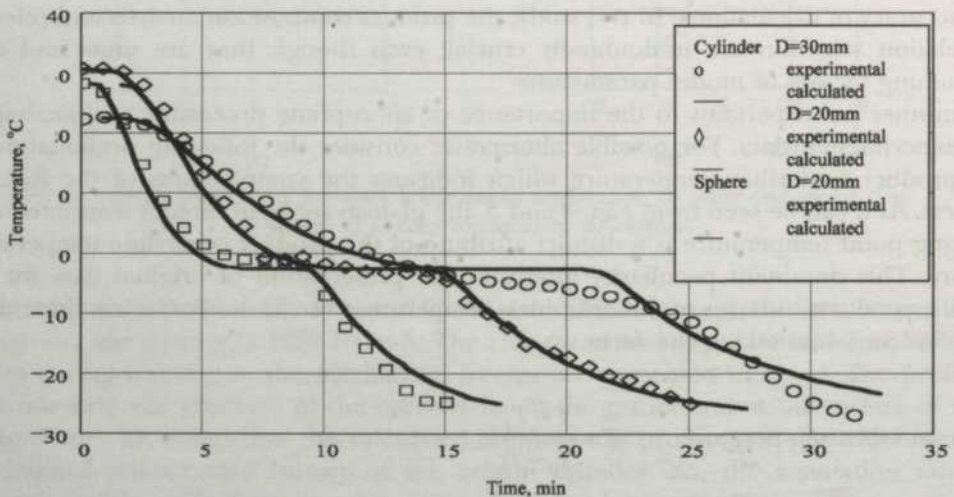


Fig. 5: Experimental and calculated temperature profile evaluated at the center for keropok lekor frozen in the mechanical freezer ( $T_{air}=-30^{\circ}\text{C}$ ), for a cylinder and a sphere samples

### CONCLUSIONS

A versatile model describing cooling and freezing process of *keropok lekor* has been developed. The simulation presented was successfully validated with the experimental results obtained from literature (gelatin cylinder) and from data obtained in this study for *keropok lekor* frozen in mechanical freezer. The fit is satisfactory for the standard geometrical shapes studied (sphere and cylinder). It has been shown that the temperature profile presents a freezing point of  $-2.6^{\circ}\text{C}$  for *keropok lekor*. The temperature history during freezing enables the prediction of the freezing time. For a 30 mm diameter cylindrical *keropok lekor* sample, the simulation model predicted a freezing time of 30

### Predicting Freezing Time for Keropok Lekor

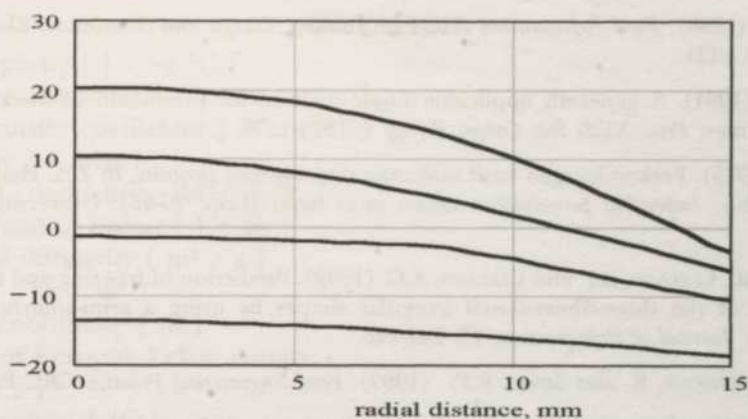


Fig. 6: Calculated temperature profiles for keropok lekor ( $R=15\text{mm}$ ) for  $t_1=200\text{s}$ ,  $t_2=400\text{s}$ ,  $t_3=800\text{s}$  and  $t_4=1600\text{s}$ .  
o - experimental temperature at axis

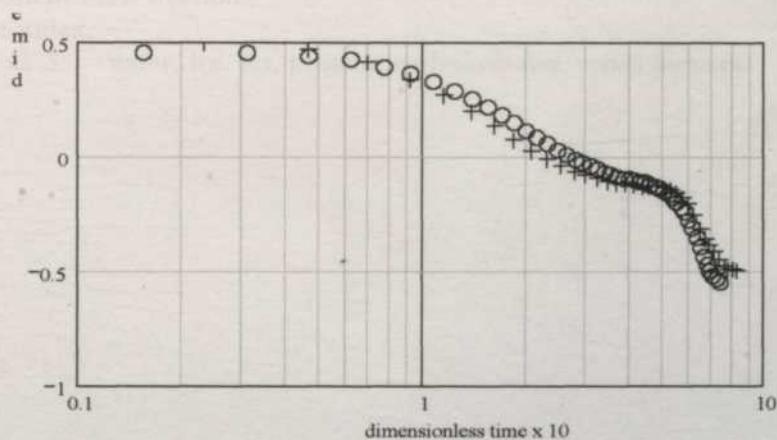


Fig. 7: Centerline temperature generalization for unsteady freezing process of keropok lekor

minutes for the core temperature to achieve the frozen temperature of  $-20\text{ }^{\circ}\text{C}$ . Likewise, for 20 mm diameter cylindrical and spherical *keropok lekor* samples, the predicted freezing time to achieve  $-20\text{ }^{\circ}\text{C}$  were 20 minutes and 15 minutes, respectively. These predicted freezing times are in good agreement with experimental freezing times. Thus the simulation model could provide a good approximation for predicting of the freezing time for *keropok lekor* with cylindrical and spherical shapes.

### REFERENCES

- AGNELLI, M.E. and MACHERONI, R.H. (2001). Cryomechanical freezing. A model for the heat transfer process. *Journal of Food Engineering*, 47, 263-270.
- CHEN, Y.L. and PAN, B.S. (1995). Freezing tilapia by air blast and liquid nitrogen - freezing point and freezing rate. *Int. J. Food Sci. and Tech.*, 30, 167-173.
- CHEVALIER, D., LE BAI, A. and GHOUL, M. (2000). Freezing and ice crystal formed in cylindrical food model: part I. Freezing at atmospheric pressure. *J. Food Eng.*, 46(4), 277-285.

- CLELAND, A.C. (1990). *Food Refrigeration Processes: Analysis, Design and Simulation*. Elsevier Science Publishers LTD.
- CLELAND, D.J. (1991). A generally applicable single method for prediction of food freezing and thawing times. *Proc. XVIII Int. Congr. Refrig.* 4, 1874-1877.
- EMBONG, M. (1988). Perkembangan hasil makanan dari sumber protein. In Z.A. Hamid and N.M. Embi (Eds.), *Imperaktif penyelidikan dalam sains hayat* (Cop. 29-46). Universiti Kebangsaan Malaysia.
- HOSSAIN, M.D.M., CLELAND, D.J. and CLELAND, A.C. (1992). Prediction of freezing and thawing times for foods of the three-dimensional irregular shapes by using a semi-analytical geometric factor. *Int. Journal of Refrigeration*, 15, 241-246.
- KENNETH, J.C., ENRIQUE, R. and SINGH, R.P. (1997). *Food Engineering Practice*. CRC Press.
- MACCHI, H. (1995). Congelation alimentaire par froid mixte: Procédé avec pretreatment par Immersion dans l'Azote Liquide. (Doctoral Thesis, ENGREF (pp. 162-166; 73-78)). Paris, France.
- PEARSON, D. (1976). *The Chemical Analysis of Foods* (7th ed.). London: Longman Group Limited.

NOTATION

- $c$  heat capacity [ J / kg °C ]
- $c_u$  heat capacity at unfrozen state [ J / kg °C ]
- $h$  heat transfer coefficient [ W / m<sup>2</sup> °C ]
- $H$  enthalpy [ J / kg ]
- $k$  thermal conductivity [ W / m °C ]
- $\lambda$  latent heat of fusion [ J / kg ]
- $\alpha$  thermal diffusivity [ m<sup>2</sup> / s ]
- $\rho$  density [ kg / m<sup>3</sup> ]
- $r$  radial coordinate [ m ]
- $R$  radius of Keropok Lekor sausage
- $t$  time [ s ]
- $T$  temperature [ (C )
- $T_f$  freezing temperature [ °C ]
- $T_b$  bulk temperature [ °C ]
- $T_s$  surface temperature [ °C ]
- $X$  component mass fraction
- $n$  space index
- $W, I, F, P, C, S$  water, ice, fat, protein, carbohydrates, solids indexes.

## Performance Evaluation of a Terrain-Accommodating Oil Palm Loose Fruit Collector

Rimfiel B. Janius & Abadanjumi Eskandar

*Department of Biological and Agricultural Engineering  
Faculty of Engineering, Universiti Putra Malaysia,  
43400 UPM, Serdang, Selangor, Malaysia*

Received: 19 May 2003

### ABSTRAK

Sebuah pemungut buah kelapa sawit terlerai jenis rantai dan jari pengaut telah direka bentuk dan dibina. Dengan kelebaran muncung 220 mm dan dua roda tukisan bergaris pusat 360mm, mesin ini boleh mengikut keadaan bentuk bumi, tumbuhan dan sisa yang berubah-ubah di sekeliling pokok kelapa sawit. Mesin diuji pada kelajuan enjin 470 psm yang menghasilkan kelajuan linear jari pengaut 52.4 m/min. Kebolehan mengutip di atas tujuh jenis permukaan dan kebolehgerakan dalam sepuluh jenis keadaan telah diuji. Penilaian kebolehan pemungut untuk mengutip menunjukkan bahawa panjang cirian (characteristic length) mesin, kelebaran serta ketinggian muncung dan kelegaan permukaan bumi-jari yang betul adalah parameter yang paling penting dalam menentukan kebolehan mesin untuk mengikut bentuk bumi. Bagi kebolehgerakan (manoeuvrability) pemungut, faktor-faktor yang mempengaruhinya adalah sokongan roda hadapan dan kedudukan roda belakang sebagai pivot. Dalam kesemua percubaan mengutip yang berjaya, mesin dapat mengutip buah tanpa sebarang kecederaan. Panjang cirian mesin menduga bentuk bumi pada peringkat makro sementara muncung pula membuatnya pada peringkat mikro. Kebolehan mesin untuk beroperasi dalam kawasan bertumbuhan dan bersisa bergantung sebahagian besarnya pada peranti pengutipan yang telah menunjukkan keupayaan menyisir kebanyakan tumbuhan dan menapis keluar sisa bersaiz kecil hingga sederhana.

### ABSTRACT

A chain-and-rake type oil palm loose fruit collector was designed and developed. With a nose width of 220 mm and two 360-mm diameter wheels the machine is able to accommodate the varying conditions of terrain, vegetation and residue around an oil palm tree. The machine was tested at an engine speed of 470 rpm resulting in a linear rake speed of 52.4 m/min. Pick-up ability on seven types of surfaces and manoeuvrability in ten different conditions was tested. Evaluation of collector pick-up ability reveals that machine characteristic length, nose width and height and correct finger-ground clearance are the most important machine parameters determining the ability of the collector to follow the terrain. For collector manoeuvrability, the affecting factors are the front wheel support and location of the rear wheels as a pivot. In all successful pick-up attempts, the machine picks up the fruits free of injury. While the characteristic length negotiates the terrain at the macro level, the nose does it at the micro level. The ability of the machine to operate in areas of vegetation and residues depends largely on the picking device, which has been able to comb through most vegetation and filter out smaller to medium size residues.

**Keywords:** Loose fruit collector, finger-fruit interaction, terrain-accommodating, vegetation, residue

## INTRODUCTION

Currently, the most effective ways of collecting loose fruits in the field are the hand and the board methods. The former entails scraping the ground with two pieces of board to gather and lift the fruits into a sack while the latter involves the same procedure but uses both hands (gloved) without the aid of board. In both methods, fruit injury is practically absent but a substantial amount of debris, small plant matter and pebbles are also collected. These non-fruit matters are separated from the fruits before the fruits are sent to the mill. Measurements made at UPM farm give a gross fruit collection rate (i.e. including all non-fruit matters) of 39.6 kg/hour. Bardaie (1987) reported that 28% of the total time required for field operations, from the cutting of the fronds to the movement of the FFB transporters to the next palm, was spent in collecting loose fruits. Earlier, Turner and Gillbanks (1974) and Webb (1977) reported that the amount of time spent to be at 25% and 39%, respectively.

Gan *et al.* (1993) reported that the average time spent to collect the fruits by hand was three minutes and this was five times the time taken to cut a fresh fruit bunch. Thus, most workers did not collect the loose fruits. Loose fruits are found not only in the fields but also at the unloading ramp. Human labour is employed to pick these fruits by hand.

At the ramp, the spread of loose fruits is confined to a small area in a relatively high concentration on flat concrete or tarred surface. Mechanised picking in this area is not a problem; in fact, the status quo is believed to be more effective and economical. The main problems faced in the use of mechanical collectors in plantations are the terrain (T), the vegetation (V) and the residue (R) in order of importance, conveniently referred to here as the TVR problems. The typical oil palm plantation has a very rough terrain. Even a flatland plantation is not flat when observed at a close range. The ground around the palm may have mounds, depressions, ridges, gullies, partially embedded rocks and loose gravels, among others. Vegetation includes grass, weeds, creepers and other undergrowths. Fruits trapped in between these plants are difficult to recover. Currently, manual picking is the only certain way of recovering them. Vegetation can be controlled relatively easily through the application of herbicides and regular use of crop upkeep equipment. Residue includes cut fronds, felled trunks, old uncollected loose fruits and debris. All these factors are a hindrance to mechanical collectors.

Various terrain, vegetation and residue characteristics are found in a plantation to give an infinite number of combinations of these elements. Even under and around a single palm loose fruits can be found in different TVR conditions, bringing up the importance of micro-terrain in design and development. The machine must be versatile enough to be able to adapt to the varying TVR requirements (micro-terrain) in order to pick up the fruits in the desired time period, free of injuries and foreign matters. However, a machine can perform only in the set range of conditions for which it is designed and developed. The small fruit size against the big terrain, vegetation and residue elements complicate the scenario, making it difficult to recover the lodged fruit. Thus, the demanding performance expected of an oil palm loose fruit collector can be appreciated.

Various collectors have been built. However, all of them suffer from the inability to accommodate the plantation terrains. They are generally too wide, could only pick up fruits on flat open ground and unable to pick up fruits near obstacles including the palm trunks. Some research carried out studied the different methods of picking rather than addressing the TVR problems. Muhammad Salih and Razak Jelani (1988) developed a cylindrical collector that collects one fruit at a time. The process is similar to individual

fruit picking by hand except that with the use of this cylinder, the labourer does not have to bend down. Mechanical collectors employing the sweep or brush mechanism were developed by Osman (1988) and Rosnita (1998). Narayanan (1992) and Harris (1995) used discs as the collecting device. Different suction methods were tested by Wan (1993), Ahmad Hitam *et al.* (1995) and Mahmud Manti (2004). The machines were big and not quite to the terrain and fruit collection rates reported were about 1.0 kg/min with debris varying between 5 and 10 %. Following that, Mohd Shahir (2006) experimented with a modified 1.2-kW domestic vacuum cleaner and managed to collect 0.64 kg/min of loose fruits under laboratory condition with debris rated at 2.1%. The whole machine weighed about 10 kg and the suction air flow rate was 4.75 m/s and reported to be insufficient. The simple method of using a gatherer and scoop was tested by Fakhurrrazy (2003) who obtained a fruit collection rate of 1.1 kg/min with 4% debris.

Although various performance levels of these machines are reported, they have yet to be used on a continuous basis. As such, no realistic indicator of performance level as a reference value can yet be available unless and until a loose fruit collector has been successfully used in a continuous manner in real field operations. An indicator obtained from simulated tests would not be representative because the real nature of loose fruit spreads on the ground upon FFB impact can never be reproduced.

There is a clear need for a collector that can be adapted to varying conditions of terrain, vegetation and residue. A prototype of such a machine is built, and being in its preliminary stage, the design and development is focused on achieving the ability to pick up fruits in different conditions rather than on its operational field performance. Hence, the present study of its performance is confined to the qualitative evaluation of its functional ability, i.e., its picking ability and manoeuvrability, detailed as follows.

1. The ability of the machine to pick up fruits free of dirt and injury
2. The ability of the machine to pick up fruits trapped in vegetation
3. The manoeuvrability of the machine on different terrains

## METHODS

The collector was designed and developed with the aim of getting a low-weight machine and addressing the TVR problems. A 1-kW grass cutter engine (Tanaka SUM328) running at about 470 rpm was used as a power source. The collector is shown in *Fig. 1*.



*Fig. 1: The oil palm loose fruit collector*

To be able to accommodate the different terrains, the collector was built as narrow and as short as possible. This would allow it to access difficult areas such as depressions, ridges and gaps between obstacles. In order to avoid the tyres from being stuck in between small obstacles and in soft ground, a pair of large pneumatic tyres was used for traction. Two small wheels at the front served as a guide. Fig. 2 shows the various important parts of the collector and Fig. 3 shows the relevant dimensions in millimetres.

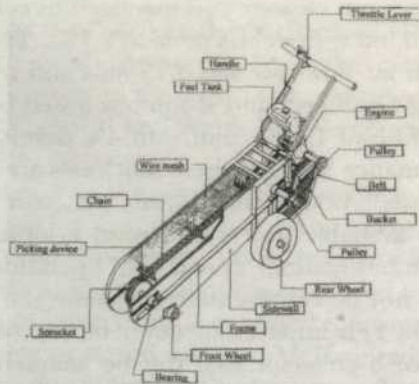


Fig. 2: Important parts of the oil palm loose fruit collector

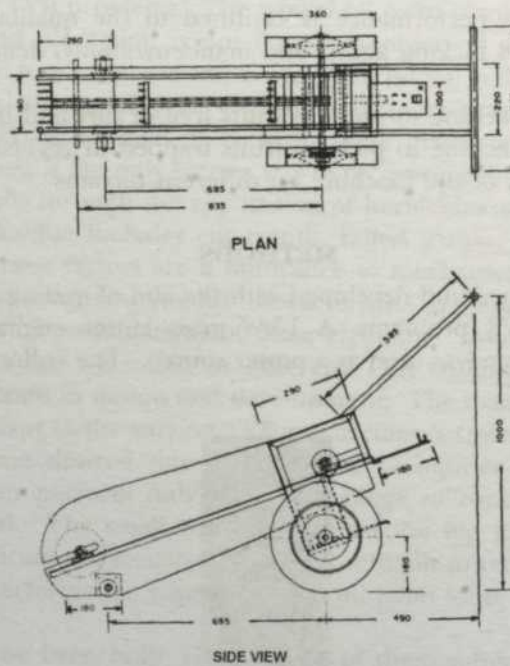


Fig. 3: Relevant dimensions of the collector in mm

Not including the handle, the total width of the machine at the rear wheels is 425 mm. The nose, i.e., the body proper part to the front of the large rear wheels (excluding the small front wheels) determines whether or not the machine can access difficult areas. This part has a width of 220 mm.

Once a difficult area is accessed, the fruit must be able to be picked up by the picking device of the collector. This device is of the continuous chain and rake type. Four steel rakes placed at equal intervals on the 1747 mm long chain travel with a linear velocity of 52.4 m/min. The rakes gather the fruits and push them up along the floor inclined horizontally at about 20° into a bucket at the end of the incline. For smoothness and to avoid rust, an aluminium sheet is used for the floor. The fingers of each rake are placed close to each other so as to avoid the fruits from slipping through and to discard small residues. A 10-mm clearance is given between the tip of the fingers and the ground to ensure the picking up of the fruits using these fingers and avoid scraping the ground. These fingers are also encased in plastic tubes to keep the fruits intact. Being of the finger type, the rakes are expected to comb through the vegetation.

The machine was tested at an engine speed of 470 rpm and a resulting linear rake speed of 52.4 m/min. The pick-up ability was tested on seven different surface categories as listed in Table 1. Description of the categories is as follows:

- a) Uneven ground: gradual mounds and depressions, gentle ridges, low surfacing roots.
- b) Frond-covered: the frond piles in between rows of palms.
- c) Grass: ordinary grass.
- d) Other vegetation: creepers, small plants, lallangs, etc.
- e) Sudden depressions: holes, shallow but steep drop in surface levels, ridges.
- f) Rocks/other obstacles: partially embedded rocks, step-like inclines, occasional thick standing plants and timber, areas within about 20 cm from trunks.
- g) Clear: relatively even, varying from flat to about 15% slope.

The manoeuvrability was tested in ten different conditions as listed in Table 2. All tests were carried out during real harvesting operations with loose-fruit spread being formed naturally upon the impact of the FFB on the ground. Except for a number of cases on uneven ground, grass and clear areas, each pick-up attempt was usually on a single fruit.

## RESULTS AND DISCUSSIONS

### *Picking Ability*

The picking ability of the collector in the various surface categories is shown in Table 1. Uneven ground, grass and clear areas were well accommodated by the machine but it totally failed in frond-covered areas as there was no way of recovering the fruits without first lifting the bulky materials. To minimize frond-covered area loss, frond piles would have to be as far away as possible from the palms. Although the 220 mm wide nose could negotiate many terrain features, there were more gaps in the TVR surroundings narrower than the nose, preventing it from accessing the fruits trapped in them. The rakes are firmly fastened to the chain but the flexible nature of the chain allows the rakes to be not truly horizontal. This can be clearly seen in *Fig. 1*. This phenomenon is undesirable as it increases the chance of missing the fruits if they happen to be under the higher sides of the rakes.

TABLE 1  
Picking ability of a terrain-accommodating loose fruit collector

Feature at pick-up areas	Total attempts	Success	Failure	
			Injured pick-up	No pick-up
Uneven ground	50	30	10	10
Fronde-covered	20	0	0	20
Grass	20	16	4	0
Other vegetation	40	22	4	14
Sudden depressions	50	11	9	30
Rocks/other obstacles	33	11	6	16
Clear	60	56	4	0

The rake fingers were able to comb through grass. However, when the vegetation was of creepers or other plants that grew perpendicular to the length of the machine, they were torn off and carried into the bucket. Tougher vegetation caused the chain rotation to slow down necessitating the depression of the throttle lever to bring the engine up to speed again. Only debris larger than the rake finger spacing was conveyed along with the fruits into the collecting bucket. A slatted floor helps to minimize this problem except for debris that happens to lie across the slats.

The picking device is the most critical and sensitive part of the machine with the finger-ground clearance very much dependent upon the terrain. Zero clearance will result in the fingers scraping the ground gathering along debris or being stuck in the ground. On the other hand, too much clearance results in either the scraping of the fruits (due to partial finger-fruit interaction) leading to injuries or the fruits totally escaping the machine. Fruits that were injured were those that the fingers interacted with only partially and could not be dislodged by the first few rakes. It was the continuous action of the fingers in trying to extricate these fruits from their trapped positions that caused the injuries. Although they were eventually picked up, these fruits are considered as a failed attempt as they otherwise would have been, if not for the persistent trying by the operator of the machine. Fruits that were properly interacted with (picked up immediately) upon tilting were not injured. It was also observed that it was a natural reaction of the operator to increase speed and tilt the machine slightly forward whenever a fruit is difficult to dislodge. This is specifically so in cases of obstacles and sudden depressions which cause the fingers to be far from the fruits. Other operations such as conveying along the incline and discharging into the bucket did not cause any injury to the collected fruits.

Palm trunks were obstacles to the machine for fruits within a 20 cm distance of the trunk perimeter. This problem was due to the front end of the sidewalls extending beyond the chain boundary. From *Fig. 2*, it can be seen that it is possible to shorten the sidewalls to result in the fingers jutting out ahead of the machine. This is expected to resolve the front obstacle problems that are in other forms such as rocks, earth walls, etc.

Other factors influencing the ability of the machine to accommodate the terrain are the characteristic length and the nose height of the machine. The characteristic length is the horizontal distance between the ground contact point of the rear traction wheel

and the point at which the nose curvature contacts the ground. The shorter this distance is, the better the machine will be able to be used on the different terrains.

The nose height has to be small to enable the machine to properly engage according to the ground physical feature at the pick-up spot. The height of the nose is characterized by its curvature, subsequently the distance between the tensioned and slacked sides of the chain. Reducing this curvature would entail using smaller front sprockets and shorter-fingered rakes. Subsequently, the sidewalls could also be replaced with low ones that would have to be high enough to prevent the fruits being conveyed from falling off the sides. When the nose size is considered together with a shortened characteristic length, the chain speed would also have to be changed accordingly. In short, with respect to the machine, the characteristic length accommodates the terrains at the macro level while the nose at the micro level.

### Manoeuvrability

Table 2 shows the difficulty level in various manoeuvring efforts for the collector. The reference level is that of manoeuvring the collector on a firm, dry and flat natural plantation ground with thin vegetation cover. A single operator carries out all the manoeuvrability assessments.

TABLE 2  
Manoeuvrability of terrain-accommodating loose fruit collector (on two traction wheels)

Manoeuvre types	Easy	Moderate	Difficult
Going up a slope		/	
Going down a slope	/		
Cornering on a slope			/
Backing up - going up a slope	/		
Backing up - going down a slope	/		
Going over obstacles (level)	/		
Going over obstacles (slope)			/
Other movements on level surface	/		
All movements on wet and soft surface (level)		/	
All movements on wet and soft surface (slope)			/

Easy: Success is achieved on the first attempt. Operator does not feel unduly stressed in applying the effort needed. This is a typical reference level achievement.

Moderate: Success is achieved on the second attempt. Operator feels that he is applying an amount of effort over and above the reference level.

Difficult: The operation is marked by two or more failed attempts or a complete failure. Operator is stressed.

Due to the small front wheels and the nature of the plantation grounds, it was found that when not picking up fruits, moving the machine on the two rear wheels were more convenient though not necessarily relaxing. On slopes, the machine was felt heavier due to the unsuitable location of the large rear wheels making manoeuvring a problem. A better pivot position for the wheels and/or an improved handle design would make the weight balance more manageable on slopes. On softer surfaces, the front wheels tended to get stuck in the ground affecting the finger-ground clearance and the manoeuvrability

of the machine. Therefore, there was a need for big pneumatic front wheels instead of small steel rollers.

Manoeuvrability on level ground was poor when the surface was bare and wet. On such a slippery condition, the need for wider rear and front wheels was again felt. However, wider wheels would increase the width of the machine especially at the important front end, in which a proper engagement with the micro-terrain is important, as discussed above. An alternative would be to use reduced inflation pressure for the rear wheels. As for bigger front wheels, though not bigger than the rear ones, their positions beneath the inclined floor would have to be moved further backwards to retain the desired nose features. This will change the overall balance and handle design of the machine. However, it should be noted that a two-wheel machine is undesirable as it encourages operator fatigue.

### CONCLUSIONS

The current terrain-accommodating loose fruit collector was able to address a major part of the TVR problems. Satisfactory picking ability was observed on uneven ground, grass and clear areas. However, the machine was found to be unsuitable in the frond-covered areas. The finger rake method of gathering and conveying fruits is successful in eliminating fruit injuries and debris. For successful picking, a correct finger-ground clearance is important to ensure adequate interaction between the fruits and fingers.

On-slope manoeuvrability is not satisfactory during cornering, overcoming obstacles and when the slope is slippery. Manoeuvrability on a level surface is only a problem if the surface is slippery. In order to improve manoeuvrability, bigger pneumatic front wheels are required and should be installed further rearwards, while relocating the rear wheels and/or redesigning the handle for a better weight balance.

### REFERENCES

- AHMAD HITAM, AHMAD ZAMRI M. Y. and MUHAMMAD SALIH. (1995). Loose fruit collector. PORIM Information Series. *PORIM Technical Bulletin*, (19). Bangi: Palm Oil Research Institute of Malaysia.
- BARDAIE, M.Z.B. and WAN ISHAK. (1987). *Mechanization of oil palm production in Malaysia*. Serdang: Department of Power and Machinery Engineering, Faculty of Engineering, UPM.
- FAKHRURRAZY ABU YAZID. 2003. *Pembangunan alat pungut buah kelapa sawit terlerai menggunakan kaedah kautan dan cedohan secara manual*. Laporan projek pelajar tahun akhir. Serdang: Fakulti Kejuruteraan, UPM.
- GAN, L.T., HO, C.Y., LAM, K.S. and CHEW, J.S. (1993). Optimum harvesting standards to maximize labour productivity and oil recovery. In *PORIM International Palm Oil Congress*. Kuala Lumpur.
- HARRIS SANDAMUDIN. (1995). *Perlakuan alat pungut buah kelapa sawit terlerai*. Laporan projek pelajar tahun akhir. Serdang: Fakulti Kejuruteraan, UPM.
- MAHMUD MANTI. (2004). *Reka bentuk mesin pungut buah kelapa sawit terlerai menggunakan kaedah sedutan secara langsung*. Laporan projek pelajar tahun akhir. Serdang: Fakulti Kejuruteraan, UPM.
- MUHAMMAD SALIH and RAZAK JELANI. (1988). Kajian awal terhadap alat memungut buah kelapa sawit terlerai. In *Seminar Penyelidikan Kejuruteraan Pertanian*, 16-17 November. Serdang: Fakulti Kejuruteraan, UPM.

- MOHD SHAHIR WAGIO. (2006). *Reka bentuk dan pembangunan mesin sedut buah kelapa sawit terlerai*. Laporan projek pelajar tahun akhir. Serdang: Fakulti Kejuruteraan, UPM.
- NARAYANAN, P. (1992). *Preliminary observations on the performance of an oil palm loose fruit collector*. Final year student project report. Serdang: Faculty of Engineering, UPM.
- OSMAN MOHD. TOP. (1988). *Reka bentuk jentera pemungut buah kelapa sawit terlerai*. Laporan projek mini. Serdang: Fakulti Kejuruteraan, UPM.
- ROSNITA ABDULLAH. (1998). *Pengubahsuaian dan perlakuan mesin pengaut buah kelapa sawit terlerai bermotor*. Laporan projek pelajar tahun akhir. Serdang: Fakulti Kejuruteraan, UPM.
- TURNER, D.D. and GILLBANKS, R.A. (1974). Oil palm cultivation and management (p. 485-504). Incorporated Society of Planters, Kuala Lumpur.
- WAN, W.T. (1993). *Design and performance of a prototype oil palm loose fruit collector using indirect suction method*. Final year student project report. Serdang: Faculty of Engineering, UPM.
- WEBB, B.H. (1977). The development of suitable infield ffb harvesting systems to improve the efficiency of oil palm production. In D.A. Earp and W. Newll (Eds.), *International Development in Oil Palm*, 14-17 June. Pub. Incorporated Society of Planters.

## Array Beampattern Using Goal

Farrukh Nagi & Wong Hung Way

*University Tenaga Nasional*

*Selangor, Malaysia*

*E-mail: farrukh@uniten.edu.my*

Received: 2 August 2004

### ABSTRAK

Corak pancaran di kedudukan jauh daripada punca bunyi boleh dibentuk dengan menukarkan amplitud dan fasa setiap kesusunan antena. Walau bagaimanapun, apabila satu atau lebih elemen gagal, corak pancaran akan terganggu. Algoritma 'Goal Attain' boleh digunakan untuk memperbaiki corak tersebut dengan mengoptimasikannya supaya sama dengan corak pancaran yang asal. Ini boleh dicapai dengan mengubah dan mengawal fasa serta amplitud setiap elemen beberapa kali. Kualiti corak yang dibaiki boleh dibandingkan dengan corak yang asal dengan satu indeks kecapaian yang tertentu. Kebaikan Goal Attain telah dikaji dalam sistem bunyi 'Uniform Planar' dan 'Linear Array'.

### ABSTRACT

The desire beampattern of a sound source at the far field can be synthesised by controlling the relative amplitudes and phases of each array element. However, when one or more elements in the array fail, the beampattern at the far field is severely distorted. The Goal Attain optimisation algorithm is used to adjust the relative gains of the remaining array elements so as to generate an optimised pattern closely resembles the original beampattern. The quality of each optimised pattern is evaluated and compared based on a defined performance index. The effectiveness of the Goal method is tested in both the Uniform Planar and Linear Array sonar systems.

**Keywords:** Beampattern, beamwidth, linear array, planar array, goal attain optimisation

### INTRODUCTION

The desire shape of the far field radiation pattern of a linear uniform array antenna system can be synthesised by controlling the relative amplitudes and phase of the array element weights.

The array antennas typically consist of individual elements that are essentially each little antenna on their own. Numbers of these elements are arrayed in patterns depending on the desired performance characteristics needed by the application such as operating frequencies, antenna gain, sensitivity, and power requirements. When one or more array elements or its associated circuitries of the antenna system become defective, the result, in severe distortion of the original far-field pattern. If all array elements operate properly, the well-known analytic techniques can be used to find the optimum amplitude and phase of each element to yield the desired pattern. However, if any elements fail, no analytic means exists to find the excitation coefficients of the array that compensates for the degradation of the pattern.

Recently, there has been an increased interest in developing methods to improve the patterns of arrays in the presence of failed elements by re-optimising the weights applied to the remaining array elements. Peters (1991) proposed a method to reconfigure the amplitude and phase distortion of the remaining elements by minimizing the average sidelobe level via Conjugate Gradient Method. Er (1992) matched the array response

over the main lobe width while minimizing the mean-square value of the array response over the sidelobe regions. This formulation results in a constrained optimization problem involving a quadratic constraint and a set of linear constraints on the element excitation. Bu *et al.* (1993) used the biquadratic programming method in reconfiguring the array by changing the phase of each remaining active element. Maxillous (1996) used the method of replacing the signals from failed elements in a digital beamforming receiving-array. Levitas *et al.* (1999) introduced a practical failure compensation technique for active phasing arrays. It is independent of the external signal environment and is capable of achieving substantial performance improvement across broad selectable angular sectors at the expense of some additional performance degradation in other less important sectors. Yeo *et al.* (1999) proposed the genetic algorithms for array failure correction in digital beamforming of arbitrary arrays. Deng *et al.* (2001) applied the optimisation algorithm, differential evolution to the radiation pattern synthesis of the array. Miaris *et al.* (2002) uses the orthogonal method to find the excitation of each non-defective element factor and considers only the array factor established with orthogonal basis.

This paper describes Goal Attain technique to restore the original far field radiation pattern by adjusting the gains of the remaining working elements. The Goal Attain technique is more relevant when dealing with faulty array elements since the Goal objective is chosen to restore maximally possible the correct beampattern to avoid degradation in performance of the array system. To use Goal Attain, two beam patterns are required; the original and the distorted pattern caused by faulty elements. The original beampattern is determined by numerically integrating the gains and phases of all the working elements in the sound source array. To synthesise the fail beam pattern, the phases and gains of the faulty array elements are null during the integration process. The effect of the faulty array elements on the beampattern is the overall reduction in the array gain factor. In addition, lobe symmetry is also affected in absence of non-coherent inter-element spacing between elements (*Fig. 1*). The original beampattern is set as the target in Goal Attain. The Goal Attain then attempt to minimize the error between the faulty and the original pattern by adjusting the gain (weights) of the remaining working elements in the array.

The availability of powerful Digital Sequel Processors (DSPs) and their efficient computation algorithms can be exploited to implement optimisation techniques in real time sonar array systems. Although the Goal Attainment optimisation technique is applied to linear and planar arrays in this paper, the procedure can be generalized for other array configurations.

#### FAR FIELD BEAMPATTERN GENERATION OF SOUND SOURCE ARRAY - BEAMFORMING

The linear and planar arrays considered in this work (Wykes *et al.*, 1992; Wykes and Nagi, 1992) operate at Ultrasonic frequency of  $f_c = 100\text{KHz}$  and the speed of sound in air at  $20^\circ\text{C}$  is  $c = 344\text{ m/sec}$ ; the inter-element distance ' $d$ ' avoiding grating is

$$\lambda = \frac{c}{f_c} \Rightarrow \frac{344}{100,000} = 3.44\text{mm}$$

$$d \leq \frac{\lambda}{2} = 1.72\text{mm}$$

The linear array consists of  $M=16$  where as planar consists of  $M \times N$  ( $8 \times 8$ ) elements. The resultant sound field at a particular far field point is determined by the vector addition of the sound field at that point radiated by the individual sound sources. Conventional beamforming calculates the time delay of the signals arriving between array elements by shifting and summing the incoming data using numerical integration.

*Linear Array*

The array factor of the beampattern is normalised with equal amplitudes  $w(m)$  of one. The beamforming output from linear array is given as

$$G(\theta) = \sum_{m=1}^M w(m) e^{i(2m-M-1) \cdot arg} \tag{1}$$

where

$$arg = \pi d \left[ \sin \left( \theta - \frac{\pi}{2} - \gamma \right) \right]$$

- $\theta$  is scanning angle,  $q = -90 : 1:90$
- $\gamma$  is steering angle
- $w(m)=[1,1,\dots,M]$ , Uniform weight on each element
- $d$ , inter-element distance between array elements
- $M=16$  array elements and  $m$  is the index on  $M$

The quantity  $|G(\theta)|^2$  is known as the beampattern, which is simply the power of the beamformer as a function of  $\theta$ .

*Planar Array*

Planar array beampattern  $G_p$  in two-dimensional is superposition of two beampatterns  $S_x$  in x-axis and  $S_y$  in y-axis

$$G_p = S_x(\theta, \varphi) * S_y(\theta, \varphi) \tag{2}$$

where

$$S_x(\theta, \varphi) = \sum_{m=1}^M w_x(m) e^{i(2m-M-1) \cdot arg_x}$$

$$arg_x = \pi d_x \left[ \cos \left( \theta - \frac{\pi}{2} - \gamma_x \right) \sin \left( \phi - \frac{\pi}{2} - \gamma_y \right) \right]$$

$\theta$  and  $\varphi = -90:1:90$ , are the scanning in x and y dimension

and

$$S_y(\theta, \varphi) = \sum_{n=1}^N w_y(n) e^{i(2n-N-1) \cdot \arg_y}$$

$$\arg_y = \pi d_y \left[ \sin\left(\theta - \frac{\pi}{2} - \gamma_x\right) \sin\left(\phi - \frac{\pi}{2} - \gamma_y\right) \right]$$

$\gamma, \theta, \varphi$  and  $w_x(m) = w_y(n) = w(m)$  are same as before.

### FAILED BEAMPATTERN

To simulate the beampattern due to failed elements, equations (1) and (2) are used. A new weight vector  $w(q)$  is used in equations (1) and (2) instead of  $w(m)$  which has zero at the positions of the failed elements.

$$w_f(q) = [1, 0, 1, 0, 0, 1, 1, \dots, Q = M-P] \text{ Array element \# } 2, 4, 5, \dots, \text{ failed} \tag{3}$$

where  $Q$  is the number of the remaining working elements and  $q$  is their index.  $P$  represent the numbers of the failed elements and  $p$  is the index of the failed elements. The beampattern of the remaining elements excluding the contribution from the failed elements is evaluated as

$$G_f(\theta) = \sum_{q=1}^Q w_f(q) e^{i(2(q+p)-Q-1) \cdot \arg} \tag{4}$$

In equation (4), index  $q+p$  cater for increased inter-element distance in multiple of  $d$ , as in Fig. 1. The purpose of  $w_f(q)$  and  $(q+p) \cdot d$  is to avoid contributions from the failed elements

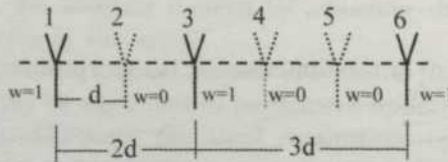


Fig. 1: Non-uniform inter-element distance

$$(q+p) \cdot d = (1, 2, 3..) \cdot d \tag{5}$$

In the planar array system, the randomly selected elements are also failed similarly in Fig. 2. The weights  $w_x$  and  $w_y$  are changed to  $w_{fx}$  and  $w_{fy}$  as in equation (3).

$$G_{pf}(\theta, \varphi) = \left[ \sum_{u=1}^U w_{fx}(u) e^{i(2(u+p)-U-1) \cdot \arg_x} \right] \left[ \sum_{v=1}^V w_{fy}(v) e^{i(2(v+p)-V-1) \cdot \arg_y} \right] \tag{6}$$

where  $u, v$  and  $U, V$  are the indexes and numbers of the failed x-y planar array respectively, similar to  $q$  and  $Q$  in equation (5) for failed linear array.

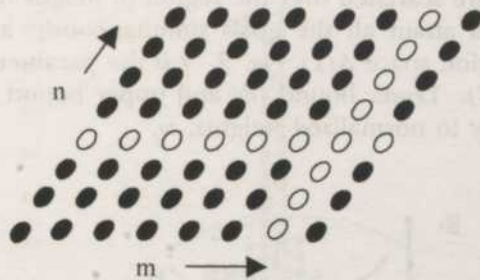


Fig. 2: Failed elements of planar array are shown white

**OPTIMISATION OBJECTIVE FUNCTION AND PATTERN**

The optimisation process evaluates the optimised weights  $w_o = [w_{o1}, w_{o2}, \dots, w_{oM}]$  compensating the failed elements weights  $w_f$ . The failed element beampattern  $G_f(w_f)$  is chosen as the optimisation objective function so that during the optimisation process, the failed array elements do not contribute to the optimised beampattern. Goal Attain then iteratively evaluates the weights of all the working elements in the array. Each weight  $w_{op}$  consists of the relative amplitude of each working element. The weights are so adjusted such that  $G_f(w_f)$  is optimised to  $G_f(w_o)$  and approaches closest to the goal  $G(q)$ . The optimised objective function is described here in the with linear array but it can be extended similarly to planar array. The optimised beam patterns can then be described as

$$G_f(w_f = w_o) = \sum_{m=1}^M w_o(m) e^{i(2(m+p) - M - 1) * arg} \tag{7}$$

and for planar array

$$G_f(\theta, \varphi)_o = Sx(\vartheta, \varphi)_o * Sy(\theta, \varphi)_o \tag{8}$$

**OPTIMISATION - GOAL ATTAINMENT**

Multi-objective optimisation method of Gembicki (1974) concerns with the minimization of a set of objectives simultaneously. According to Hiller and Lieberman (2001) "The basic idea is to establish a numerical goal for each of the objectives, formulate an objective function for each objective and seek a solution from their respective goals". Mathematically, for array gain optimisation, the problem can be stated

$$\begin{aligned} \text{Minimize}_{\gamma, w \in \Omega} \quad & \Theta * \gamma = G_f(w) - G^* \\ \text{or} \quad & G_f(w) - \Theta * \gamma \leq G^* \\ & 0 \leq w_j \leq 1 \quad (ub) \end{aligned} \tag{9}$$

$G^* = [g_1^*, g_2^*, \dots, g_m^*]$  are goals to be achieved by set of objective  $G_f = [g_{f1}(w_f), g_{f2}(w_f), \dots, g_{fm}(w_f)]$ . Where  $g^*$  is described as isotropic field of radiation of individual array element and  $g_f$  is describe as radiation pattern as a function of  $w_f$ . Each objective function  $g_f$  and its corresponding goal  $g^*$  are searched over the region of weight vector  $[w_{f1} w_{f2} \dots w_{fm}]$ . Since it is not possible to attain all the goals simultaneously, a feasible region  $\Omega$  is explicitly defined by function space  $\Lambda(\gamma)$ . Fig. 3,  $\gamma$  is the parameter which changes the size of function space  $\Lambda(\gamma)$ . Lower bound (*lb*) and upper bound (*ub*) are constraint in (9) to 0 and 1 respectively to normalized weights,  $w_f$ .

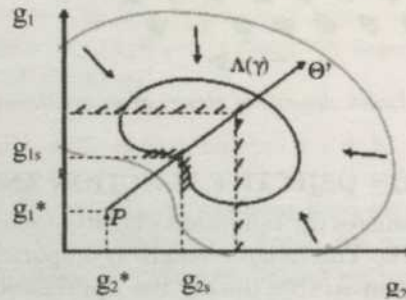


Fig. 3: Two dimensional optimisation problem

The sign of  $\Theta$  determines the direction of search of the feasible function space from goal point  $P$   $g_1^*, g_2^*$ . The +ve of  $\Theta$  in equ.(9) makes the  $G_f(w_f)$  less than  $G^*$ , while -ve makes  $G_f(w_f)$  greater than  $G^*$  and function converges closer to the solution. The starting weights  $w_f(M)$  are carefully chosen so as not to produce local minima. The starting optimisation function  $|G_f(w_f)|$  then would be less than  $|G^*|$ , so

$$w_f = -(1 \text{ to } 2)$$

The magnitude of 1 to 2 is selected for the slackness in the solution and helps to increase speed of convergence. After optimisation the optimised weights are then

$$w_{op} = (w_f)^*$$

### PERFORMANCE MEASURE

After the optimised pattern has been determined, it is compared with the failed beam pattern to evaluate if any improvement in performance has occurred. Gain performance indicator  $\eta$  (SNR) is set to the ratio of the beamwidth defined as the gain of the main beam above -3db, to the side lobes as

$$SNR \Rightarrow \eta_{(f,op)} = 20 \log_{10} \left[ \frac{\Sigma G_{BW_{-3db}}}{\Sigma [G_f(w_o) - G_{BW_{-3db}}]} \right]$$

Fig. 4 depicts the above expression. The rationale for  $\eta$  is that the main beam is pointing towards the desired direction and the side lobes give rise to undesirable noise entering in the receiver from other undesirable direction.

### Array Beampattern Using Goal

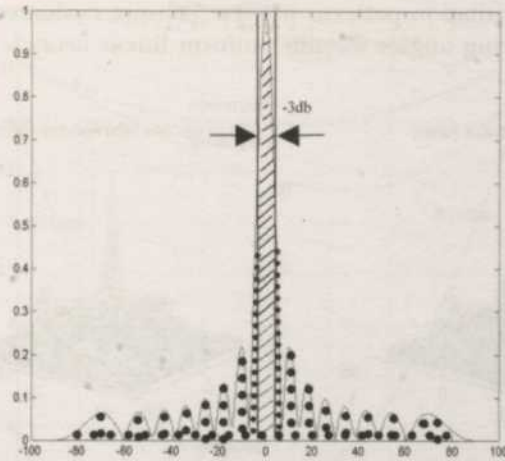


Fig. 4: 3db beamwidth used in equ. (9)

### RESULTS

Sixteen element uniform linear array optimisation results were evaluated at different steering angles with different positions of failed elements. Matlab's optimization toolbox (1996) 'fgoalattain' command was used for implementation of algorithm in section 5. Figs. 5-6 illustrate the beampattern results. The reference pattern  $|G(q)|$  is obtained equations (1) and (2), failed patterns  $|G_f(q)|$  from equations (4) and (6), optimised beampattern  $|G_{opt}(q)|$  from equations (7) and (8). The selected failed elements in equation (2) are set as '0.000' in the weight column at the left of Fig. 5.

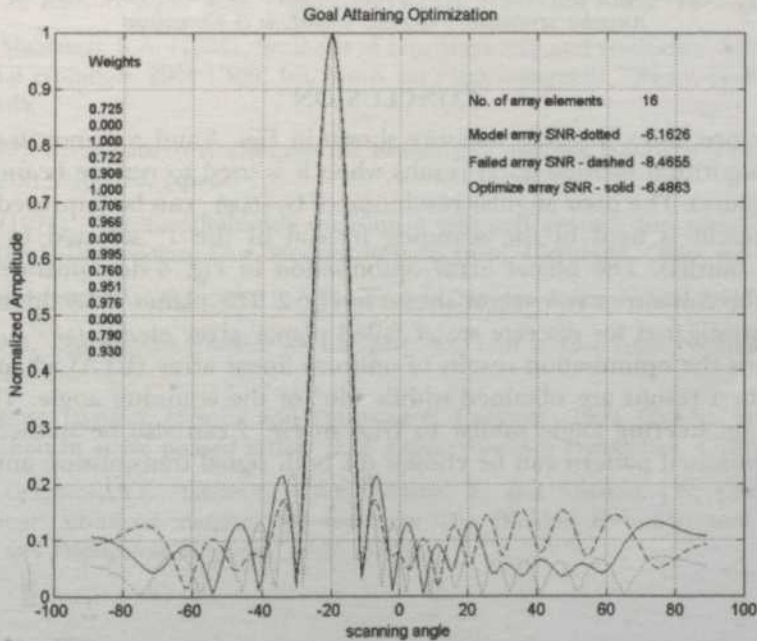


Fig. 5: Goal optimisation for failed elements numbers 2, 9 and 14. Element separation  $d=1.72mm$

The  $\eta$  of the three-radiation patterns in Figs. 5-6 were evaluated using equation (10). The  $\eta$  at different steering angles for the uniform linear array is shown in Fig. 7.

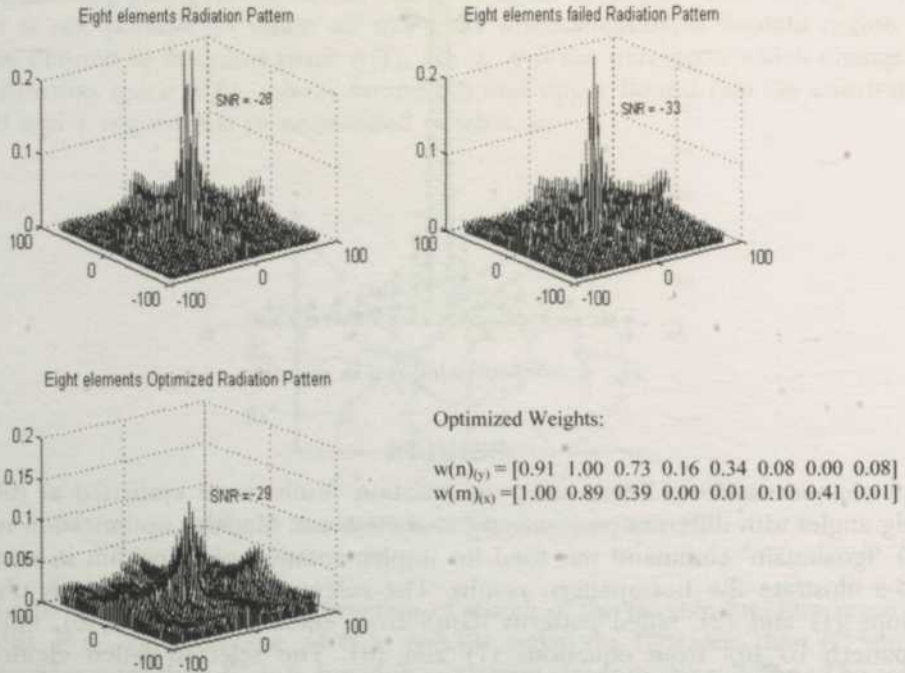


Fig. 6: Failed element vector three or x-axis and vector seven on x-axis, see fig. 2. Scanning angles theta and psi range -90 to 90 degrees. SNR =  $\eta$ , Angular resolution 5 degrees, amplitude is normalized

### CONCLUSION

The performance index  $\eta$  (SNR) measure shown in Figs. 5 and 6 demonstrates that the Goal Attain algorithm provide good results when it is used to restore beampattern due to element failures. The poor angular resolution of  $G_f(\theta, \varphi)_0$  can be improved if a smaller degree increment is used in the scanning instead of the  $1^\circ$  selected to reduce the computation burden. The planar array optimisation in Fig. 6 demonstrates the failed elements in the column or row vector shown in Fig. 2. The planar array optimisation can be further investigated for discrete scalar failed planar array elements.

Fig. 7 shows the optimisation results of uniform linear array (ULA) when steered off centre. The best results are obtained within  $\pm 40^\circ$  of the scanning angle. The effect of optimisation on steering angle similar to ULA in Fig. 7 can also be studied for planar array. The optimised pattern can be chosen for both signal transmission and reception.

## Array Beampattern Using Goal

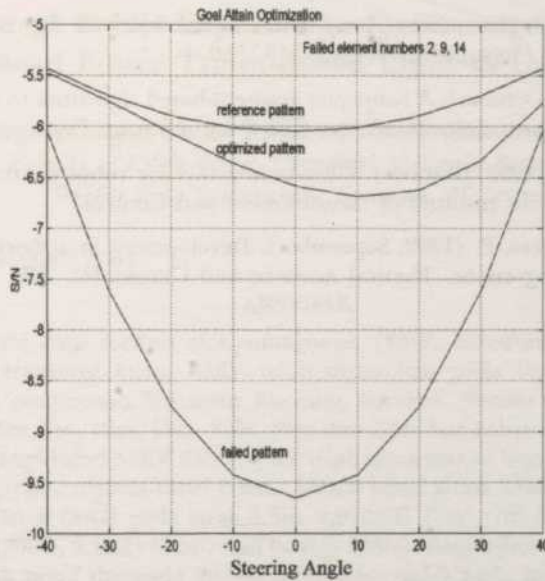


Fig. 7:  $h$  (SNR) vs. scanning angle plot of uniform linear failed elements array in Fig. 5

### REFERENCES

- BENG-KIONG YEO and YILONG LU. (1999, May). Array failure correction with a genetic algorithm. *IEEE Trans., Antennas Propagation*, 47(5), 823-828.
- BU, S.Z. and DARYOUSH, A.S. (1993). Comparison of reconfigurable methods of active phased array antenna. In *IEEE AP-S Int. Symp. Digest* (p. 214-217). USA: Ann Arbor, Michigan.
- DENG, Z. and MICHALSKI, K.A. (2001). Synthesis of reconfigurable and conformal antenna arrays by differential evolution. 2001 URSI, Int. Symp. on Electromagnetic Theory, pp.80-82, Victoria, BC, Canada,
- ER, M.H. (1992). Array pattern synthesis in the presence of element failure. In *Proceeding of (SAP' 92)* (p. 9-12). Sapporo, Japan.
- GEMBICKI, W. (1974). Vector optimization for control with performance and parameter sensitivity indices. (Ph.D Dissertation, Case Western Reserve Univ., Cleveland, Ohio, 1974).
- HILLER, F.S. and LIEBERMAN, G.J. (2001). *Introduction to Operation Research*. New York: McGraw Hill.
- \_\_\_\_\_. (1996). *Optimization Toolbox for Use with MATLAB – User Guide*. Natick, Mass. USA: MathWorks, Inc.
- MENACHEM LEVITAS, DAVID A. HORTON and THEODORE C. CHESTON. (1999, March). Practical failure compensation in active phased arrays. *IEEE Trans., Antennas Propagation*, 47(3), 524-535.
- MIARIS, G.S., GOUNDOS, S.K., IAKOVIDIS, C.H.R, VAFIADIS, E. and SAHALOS, J.N. (2002, October). "Orthogonal" advanced methods for antennas: The ORAMA computer tool. *IEEE Trans. Antennas and Propagation Magazine*, 44(5), 62-74.

- ROBERT J. MAILLOUX. (1996, December). Array failure correction with digitally beamformed array. *IEEE Trans. Antennas Propagation*, 44(12), 1543-1550.
- TIMOTHY J. PETERS. (1991, October). A conjugate gradient-based algorithm to minimize the sidelobe level of planar arrays with element failures. *IEEE Trans. Antennas Propagation*, 39(10), 1497-1504.
- WYKES, C. and NAGI, F. (1992, October). Ultrasonic arrays for robot control. Sensory system for robots symposium. UK: Institute of Measurement and Control.
- WYKES, C., NAGI, F. and WEBB, P. (1992, September). Development in airborne ultrasonic ranging. Annual review of progress on 'Physical Acoustic and Ultrasonic'. UK.

## Assessment of Public Exposure to Electromagnetic Fields by Overhead Power Transmission Lines: A Case Study

Law Puong Ling, Awangku Abdul Rahman, Azhaili Baharun & Ngu Lock Hei

*Faculty of Engineering, Universiti Malaysia Sarawak  
94300 Kota Samarahan, Sarawak, Malaysia*

Received: 30 November 2004

### ABSTRAK

Pengumpulan data bagi medan elektromagnetik (EMF, Electromagnetic Fields) yang dihasilkan oleh transmisi kuasa 33KV telah dijalankan pada Ogos 2002 di 3 lokasi berlainan dalam rangkaian Bahagian Kuching, Sarawak. Semua bacaan diambil pada jarak cerunan 3.5m, 7m, 10m, 15m, 20m, 30m dan 40m dari kabel kuasa. Data EMF dari 3 lokasi tersebut bagi kabel 33KV dan 132 KV telah dipuratakan bagi mendapatkan purata hasil bagi setiap jarak daripada kabel kuasa. Untuk kabel kuasa 33KV, jumlah purata EMF ialah 8608 milliGauss (mG) pada jarak 3.5m, 4,972mG (7m), 785.5mG (10m), 114.3mG (15m), 41.6mG (20m), 6.1mG (30m) and 0.2mG (40m). Bagi kabel 132KV, jumlah purata EMF adalah lebih besar daripada 20,000 milliGauss (mG) pada jarak 3.5m, 10,1612mG (7m), 4,164mG (10m), 1,720mG (15m), 802mG (20m), 139mG(25m), 9mG (30m), and 0.9mG (40m). Tahap standard normal ketinggian bagi kabel kuasa 33KV dan 132 KV ialah 12m dari paras bumi dengan jarak perantaraan 20m pada kedua-dua belah kabel, dan aktiviti manusia kebiasaannya berlaku pada jarak lebih daripada 50m (jarak cerunan) dari kabel kuasa. Kuasa EMF yang dihasilkan oleh kabel kuasa 33KV dan 132 KV tidak mendatangkan sebarang kesan buruk terhadap kesihatan orang ramai yang pada kebiasaannya terdedah pada tahap kuasa EMF di bawah 4.0 mG.

### ABSTRACT

Data collection of the electromagnetic fields (EMF) produced by 33KV and 132KV power transmission lines were carried out in August 2003 at 3 different locations in Kuching Division, Sarawak, Malaysia. All readings were taken at a slope distance of 3.5m, 7m, 10m, 15m, 20m, 30m, and 40m, respectively from the power lines. The EMF values measured from the three locations of 33KV and 132KV lines were averaged to obtain the mean values of each distance from the power lines. For the 33KV power lines, it was found that the mean EMF values were 8,608 milliGauss (mG) at 3.5m away, 4,972mG (7m), 785.5mG (10m), 114.3mG (15m), 41.6mG (20m), 6.1mG (30m) and 0.2mG (40m). For the 132KV power lines, the mean EMF values were greater than 20,000 milliGauss (mG) at 3.5m, 10,1612mG (7m), 4,164mG (10m), 1,720mG (15m), 802mG (20m), 139mG(25m), 9mG (30m), and 0.9mG (40m). The normal standard height of both 33KV and 132 KV power lines are 12 m above ground level and an easement width of 20 m on both sides of the power lines, and human activities generally occur at a distance greater than 50m (slope distance) from the power lines. It was found that the EMF produced by both 33KV and 132KV power transmission lines do not pose adverse health effects on the public who are generally exposed to EMF levels below 4.0 mG.

**Keywords:** Kilovolts, electromagnetic fields, milliGaus

### INTRODUCTION

In Malaysia, the electric and magnetic field (EMF) issue has become an area of increasing public concern (Wertheimer and Leeper, 1979). Epidemiological and laboratory studies suggested that EMF may act as promoters of carcinogenesis, especially brain tumours and

leukaemia, while the epidemiological results remain inconsistent (Tomenius, 1986; Savitz *et al.*, 1989). There are a number of researches conducted on the effects of EMF on human population, animals and isolated cells (London *et al.*, 1991; Feychting and Ahlbom, 1992), and some of the scientific evidences have suggested that the EMF exposures pose any health risk is rather weak (Morgan, 1989; Portier and Wolfe, 1997). The strongest evidences for health effects in association with EMF exposures observed in human populations in the forms of cancer are childhood leukaemia and chronic lymphocytic leukaemia among occupationally exposed adults (Hatch *et al.*, 1998).

In some researches, they claimed that a long-term exposure to 16mG or greater EMF may cause miscarriage in humans (Belanger *et al.*, 1998). There is also an association found between the long-term EMF exposure to 4mG or above and the children leukaemia (Washburn *et al.*, 1994). For animals, when they are directly below the conductors, where the clearance is about 9 meters and the EMF level is more than 1.0 Gauss, it may promote increased growth and size of tumour. However, it is also claimed that EMF alone does not cause any tumours in animals (Tsurita *et al.*, 2000). A study claimed that a 500mG magnetic field exposure of rats treated with carcinogens may increase their incidence of breast cancer, but did not affect tumour growth in individual animals. Another study found that there was an increase in the DNA strand breaks in brain cells of rats when exposed to more than 1 Gauss of EMF (Lai and Singh, 1997).

#### METHODOLOGY

A total of three 33KV transmission lines at 3 different locations, Jalan Stampin (near SRJK Stampin), Jalan Tun Jugah (near Petronas Petrol Station) and at the junction of Jalan Tun Razak and Jalan Foochow Road No.1 (*Fig. 1*) were identified for this study. All the power transmission lines are located along the main roads and all the EMF readings were taken based on the slope distance of 3.5, 7, 10, 15, 20, 30, and 40 m from the 33KV power lines. The EMF readings were taken on 22 and 23 August 2002 during peak demand hours between 11:00 A.M and 1:00 P.M.

Similarly, three 132KV power transmission lines at 3 different locations within Kuching Division, namely Muara Tebas, Muara Tabuan and Mambong (*Fig. 2*). All the power transmission lines are located along the main roads and all the EMF readings were taken based on the slope distance of 3.5, 7, 10, 15, 20, 25, 30, and 40 m from the 132KV power lines. The EMF readings were taken on 26, 27 and 30 August 2002 during peak demand hours between 11:00 A.M. and 1:00 P.M.

The instrument used to collect the data is called Lutron EMF-827 Detector. Lutron EMF-827 Detector has wide measuring range with 3 ranges; 200 mG, equivalent to 20 microTesla ( $\mu\text{T}$ ), 2,000mG (200 $\mu\text{T}$ ), 20,000mG (2,000 $\mu\text{T}$ ). This EMF tester is a handheld instrument designed and calibrated to measure EMF radiation at different bandwidths down to 50Hz/60Hz. It has a separate probe serving as receiver to the main meter. The probe will detect the amplitude and frequency of EMF. Hence, depending on the amplitude of the electromagnetic field frequency within the range, the display unit on the main meter will then display the level of EMF detected by the probe.

Precautions were taken during the data collection to make sure that the readings from the display unit of the EMF tester were stable before recording. Even though the manufacturer of the instrument claims that the sampling time takes about 0.4 second, it is always wise to stay long on the sampling point to let the reading stabilize. In this study, only highest readings were recorded. It is worth noting that the EMF is not necessary



Fig. 1: Sampling locations for 33KV power transmission lines in Kuching City

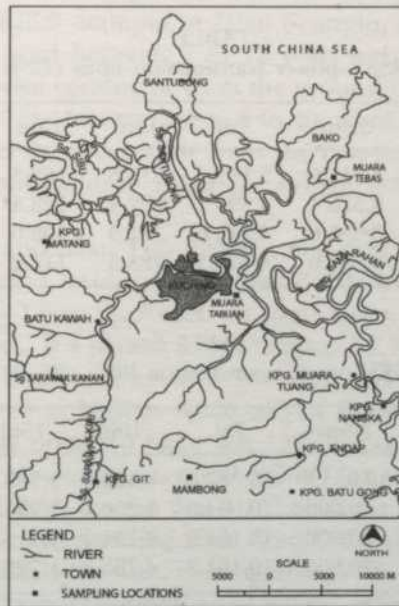


Fig. 2: Sampling locations for 132KV power transmission lines

stable at all times, generally due to fluctuations of the current levels in the conductors (related to power demand) at different times of the day. Sometimes, the EMF might drop significantly for a short while before rising back again to its normal level. Thus, about 5 to 10 minutes are needed at each sampling point.

### RESULTS AND DISCUSSIONS

The EMF readings for all the 33KV transmission lines were taken at 3 different locations, namely Jalan Stampin, Jalan Tun Jugah, and Jalan Tun Razak. All the power transmission lines are located along the main roads and all the EMF readings were taken based on the slope distances of 3.5, 7, 10, 15, 20, 30, and 40 m from the power lines. The EMF

readings for the 33KV for individual transmission lines taken on 22 and 23 August 2002 are shown in Table 1, whereas the plots of mean EMF levels versus slope distances are illustrated in Fig. 3.

The EMF Readings for all the 132KV transmission lines were taken at 3 different locations, namely Muara Tebas, Muara Tabuan, and Mambong. All the power transmission lines are located along the main roads and all the EMF readings were taken based on the slope distance of 3.5, 7, 10, 15, 20, 30, and 40 meters from the power lines. The EMF readings for the individual 132KV transmission lines taken on 26, 27 and 30 August 2002 are shown in Table 2, and plots of mean EMF levels versus slope distances are illustrated in Fig. 4.

The mean EMF readings obtained from the 33KV transmission lines along Jalan Stampin, Jalan Tun Jugah and Jalan Tun Razak were 8,608.6mG for a slope distance of 3.5m away from the power line, 4,972.7mG for the 7m, 783.5mG for the 10m, 114.2mG for the 15m, 41.6mG for the 20m, 6.1mG for 30m, and 0.2mG for the 40m. For the 33KV transmission lines investigated, it was noticed that all the power lines are located higher

TABLE 1  
EMF data for 33KV power transmission lines (22 & 23 Aug 2005)

Slope Distance (m)	3.5m	7m	10m	15m	20m	30m	40m
Jalan Stampin (mG)	8,812.6	5,113.4	816.6	108.3	42.9	6.9	0.3
Jalan Tun Jugah (mG)	8,526.4	4,894.1	772.4	128.4	41.6	6.2	0.2
Jalan Tun Razak (mG)	8,486.6	4,910.6	761.9	105.6	40.3	5.3	0.2
Mean (mG)	8,608.6	4,972.7	783.5	114.2	41.6	6.1	0.2

TABLE 2  
EMF data for 132KV power transmission lines (26, 27 & 30 Aug 2005)

Slope Distance (m)	3.5m	7m	10m	15m	20m	30m	40m
Muara Tebas, Kuching	19,961.8	10,287.6	4,140.9	1,708.2	801.4	8.9	1.5
Muara Tabuan, Kuching	>20,000	10,094.5	4,206.1	1,734.0	829.1	9.2	0.5
Mambong, Kuching	>20,000	10,101.6	4,144.4	1,718.9	776.0	8.7	0.7
Mean (mG)	>20,000	10,161.2	4,163.8	1,720.4	802.2	8.9	0.9

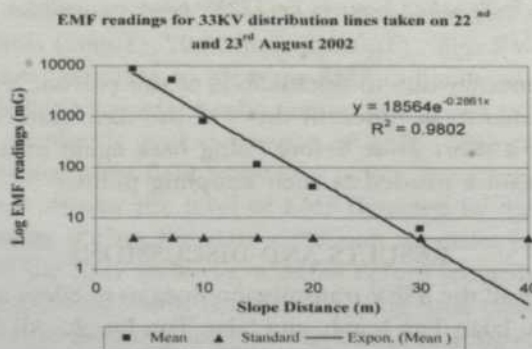


Fig. 3: Mean EMF vs. slope distance (33KV)

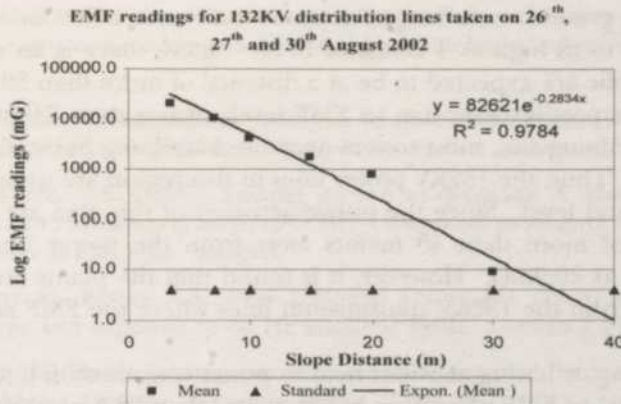


Fig. 4: Mean EMF vs slope distance (132 KV)

than the standard height of 8m above ground level. However, one of the towers is located inside the compound of SRJK© Stampin at Jalan Stampin, a primary school which has more than 1,000 students aged between 7 to 12 years old. Even though the tower is properly fenced and the lowest conductor from the ground level is more than 10 meters, the school children are likely to be exposed to 6 to 40mG of EMF. At the same location, the 33KV power lines are as far as 5m away from the overhead pedestrian road-crossing bridge. The public or school children using the bridge may be exposed to as high as 5,000mG of EMF.

Along Jalan Tun Jugah and Jalan Tun Razak, some stretches of the road levels is 1.5 to 2m higher than the ground levels on the roadside. Thus, the towers built alongside the roads are approximately 1.5 to 2m lower. At some spots, the power lines are actually less than 7m above road level. If a person with a height of 1.70m standing below the lines at those spots, the lines are approximately 5.3m above his head. This means that the individual may be exposed to as high as 6,000 mG of EMF.

The mean EMF readings obtained from the 132KV transmission lines along Muara Tebas, Muara Tabuan, and Mambong were >20,000mG for a slope distance of 3.5m away from the power line, 10,161.2mG for the 7m, 4,163.8mG for the 10m, 1,720.4mG for the 15m, 802.2mG for the 20m, 138.5mG for 25m, 8.9mG for the 30m, and 0.9mG for the 40m. For all the 132KV transmission lines investigated, it was noticed that the power lines are located well above the normal recommended height of 9m, i.e., the distance between the lowest conductor and the ground level. The minimum requirement of clearance for power lines that are not exceeding 132KV is 6.7 meters above the ground level. In Muara Tebas area, some of the towers located near to the commercial centres, schools and housing areas are found to have approximately 6.0 meters clearance distance from ground, and the nearest row of shops of 10.0 meters high are located approximately 9.0 meters from the power lines. As such, the 132KV power lines are approximately 4m to 5m above the head of a pedestrian crossing the power line zone. Generally, human activities occur at distances greater than 30m (slope distance) from the power lines, taking into consideration the easement width of 20 m on both sides of the power lines, the public staying outside the easement zone may be exposed to less than 8.9 mG EMF.

In Muara Tabuan area, it was found that the 132KV power transmission lines running near Sekolah Menengah Kerajaan Tabuan Laru could pose a potential adverse health impact to the public. At this zone, even though the power lines are generally more than

10.0 meters above ground, a student or anyone who stands below or nearby to the lines could be exposed to as high as 4 Gauss of EMF. Again, there is an easement width of 20 meters, the public are expected to be at a distance of more than 30 meters away from 132KV power lines possibly exposing to EMF levels of less than 8.9mG.

As for the Mambong site, most towers near the Mambong Substation are located on top of a small hill. Thus, the 132KV power lines in this region are usually more than 15.0 meters above ground level. Since the public activities of this area are found to occur at a slope distance of more than 40 meters away from the power lines, they could be exposed to as low as <0.9mG. However, it is found that the plants are usually less than 19.0 meters away from the 132KV transmission lines where the EMF could be as high as 1.0 Gauss.

The public living or having activities near to power transmission lines may be exposed to 16 mG and 4 mG of EMF when they are at or less than 28 meters and 35 meters away from the 132KV transmission lines, respectively. As the normal standard height of 132 KV transmission lines are usually 10 to 12 meters above ground levels, where the ground level EMF is about 4 Gauss or 4,000 mG, it is advised to avoid prolonged exposure underneath or near to those power lines especially the conceived women and children. A study found that there is a correlation between increased incidences of leukaemia among adults living within 50 meters of a high voltage power line [3]. Therefore, the public should minimize their outdoor activities near the 132KV power lines or to keep a slope distance of more than 50 meters.

### CONCLUSIONS

From the data gathered, it is found that one could be exposed to about 16mG of EMF at about 26 meters away from the 33KV transmission line; and 4mG of EMF at about 32 meters away. It is also concluded that an individual standing below 33KV transmission power lines at a slope distance of less than 7 meters could be exposed to the EMF higher than the permissible level of 4 mG.

From this study, it is demonstrated that one could be exposed to about 16mG at about 28 meters away from the 132KV power transmission lines; and exposed to 4mG of EMF at about 35 meters away. Since the safety clearance slope distance of 132KV and 33KV transmission lines are about 50 meters or more, it is concluded that the EMF of power transmission lines are unlikely to pose any adverse health effects to the public.

### REFERENCES

- BELANGER, K., LEADERER, B., KEENBRAND, K., HOLFORD, T., MCSHARRY, J.E., POWER, M.E. and BRANGEN, M. (1998). Spontaneous abortion and exposure to electric blankets and heated water beds. *Epidemiology*, 9, 36-42.
- HATCH, E.E., LINET, M.S., KLEINERMAN, R.A., TARONE, R.E., SEVERSON, R.K., HARTSOCK, C.T., HAINES, C., KAUNE, E.T., FREIDMAN, D., ROBISON, L.L. and WACHOLDER, S. (1998). Association between childhood acute lymphoblastic leukemia and use of electric appliances during pregnancy and childhood. *Epidemiology*, 9, 234-245.
- FEYCHTING, M. and AHLBOM, A. (1992). Magnetic fields and cancer in people residing near Swedish high voltage power lines (IMM Report 6/92). Stockholm, Sweden: Institute of Environmental Medicine (IMM), Karolinska Institute.
- LAI, H. and SINGH, N.P. (1997). Acute exposure to a 60Hz magnetic field increases DNA strand breaks in rat brain cells. *Bioelectromagnetics*, 18, 156-165.

- LONDON, S.J., THOMAS, D.C., BOWMAN, J.D., SOBEL, E., CHENG, T.C. and PETERS, J. (1991). Exposure to residential electric and magnetic fields and risk of childhood leukemia. *American J. Epidem.*, 134, 923-937.
- MORGAN, M.C. (1989). *Electric and Magnetic Fields from 60 Hertz Electric Power. What do We Know About Possible Health Risk?* Pittsburgh, P.A. USA: Cornegie-Mellon University.
- PORTIER, C.J. and WOLFE, M.S. (1997). Linking science to decisions: A strategy for electric and magnetic fields. In *Proceedings of the ICNIRP/WHO Symposium on Research Priorities for Evaluating Risks from Exposure to EM*, June. Bologna.
- SAVITZ, D.A., WACHTEL, H., BARNES, A.A., JOHN, E.M. and TURDIK, J.G. (1988). Case-control study of childhood cancer and exposure to 60 Hz magnetic fields. *American J. Epidem.*, 128, 21-38.
- TOMENIUS, L. (1986). 50 Hz electromagnetic field environments and the incidence of childhood tumors in Stockholm County. *Bioelectromagnetics*, 7, 191-207.
- TSURITA, G., NAGAWA, H., UENO, S., WATANABE, S. and TAKI, M. (2000). Biological and morphological effects on the brain after exposure of rats to a 1439 MHz TDMA field. *Bioelectromagnetics*, 21(5), 364-371.
- WASHBURN, E.P., ORZA, M.J., BERLIN, J.A., NICHOLSON, W.J., TODD, A.C., FRUNKIN, H. and CHALMERS, T.C. (1994). Residential proximity to electricity transmission and transmission equipment and risk of childhood leukaemia, childhood lymphoma, and childhood nervous system tumours: systematic review, evaluation, and meta-analysis. *Cancer Causes and Control*, 5, 299-309.
- WERTHEIMER, N. and LEEPER, E. (1979). Electrical wiring configurations and childhood cancer. *American J. Epidem.*, 109, 1273-1284.

## Anthraquinones and Xanthenes from *Cratoxylum glaucum* (Guttiferae)

\*G.C.L. Ee, A.S.M. Kua & M. Rahmani

Department of Chemistry, Faculty of Science,  
Universiti Putra Malaysia, 43400 UPM,  
Serdang, Selangor, Malaysia

Received: 27 February 2006

### ABSTRAK

Dalam pencarian berterusan untuk sebatian xanton dan kuinon daripada famili Guttiferae, kami telah membuat keputusan untuk meneliti genus *Cratoxylum*. Satu kajian kimia teliti ke atas *Cratoxylum glaucum* telah menghasilkan dua triterpenoid iaitu friedelin (1) dan stigmasterol (2) dua antraquinon 1,8-dihidroksi-3-metil-6-metoksiantraquinon (3) dan vismiaquinon (4) and satu xanton dimetilmangostin (5). Sebatian-sebatian ini telah dikenal pasti menggunakan Spektroskopi RMN 1D dan 2D. Ini adalah laporan pertama mengenai ciri kimia *Cratoxylum glaucum*.

### ABSTRACT

In a continuing search for xanthenes and quinones from the Guttiferae family, we decided to look at the genus *Cratoxylum*. A detailed chemical study on *Cratoxylum glaucum* has led to the isolation of two triterpenoids, friedelin(1) and stigmasterol (2), two anthraquinones 1,8-dihydroxy-6-methyl-3-methoxyanthraquinone (3) and vismiaquinone(4) and one xanthone dimethylmangostin(5). These compounds were identified using the 1D and 2D NMR spectroscopy. This is the first report done on the chemistry of *Cratoxylum glaucum*.

**Keywords:** *Cratoxylum glaucum*, Guttiferae, anthraquinones, xanthenes, triterpenoids

### INTRODUCTION

The genus *Cratoxylum* which consists of a total of six species is a small genus of South East Asian trees belonging to Guttiferae, which it is sometimes categorized under the family of Hypericaceae. The stem bark of *Cratoxylum* species is known to be used in traditional medicine (Bennet *et al.*, 1993). The wood of *Cratoxylum glaucum* is used for house and farm hut construction. Poles from moderately big trees are used as beams, joists, rafters and posts in the farm hut construction (Pearce *et al.*, 1987). The bark, roots and leaves are reported to be used in folk medicine to treat fevers, cough, diarrhoea, itches, ulcers and abdominal complaints (Lien *et al.*, 1998). There are not many reports on the chemistry of the *Cratoxylum* species. However, some phytochemical studies on this genus have revealed it to be rich in xanthenes, triterpenoids and tocotrienols (Iinuma *et al.*, 1996; Bennett *et al.*, 1993; Sia *et al.*, 1995; Nguyen *et al.*, 1998; Bennett and Lee, 1989). This paper describes the isolation and identification of anthraquinones and xanthenes from the not-so-common *Cratoxylum glaucum*.

\* Corresponding Author:  
E-mail: gwen@fsas.upm.edu.my

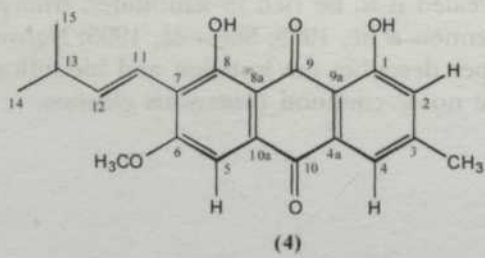
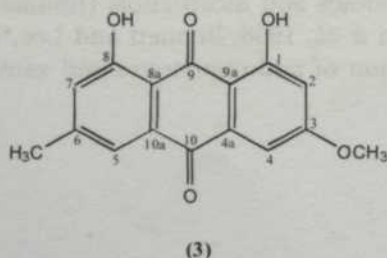
## MATERIALS AND METHOD

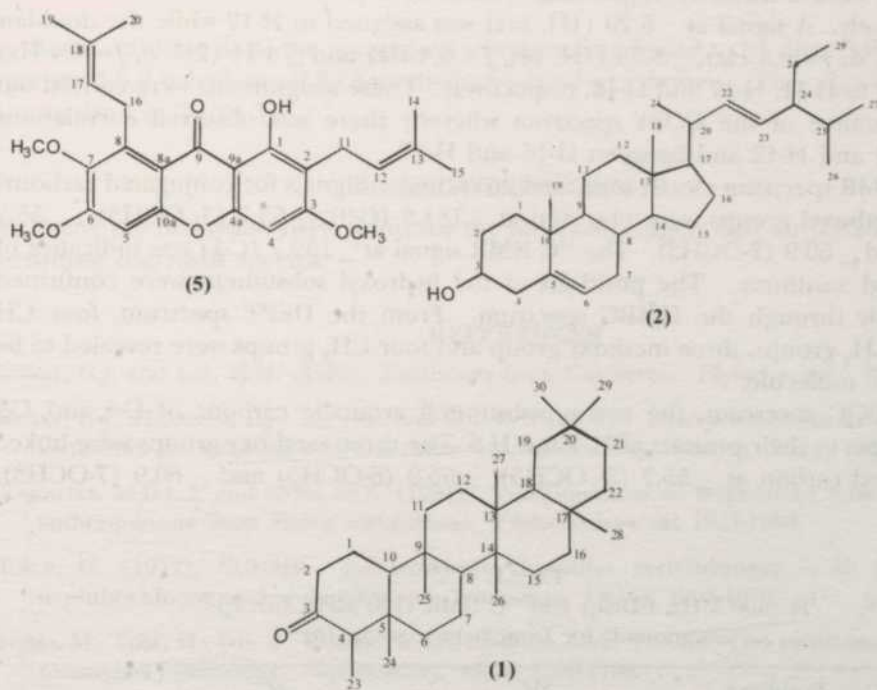
*Plant Material* – The stem bark of the *Cratoxylum glaucum* was collected from Sri Aman Sarawak, Malaysia. The plant materials were identified by Ms Runi Sylvester from the Herbarium of Sarawak Forestry Department, Kuching, Sarawak, Malaysia.

*General* – Infrared spectra were measured in KBr/NaCl pellet on a Perkin-Elmer FTIR Spectrum BX spectrometer. EIMS were recorded on a Shimadzu GCMS-QP5050A spectrometer. NMR spectra were obtained using a Unity INOVA 500MHz NMR/ JEOL 400MHz FT NMR spectrometer using tetramethylsilane (TMS) as the internal standard. Ultra violet spectra were recorded in  $\text{CHCl}_3$  on a Shimadzu UV-160A, UV-Visible Recording Spectrophotometer.

*Extraction and Isolation* – The air-dried and powdered stem bark of the *Cratoxylum glaucum* (1.0 kg) was extracted successively with hexane, chloroform, ethyl acetate and methanol at room temperature. The extracts were evaporated to dryness under a reduced pressure to yield 16.4 g of crude hexane extract, 15.3 g of crude chloroform extract, 16.8 g of crude ethyl acetate extract and 18.7 g of crude methanol extract. Each of the crude extracts was subjected to a series of column chromatography over silica gel columns using a stepwise gradient system (hexane/chloroform, chloroform/ethyl acetate and ethyl acetate/methanol). The elements were collected in a range volume of 50 to 250 ml, depending on the size of the columns used. The column chromatography of the hexane extract gave two terpenoids, friedelin (1) (20mg) and stigmasterol (2) (15 mg). The ethyl acetate extract yielded 1,8-dihydroxy-3-methyl-6-methoxyanthraquinone (3) (10 mg) while the chloroform extract gave vismiaquinone (4) (20 mg). The methanol extract gave 10 mg of dimethylmangostin (5).

1,8-Dihydroxy-3-methyl-6-methoxyanthraquinone (3): Orange crystals, m.p. 209-210 °C (Lit. 208-209 °C, Hofle, 1977). UV (EtOH)  $\lambda_{\text{max}}$  nm (log  $\epsilon$ ): 287 (0.73), 266 (0.75); IR  $\nu_{\text{max}}$   $\text{cm}^{-1}$  (KBr): 3418 (broad, OH), 2924 (C-H stretching), 1676 (C=O), 1622 (C=O), 1564 (C=C), 1480 ( $\text{CH}_2$  bending), 1316 ( $\text{CH}_3$  bending), 1158 (C-O); EI-MS m/z (rel. int.): 284 (100), 255 (18), 241 (16), 213 (12), 128 (18);  $^1\text{H}$  NMR (400 MHz,  $\text{CDCl}_3$ ):  $\delta$ 12.28 (1H, s, OH-1),  $\delta$ 12.05 (1H, s, OH-8),  $\delta$ 7.56 (1H, brs, H-7),  $\delta$ 7.29 (1H, d,  $J = 2.8$  Hz, H-4),  $\delta$ 7.05 (1H, brs, H-5),  $\delta$ 6.62 (1H, d,  $J = 2.8$  Hz, H-2),  $\delta$ 3.87 (1H, s,  $\text{OCH}_3$ ),  $\delta$ 2.38 (1H, s,  $\text{CH}_3$ );  $^{13}\text{C}$  NMR (100 MHz,  $\text{CDCl}_3$ ):  $\delta$ 190.7 (C-9),  $\delta$ 182.0 (C-10),  $\delta$ 166.6 (C-3),  $\delta$ 165.2 (C-1),  $\delta$ 162.5 (C-8),  $\delta$ 148.4 (C-6),  $\delta$ 135.2 (C-10a),  $\delta$ 133.2 (C-4a),  $\delta$ 124.5 (C-7),  $\delta$ 121.3 (C-5),  $\delta$ 110.2 (C-8a),  $\delta$ 113.5 (C-9a),  $\delta$ 108.2 (C-4),  $\delta$ 106.8 (C-2),  $\delta$ 56.1 ( $\text{OCH}_3$ ),  $\delta$ 22.2 ( $\text{CH}_3$ ).





Vismiaquinone (4): Dark reddish crystals, m.p. 201-203 °C (Lit. 202-204 °C, Gonçalves *et al.*, 1981). UV (EtOH)  $\lambda_{\max}$  nm (log  $\epsilon$ ): 294 (0.84), 263 (0.57). IR  $\nu_{\max}$   $\text{cm}^{-1}$  (KBr): 3440 (broad, OH), 2952 (C-H stretching), 1626 (C=O), 1560 (C=C), 1482 ( $\text{CH}_2$  bending), 1374 ( $\text{CH}_3$  bending), 1174 (C-O); EI-MS  $m/z$  (rel. int.): 352 [ $M^+$ , 48], 337 (20), 309 (100), 297 (31), 161 (11);  $^1\text{H}$  NMR (400 MHz,  $\text{CDCl}_3$ ):  $\delta$  12.86 (OH-1, s),  $\delta$  12.02 (OH-8, s),  $\delta$  7.52 (1H, s, H-4),  $\delta$  7.30 (1H, s, H-5),  $\delta$  7.05 (1H, s, H-2),  $\delta$  6.99 (1H, dd,  $J = 16.0$  Hz & 6.4 Hz, H-12),  $\delta$  6.61 (1H, dd,  $J = 16.0$  Hz, H-11),  $\delta$  3.99 (3H, s,  $\text{OCH}_3$ -6),  $\delta$  2.49 (1H, m, H-13),  $\delta$  2.40 (3H, s, H-3),  $\delta$  1.11 (6H, d,  $J = 6.5$  Hz, H-14 & H-15);  $^{13}\text{C}$  NMR (100 MHz,  $\text{CDCl}_3$ ):  $\delta$  191.2 (C-9),  $\delta$  181.7 (C-10),  $\delta$  162.9 (C-6),  $\delta$  162.4 (C-8),  $\delta$  162.0 (C-1),  $\delta$  148.4 (C-3),  $\delta$  146.7 (C-12),  $\delta$  133.1 (C-4a),  $\delta$  131.9 (C-10a),  $\delta$  124.3 (C-2),  $\delta$  121.0 (C-4),  $\delta$  119.9 (C-7),  $\delta$  115.7 (C-11),  $\delta$  113.6 (C-9a),  $\delta$  110.4 (C-8a),  $\delta$  103.3 (C-5),  $\delta$  56.26 (6-OMe),  $\delta$  33.4 (C-13),  $\delta$  22.4 (C-14 & C-15),  $\delta$  22.1 (3- $\text{CH}_3$ ).

## RESULTS AND DISCUSSIONS

Dimethylmangostin (5) was isolated as pale yellow crystals with a melting point of 111-113 °C (Lit. 110-106 °C, Yates *et al.*, 1958). It has a molecular formula of  $\text{C}_{26}\text{H}_{30}\text{O}_6$  as established by EI mass spectrometry ( $m/z$  438 [ $M^+$ ]). A positive test with alcoholic  $\text{FeCl}_3$  revealed its phenolic nature. The UV spectrum exhibited the characteristic absorption bands of a xanthone at 312.0, 294.0 and 247.0 nm. The IR spectrum also indicated the presence of the chelated hydroxyl and conjugated carbonyl group characteristic of a xanthone at 3446 and 1600  $\text{cm}^{-1}$ .

The  $^1\text{H}$  NMR spectra showed the presence of a low field chelated hydroxyl group at  $\delta$  13.46 (OH-1) which is attached to C-1. Two aromatic proton singlets observed at  $\delta$

6.27 and  $\delta$  6.69 were assigned to H-4 and H-5, respectively. Meanwhile, three methoxy groups which show a three hydrogen singlet each were present at  $\delta$  3.87,  $\delta$  3.93 and  $\delta$  3.77, respectively. A signal at  $\delta$  5.20 (1H, brs) was assigned to H-12 while the doublets at  $\delta$  3.32 (2H, d,  $J = 6.4$  Hz),  $\delta$  5.23 (1H, brt,  $J = 6.4$  Hz) and  $\delta$  4.11 (2H, d,  $J = 6.4$  Hz) were assigned to H-11, H-17 and H-16, respectively. These assignments were carried out with the assistance of the COSY spectrum whereby there was observed correlations between H-11 and H-12 and between H-16 and H-17.

The  $^{13}\text{C}$  NMR spectrum clearly indicated 26 carbons. Signals for conjugated carbonyl and three methoxyl groups were observed at  $\delta$  181.9 (C-9),  $\delta$  55.7 (3-OCH<sub>3</sub>),  $\delta$  55.9 (6-OCH<sub>3</sub>) and  $\delta$  60.9 (7-OCH<sub>3</sub>). The  $^{13}\text{C}$  NMR signal at  $\delta$  159.7 (C-1) was indicative of an oxygenated xanthone. The positions of the hydroxyl substituent were confirmed unambiguously through the HMBC spectrum. From the DEPT spectrum, four CH groups, two CH<sub>2</sub> groups, three methoxy group and four CH<sub>3</sub> groups were revealed to be present in the molecule.

In the HSQC spectrum, the two unsubstituted aromatic carbons of C-4 and C-5 showed linkages to their protons of H-4 and H-5. The three methoxy groups were linked to the assigned carbon at  $\delta$  55.7 (3-OCH<sub>3</sub>),  $\delta$  55.9 (6-OCH<sub>3</sub>) and  $\delta$  60.9 (7-OCH<sub>3</sub>).

TABLE 1  
 $^1\text{H}$  (400 MHz, CDCl<sub>3</sub>) and  $^{13}\text{C}$  NMR (100 MHz, CDCl<sub>3</sub>)  
assignments for Dimethylmangostin (5)

Position	$\delta\text{H}$	$\delta\text{C}$
1	13.46 (1H, s)	159.7
2		111.4
3		163.3
4	6.27 (1H,s)	88.6
4a		155.2
5	6.69 (1H, s)	98.1
6		157.9
7		143.9
8		137.2
8a		112.0
9		181.9
9a		103.9
10a		155.1
11	3.32 (2H, d, $J=6.4$ Hz)	21.3
12	5.20 (1H, brs)	122.3
13		131.6
14	1.83 (3H, s)	17.8
15	1.78 (3H, s)	25.8
16	4.11 (2H, d, $J = 6.4$ Hz)	26.1
17	5.23 (1H, brt, $J=6.4\text{Hz}$ )	123.2
18		131.7
19	1.66 (6H, s)	18.2
20	1.66 (6H, s)	25.9
3-OCH <sub>3</sub>	3.87 (3H, s)	55.7
6-OCH <sub>3</sub>	3.93 (3H, s)	55.9
7-OCH <sub>3</sub>	3.77 (3H, s)	60.9

From the HMBC experiment, the chelated hydroxyl functional of OH-1 group gave linkages to the carbons of C-1, C-2 and C-9a, thus supporting the location of the OH at C-1.

Based on these data, the compound was therefore found to be dimethylmangostin, 1-hydroxy-3,6,7-trihydroxy-2,8-(3-methylbut-2-enyl)-xanthone. The spectral data are summarized in Table 1.

#### ACKNOWLEDGEMENTS

We thank the Malaysian IRPA grant for the financial support and Mr Johadi Iskander for recording the NMR spectra.

#### REFERENCES

- BENNET, G.J. and LEE, H.H. (1989). Xanthenes from Guttiferae. *Phytochemistry*, 28(4), 967-998.
- BENNET, G.J., HARRISON, L.J., SIA, G-L. and SIM, K-Y. (1993). Triterpenoids, tocotrienols and xanthenes from the bark of *Cratoxylum cochinchinense*. *Phytochemistry*, 32(5), 1245-1251.
- GONCALVES, M.D.L.S. and MORS, M.B. (1981). Vismiaquinone an isopentenyl substituted anthraquinone from *Vismia reichardtiana*. *Phytochemistry*, 20, 1947-1950.
- HOFLE, G. (1977). <sup>13</sup>CNMR spektroskopie chinoider verbindungen - II: Substitute 1,4-naphthochinone and anthrachinone. *Tetrahedron*, 33(15), 1963-1970.
- IINUMA, M., TOSA, H., ITO, T., TANAKA, T. and MADULID, D.A. (1996). Two xanthenes from roots of *Cratoxylum formosanum*. *Phytochemistry*, 43(4), 1195-1198.
- LIEN, H.D.N. and HARRISON, L.J. (1998). Triterpenoid and xanthone constituents of *Cratoxylum cochinchinense*. *Phytochemistry*, 50, 471-476.
- NGUYEN, L.H.D. and HARRISON, L.J. (1998). Triterpenoid and xanthenes constituents of *Cratoxylum cochinchinense*. *Phytochemistry*, 50, 471-476.
- PEARCE, K.G., AMEN, V.L. and JOK, S. (1987). An ethnobotanical study of an iban community of the Pantu sub-district, Sri Aman, Division 2, Sarawak. *The Sarawak Museum Journal*, XXXVII (58), 193-270.
- SIA, G.L., BENNETT, G.J., HARRISON, L.J. and SIM, K.Y. (1995). Minor xanthenes from the bark of *Cratoxylum cochinchinense*. *Phytochemistry*, 38(6), 1521-1528.
- YATES, P. and STOUT, G.H. (1958). The structure of mangostin. *Journal of American Chemical Society*, 80(7), 1691-1700.

## Determining the Optimum Process Mean Based on Manufacturing Cost and Quality Loss

Chung-Ho Chen

*Department of Industrial Management  
Southern Taiwan University of Technology  
1 Nan-Tai Street, Yung-Kang City  
Tainan 710, Taiwan  
Republic of China*

Received: 12 January 2005

### ABSTRAK

Wen dan Mergen (1999) mengemukakan satu kaedah untuk menentukan min proses optimum berdasarkan pengimbangan kos untuk tidak menemukan had spesifikasi atas dan bawah. Walau bagaimanapun, mereka tidak mengambil kira kehilangan kualiti sesuatu produk yang ada di dalam spesifikasi model. Dalam kertas ini, dicadangkan model Wen dan Mergen (1999) yang telah diubah suai untuk menentukan min proses optimum mengandungi kos pembuatan dan kehilangan kualiti. Fungsi kehilangan kualiti kuadratik dan linear digunakan dalam mengukur kehilangan kualiti produk. Kos pembuatan dianggap berkadar negatif dan linear kepada lencongan daripada nilai sasaran apabila ciri kualiti adalah di dalam spesifikasi dan kos pembuatan malar berlaku apabila ciri kualiti melebihi spesifikasi.

### ABSTRACT

Wen and Mergen (1999) presented a method for determining the optimum process mean based on balancing the cost of not meeting upper and lower specification limits. However, they have not considered the quality loss for a product which is within specifications in the model. In this paper, we propose the modified Wen and Mergen's (1999) model for determining the optimum process mean consisting of manufacturing cost and quality loss. The quadratic and linear quality loss functions are used in measuring the quality loss of product. The manufacturing cost is assumed to be negatively and linearly proportional to deviation from the target value when the quality characteristic is within specifications and constant manufacturing cost happens when the quality characteristic exceeds specifications.

**Keywords:** Process control, process mean, quality loss function, specification limits, manufacturing cost

### INTRODUCTION

Traditionally, the step quality loss function is used for deciding if the product is a conformance. If the quality characteristic of product is within specifications, then the product can be accepted and there is no quality loss. In 1986, Taguchi redefined that the product quality is the total losses to society, see Taguchi (1986). Hence, he proposed the quadratic quality loss function for reducing the expected losses. The advantage of the quadratic quality loss function is that we can evaluate losses in term of process mean and process standard deviation. However, the regular quadratic loss function is patently inappropriate in some situations. Trietsch (1999, p. 69) remarked that One such case occurs when the expected cost of exceeding the tolerance limits is not equal to the right and to the left of the target. Missing by cutting too much, for instance, may imply scrap,

while cutting too little only causes rework. When this is the case one possible response is fitting a loss function that is not symmetric and not necessarily quadratic. In some cases, a linear quality loss function is more appropriate in many industrial applications than that of quadratic quality loss function.

The optimum process mean setting has been a major topic of statistical process control. The selection of optimum process mean will directly affect the process defective rate, manufacturing cost, scrap cost, rework cost, and the cost of use. There are considerable attentions paid to the study of economic selection of process mean. The asymmetric quadratic quality loss function and asymmetric linear quality loss function are usually used in the related problems, e.g. Wu and Tang (1998), Li (1997, 1998, 2000, 2002a, 2002b), Li and Chirng (1999), Li and Cherng (2000), Maghsoodloo and Li (2000), Phillips and Cho (2000), Li and Chou (2001), and Li and Wu (2001,2002), etc.

Wen and Mergen (1999) presented a method for determining the optimum process mean based on balancing the cost of not meeting upper and lower specification limits. However, they have neglected to consider the quality loss for a product which is within specifications in the model. In this paper, we propose the modified Wen and Mergen's (1999) model for determining the optimum process mean consisting of manufacturing cost and quality loss. The quadratic and linear quality loss functions are used in measuring the quality loss of product. In order to reduce the expected quality losses of product, we have to reduce the bias (the deviation from the target value to process mean) and the standard deviation of the process. However, we usually face the manufacturing cost increases, e. g., inputting the high class of material, the advanced technology of machine and the high technology of people, when the quality improves. The manufacturing cost is assumed to be negatively and linearly proportional to deviation from the target value when the quality characteristic is within specifications and constant manufacturing cost happens when the quality characteristic exceeds specifications. The normal quality characteristic is considered in the modified model and a numerical example is provided for illustration.

## QUALITY LOSS FUNCTION

### *Quadratic Quality Loss Function*

Assume that  $X$  represents the nominal-is-best type quality characteristic. For such quality characteristic, we have a nominal value or target value, and on each side of this value the performance of the product deteriorates as we move from the target value. For such characteristic, engineers generally have the lower and the upper specification limits. We can use the quality loss coefficients  $k_1$  and  $k_2$  to represent the left and right directions of deviation from the target value  $T$ . If tolerances for both sides are  $D_L$  and  $D_U$ , the quality losses at the specification limits are defined as  $D_L$  and  $D_U$ , respectively. The asymmetric quadratic quality loss function is defined, see Taguchi (1986) as

$$L(X) = \begin{cases} D_L, & X < T_L \\ k_1(T-X)^2, & T_L \\ K_2(X-T)^2, & T < X \leq T_U \\ D_U, & X > T_U \end{cases} \quad (1)$$

where

$T_U$  the upper specification limit

$T_L$  the lower specification limit

$$k_1 = \frac{D_L}{\Delta_1^2}$$

$$k_2 = \frac{D_U}{\Delta_2^2}$$

If  $D_L = D_U$  and  $\Delta_1 = \Delta_2$ , Equation (1) is called symmetric quadratic quality loss function.

*Linear Quality Loss Function*

Under the same hypothesis as in subsection 2.1, the asymmetric linear quality loss function is defined, see Trietsch (1999) as

$$L(X) = \begin{cases} D_L, & X < T_L \\ k_1(T - X), & T_L \leq X < T \\ k_2(X - T), & T < X \leq T_U \\ D_U, & X > T_U \end{cases} \quad (2)$$

where

$$k_1 = \frac{D_L}{\Delta_1}$$

$$k_2 = \frac{D_U}{\Delta_2}$$

Again if  $D_L = D_U$  and  $\Delta_1 = \Delta_2$ , Equation (2) is called symmetric linear quality loss function.

**MANUFACTURING COST**

For the nominal-is-best type product, the nominal value of quality characteristic is a constant. It is called design target. If the output value of quality characteristic is the design target, then the product has the highest evaluation. We usually need to adopt the advanced technology of manufacturing, machine, people and material to achieve the highest class output. That is, we usually face the manufacturing cost increases when the quality improves. Assume that the manufacturing cost is negatively and linearly proportional to deviation from the target value when the quality characteristic is within specifications and constant manufacturing cost happens when the quality characteristic exceeds specifications. Then we define the manufacturing cost function for the nominal-is-best type product as

$$M(X) = \begin{cases} a, & X < T_L \\ a + b \frac{X - T_L}{T - T_L}, & T_L \leq X < T \\ a + b \frac{T_U - X}{T_U - T}, & T \leq X \leq T_U \\ a, & X > T_U \end{cases} \quad (3)$$

where

- $a$  the constant manufacturing cost
- $b$  the variable manufacturing cost coefficient per unit.

### WEN AND MERGEN'S COST MODEL

There are three assumptions in Wen and Mergen's (1999) model: (1) the quality characteristic, say  $X$ , is normally distributed with unknown mean  $\mu$  and known variance  $\sigma^2$ , or estimated in advance; (2)  $X$  is nominal-is-best type; (3) the target value, say  $T$ , is the middle value of the specifications, i.e.,  $T = (T_U + T_L)/2$ .

According to Wen and Mergen (1999, p. 508), if  $f$  represents the probability density function of  $X$  and  $\Phi$  is the distribution function of standard normal distribution, the total loss per item is

$$\begin{aligned} C_T &= D_U \int_{T_U}^{\infty} f(x) dx + D_L \int_{-\infty}^{T_L} f(x) dx \\ &= D_U \left[ 1 - \Phi \left( \frac{T_U - \mu}{\sigma} \right) \right] + D_L \Phi \left( \frac{T_L - \mu}{\sigma} \right) \end{aligned} \quad (4)$$

$C_T$  in Equation (4) is a function of  $\mu$ . In order to minimize  $C_T$ , Wen and Mergen (1999) consider the first and second derivative of Equation (4) with respect to  $\mu$ . Due to the fact that the second derivative is positive for all  $\mu$ , Wen and Mergen (1999) set the first derivative equal to zero and found the following optimal value of  $\mu$ , say  $\mu^*$  that minimized the total loss per item:

$$\mu^* = T + \frac{\sigma^2}{T_U - T_L} \ln \frac{D_L}{D_U} \quad (5)$$

### MODIFIED WEN AND MERGEN'S COST MODEL

*With Manufacturing Cost and Quadratic Quality Loss Function*

Assume that the normal quality characteristic  $X$  has unknown mean  $\mu$  and known variance  $\sigma^2$ , or estimated in advance. If  $\Phi$  and  $\phi$  represent the distribution function and the probability density function of standard normal distribution, the objective is to minimize the following total losses to society per item consisting of the producer's manufacturing cost and the customer's quadratic quality loss:

$$\begin{aligned}
 C_{T_1} &= D_U \left[ 1 - \Phi \left( \frac{T_U - \mu}{\sigma} \right) \right] + D_L \Phi \left( \frac{T_L - \mu}{\sigma} \right) + k_1 \left\{ \left[ \left( \sigma^2 + \mu^2 \right) \Phi \left( \frac{T - \mu}{\sigma} \right) - \sigma (T + \mu) \phi \left( \frac{T - \mu}{\sigma} \right) \right. \right. \\
 &\quad \left. \left. - \left( \sigma^2 + \mu^2 \right) \Phi \left( \frac{T_L - \mu}{\sigma} \right) + \sigma (T_L + \mu) \phi \left( \frac{T_L - \mu}{\sigma} \right) \right] - 2T \left[ -\sigma \phi \left( \frac{T - \mu}{\sigma} \right) + \mu \Phi \left( \frac{T - \mu}{\sigma} \right) \right. \right. \\
 &\quad \left. \left. + \sigma \phi \left( \frac{T_L - \mu}{\sigma} \right) - \mu \Phi \left( \frac{T_L - \mu}{\sigma} \right) \right] + T^2 \left[ \Phi \left( \frac{T - \mu}{\sigma} \right) - \Phi \left( \frac{T_L - \mu}{\sigma} \right) \right] \right\} \\
 &\quad + k_2 \left\{ \left[ \left( \sigma^2 + \mu^2 \right) \Phi \left( \frac{T_U - \mu}{\sigma} \right) - \sigma (T_U + \mu) \phi \left( \frac{T_U - \mu}{\sigma} \right) \right. \right. \\
 &\quad \left. \left. - \left( \sigma^2 + \mu^2 \right) \Phi \left( \frac{T - \mu}{\sigma} \right) + \sigma (T + \mu) \phi \left( \frac{T - \mu}{\sigma} \right) \right] - 2T \left[ -\sigma \phi \left( \frac{T_U - \mu}{\sigma} \right) + \mu \Phi \left( \frac{T_U - \mu}{\sigma} \right) \right. \right. \\
 &\quad \left. \left. + \sigma \phi \left( \frac{T - \mu}{\sigma} \right) - \mu \Phi \left( \frac{T - \mu}{\sigma} \right) \right] + T^2 \left[ \Phi \left( \frac{T_U - \mu}{\sigma} \right) - \Phi \left( \frac{T - \mu}{\sigma} \right) \right] \right\} \\
 &\quad + a \left[ \Phi \left( \frac{T_L - \mu}{\sigma} \right) + 1 - \Phi \left( \frac{T_U - \mu}{\sigma} \right) \right] + \left( a - b \frac{T_L}{T - T_L} \right) \left[ \Phi \left( \frac{T - \mu}{\sigma} \right) - \Phi \left( \frac{T_L - \mu}{\sigma} \right) \right] \\
 &\quad + \frac{b}{T - T_L} \left[ \mu \Phi \left( \frac{T - \mu}{\sigma} \right) - \mu \Phi \left( \frac{T_L - \mu}{\sigma} \right) - \sigma \phi \left( \frac{T - \mu}{\sigma} \right) + \sigma \phi \left( \frac{T_L - \mu}{\sigma} \right) \right] + \\
 &\quad \left( a + b \frac{T_U}{T_U - T} \right) \left[ \Phi \left( \frac{T_U - \mu}{\sigma} \right) - \Phi \left( \frac{T - \mu}{\sigma} \right) \right] - \frac{b}{T_U - T} \left[ \mu \Phi \left( \frac{T_U - \mu}{\sigma} \right) - \right. \\
 &\quad \left. \mu \Phi \left( \frac{T - \mu}{\sigma} \right) - \sigma \phi \left( \frac{T_U - \mu}{\sigma} \right) + \sigma \phi \left( \frac{T - \mu}{\sigma} \right) \right] \tag{6}
 \end{aligned}$$

The detail derivation of Equation (6) is shown in Appendix A. It is difficult to show a closed-form solution for Equation (6) because the total losses to society per item,  $C_{T_1}$ , includes  $\phi$  and  $\Phi$ . For the given parameters  $k_1$ ,  $k_2$ ,  $T$ ,  $T_L$ ,  $T_U$ ,  $\sigma$ ,  $a$ ,  $b$ ,  $D_U$ , and  $D_L$ , the optimum process mean  $\mu^*$  for Equation (6) can be obtained by using the direct search method. One can set  $\mu$  values from  $T_L - 2$ , through  $T_U + 2$ , in step 0.0001 for example, in order to search the minimum  $C_{T_1}$ .

*With Manufacturing Cost and Linear Quality Loss Function*

Using the same assumption as 5.1, here the objective is to minimize the following total losses to society per item consisting of the producer's manufacturing cost and the customer's linear quality loss,

$$\begin{aligned}
 C_{T_2} &= D_U \left[ 1 - \Phi \left( \frac{T_U - \mu}{\sigma} \right) \right] + D_L \Phi \left( \frac{T_L - \mu}{\sigma} \right) + k_1 T \left[ \Phi \left( \frac{T - \mu}{\sigma} \right) - \Phi \left( \frac{T_L - \mu}{\sigma} \right) \right]
 \end{aligned}$$

$$\begin{aligned}
 & -k_1 \left[ -\sigma \phi \left( \frac{T-\mu}{\sigma} \right) + \mu \Phi \left( \frac{T-\mu}{\sigma} \right) \right] + \sigma \phi \left( \frac{T_L-\mu}{\sigma} \right) - \mu \Phi \left( \frac{T_L-\mu}{\sigma} \right) \\
 & -k_2 T \left[ \Phi \left( \frac{T_U-\mu}{\sigma} \right) - \Phi \left( \frac{T-\mu}{\sigma} \right) \right] + k_2 \left[ -\sigma \phi \left( \frac{T_U-\mu}{\sigma} \right) + \mu \Phi \left( \frac{T_U-\mu}{\sigma} \right) \right] \\
 & + \sigma \phi \left( \frac{T-\mu}{\sigma} \right) - \mu \Phi \left( \frac{T-\mu}{\sigma} \right) \\
 & + a \left[ \Phi \left( \frac{T_L-\mu}{\sigma} \right) + 1 - \Phi \left( \frac{T_U-\mu}{\sigma} \right) \right] + \left( a - b \frac{T_L}{T-T_L} \right) \left[ \Phi \left( \frac{T-\mu}{\sigma} \right) - \Phi \left( \frac{T_L-\mu}{\sigma} \right) \right] \\
 & + \frac{b}{T-T_L} \left[ \mu \Phi \left( \frac{T-\mu}{\sigma} \right) - \mu \Phi \left( \frac{T_L-\mu}{\sigma} \right) - \sigma \phi \left( \frac{T-\mu}{\sigma} \right) + \sigma \phi \left( \frac{T_L-\mu}{\sigma} \right) \right] + \\
 & \left( a + b \frac{T_U}{T_U-T} \right) \left[ \Phi \left( \frac{T_U-\mu}{\sigma} \right) - \Phi \left( \frac{T-\mu}{\sigma} \right) \right] - \frac{b}{T_U-T} \left[ \mu \Phi \left( \frac{T_U-\mu}{\sigma} \right) - \mu \Phi \left( \frac{T-\mu}{\sigma} \right) - \right. \\
 & \left. \sigma \phi \left( \frac{T_U-\mu}{\sigma} \right) + \sigma \phi \left( \frac{T-\mu}{\sigma} \right) \right]
 \end{aligned}$$

The detail derivation of Equation (7) is shown in Appendix B. The optimum process mean  $\mu^*$  for Equation (7) can be obtained by using the same manner as in the previous subsection.

### NUMERICAL EXAMPLE

A production line which is manufacturing ball bearings in a factory, the grinding process creases the bore of the inner ring. The specifications of the bore diameter are 8 and 12 mm. Suppose that in this process, when the bore diameter is greater than 12 mm, the inner rings would be waste, and when the bore diameter is less than 8 mm, the inner rings could be recycled. The loss per waste inner ring is \$25; the loss per recycled inner ring is \$18. The inner ring bore diameter follows a normal distribution and the standard deviation of the process is estimated as  $\sigma = 0.5$ . The target value of inner ring  $T = 9.5$  mm.

The constant manufacturing cost per item  $a = 5$  and the variable manufacturing cost coefficient per item  $b = 9$ . The manufacturing cost is negatively and linearly proportional to deviation from the target value when the quality characteristic is within specifications and constant manufacturing cost happens when the quality characteristic exceeds specifications. The objective is to find an optimal process mean that it will be at the optimum level possible, while the same time minimizing the manufacturing cost and quality loss.

#### *With Manufacturing Cost and Quadratic Quality Loss Function*

The quality loss coefficient  $k_1$  to represent the left direction of deviation from the target value  $T$  is  $k_1 = \frac{18}{(1.5)^2}$ . The quality loss coefficient  $k_2$  for representing the right direction

of deviation from the target value  $T$  is  $k_2 = \frac{25}{(2.5)^2} = 4$ . By solving Equation (6), the

optimum process mean for the nominal-is-best type normal quality characteristic is  $\mu^* = 9.5972$  with the optimum total losses to society per item  $C_{T_1}^* = 13.5643$ .

*With Manufacturing Cost and Linear Quality Loss Function*

The quality loss coefficient  $k_1$  for representing the left direction of deviation from the target value  $T$  is  $k_1 = \frac{18}{1.5} = 12$ . The quality loss coefficient  $k_2$  for representing the right

direction of deviation from the target value  $T$  is  $k_2 = \frac{25}{2.5} = 10$ . By solving Equation (7),

the optimum process mean for the nominal-is-best type normal quality characteristic is  $m^* = 9.9844$  with the optimum total losses to society per item  $C_{T_2}^* = 14.3005$ .

From the above numerical example, we have the following results:

1. The large  $k_1$  and  $k_2$  values have large total losses to society per item. That is because the large quality loss coefficients  $k_1$  and  $k_2$  values usually show the large quality cost within specifications. Hence, the larger  $k_1$  and  $k_2$  values, the larger total losses to society per item will be.
2. The linear quality loss function of modified model has larger total losses to society per item than that of quadratic quality loss of modified model. The former shows larger quality loss within specifications than that of the latter. We need to consider which quality loss function should be adopted for measuring the product quality within specifications.
3. The large total losses to society per item represent the large opportunity cost to the society. The optimum process mean setting is an approach for improving product. For the long-term, we need to improve the production process to obtain the optimum output value of product. One needs to address Taguchi's (1986) parameter design method of off-line quality control, adopt statistical process control method and apply the advanced manufacturing technology to reduce the total losses to society.

**CONCLUSIONS**

The mathematical models for determining the optimum process mean of modified Wen and Mergen's (1999) model have been proposed in this article. The process target value may be different from the design target value because the optimum value setting of the former is based on minimizing the total loss to society per item consisting of the producer's manufacturing cost and the customer's quality loss. Further direction of study should address the modified model with manufacturing cost and quality loss for a one-sided specification limit product.

**REFERENCES**

Li, M.-H.C. (1997). Optimal setting of the process mean for asymmetrical quadratic quality loss function. In *Proceedings of the Chinese Institute of Industrial Engineers Conference* (p. 415-419).

Li, M.-H.C. (1998). Optimal setting of the process mean for an asymmetrical truncated loss function. In *Proceedings of the Chinese Institute of Industrial Engineers Conference* (p. 532-537).

- LI, M.-H.C. (2000). Quality loss function based manufacturing process setting models for unbalanced tolerance design. *International Journal of Advanced Manufacturing Technology*, 16, 39-45.
- LI, M.-H.C. (2002a). Unbalanced tolerance design and manufacturing setting with asymmetrical linear loss function. *International Journal of Advanced Manufacturing Technology*, 20, 334-340.
- LI, M.-H.C. (2002b). Optimal process setting for unbalanced tolerance design with linear loss function. *Journal of the Chinese Institute of Industrial Engineers*, 19, 17-22.
- LI, M.-H.C. and CHERNG, H.-S. (2000). Unbalanced tolerance design with asymmetric truncated linear loss function. In *The 14th Asia Quality Symposium* (p. 162-165).
- LI, M.-H.C. and CHIRNG, H.-S. (1999). Optimal setting of the process mean for asymmetrical linear quality loss function. In *1999 Conference on Technology and Applications of Quality Management for Twenty-first Century* (p. 2-6-2-11).
- LI, M.-H.C. and CHOU, C.-Y. (2001). Target selection for an indirectly measurable quality characteristic in unbalanced tolerance design. *International Journal of Advanced Manufacturing Technology*, 17, 516-522.
- LI, M.-H.C. and WU, F.-W. (2001). A general model of unbalanced tolerance design and manufacturing setting with asymmetric quadratic loss function. In *Proceedings of Conference of the Chinese Society for Quality* (p. 403-409).
- LI, M.-H.C. and WU, F.-W. (2002). A general model of manufacturing setting with asymmetric linear loss function. In *The 38th Annual Conference of Chinese Society for Quality and The 6th National Quality Management Symposium* (p. 1137-1143).
- MAGHSOOLBLOO, S. and LI, M.-H.C. (2000). Optimal asymmetrical tolerance design. *IIE Transactions*, 32, 1127-1137.
- PHILLIPS, M.D. and CHO, B.-R. (2000). A nonlinear model for determining the most economic process mean under a beta distribution. *International Journal of Reliability, Quality and Safety Engineering*, 7, 61-74.
- TAGUCHI, G. (1986). *Introduction to Quality Engineering*. Tokyo, Japan: Asian Productivity Organization.
- TRIETSCH, D. (1999). *Statistical Quality Control-A Loss Minimization Approach*. Singapore: World Scientific Publishing Co.
- WEN, D. and MERGEN, A.E. (1999). Running a process with poor capability. *Quality Engineering*, 11, 505-509.
- WU, C.C. and TANG, G.R. (1998). Tolerance design for products with asymmetric quality losses. *International Journal of Production Research*, 39, 2529-2541.

**Appendix A: The Detail Derivation of Equation (6)**

$$\begin{aligned}
 C_{T_1} &= D_L \int_{-\infty}^{T_U} f(x) dx + \int_{T_L}^T k_1(T-x)^2 f(x) dx + \int_T^{T_U} k_2(x-T)^2 f(x) dx + \\
 &D_U \int_{T_U}^{\infty} f(x) dx + a \int_{-\infty}^{T_U} f(x) dx + \int_{T_L}^T \left[ a + b \frac{x-T_L}{T-T_L} \right] f(x) dx + \\
 &\int_T^{T_U} \left[ a + b \frac{T_U-x}{T_U-T} \right] f(x) dx + a \int_{T_U}^{\infty} f(x) dx
 \end{aligned} \tag{A1}$$

We have

$$\begin{aligned}
 &\int_{T_L}^T k_1(T-x)^2 f(x) dx \\
 &= k_1 \left\{ \left[ (\sigma^2 + \mu^2) \Phi\left(\frac{T-\mu}{\sigma}\right) - \sigma(T+\mu)\phi\left(\frac{T-\mu}{\sigma}\right) - (\sigma^2 + \mu^2) \Phi\left(\frac{T_L-\mu}{\sigma}\right) + \right. \right. \\
 &\left. \left. \sigma(T_L+\mu)\phi\left(\frac{T_L-\mu}{\sigma}\right) \right] - 2T \left[ -\sigma\phi\left(\frac{T-\mu}{\sigma}\right) + \mu\Phi\left(\frac{T-\mu}{\sigma}\right) + \sigma\phi\left(\frac{T_L-\mu}{\sigma}\right) - \right. \right. \\
 &\left. \left. \mu\Phi\left(\frac{T_L-\mu}{\sigma}\right) \right] + T^2 \left[ \Phi\left(\frac{T-\mu}{\sigma}\right) - \Phi\left(\frac{T_L-\mu}{\sigma}\right) \right] \right\}
 \end{aligned} \tag{A2}$$

$$\begin{aligned}
 &\int_T^{T_U} k_2(x-T)^2 f(x) dx \\
 &= k_2 \left\{ \left[ (\sigma^2 + \mu^2) \Phi\left(\frac{T_U-\mu}{\sigma}\right) - \sigma(T_U+\mu)\phi\left(\frac{T_U-\mu}{\sigma}\right) - (\sigma^2 + \mu^2) \Phi\left(\frac{T-\mu}{\sigma}\right) + \right. \right. \\
 &\left. \left. \sigma(T+\mu)\phi\left(\frac{T-\mu}{\sigma}\right) \right] - 2T \left[ -\sigma\phi\left(\frac{T_U-\mu}{\sigma}\right) + \mu\Phi\left(\frac{T_U-\mu}{\sigma}\right) + \sigma\phi\left(\frac{T-\mu}{\sigma}\right) - \right. \right. \\
 &\left. \left. \mu\Phi\left(\frac{T-\mu}{\sigma}\right) \right] + T^2 \left[ \Phi\left(\frac{T_U-\mu}{\sigma}\right) - \Phi\left(\frac{T-\mu}{\sigma}\right) \right] \right\}
 \end{aligned} \tag{A3}$$

$$\int_{T_L}^T \left[ a + b \frac{x - T_L}{T - T_L} \right] f(x) dx$$

$$= \left( a - b \frac{T_L}{T - T_L} \right) \left[ \Phi \left( \frac{T - \mu}{\sigma} \right) - \Phi \left( \frac{T - \mu}{\sigma} \right) \right] + \frac{b}{T - T_L} \left[ \mu \Phi \left( \frac{T - \mu}{\sigma} \right) - \mu \Phi \left( \frac{T_L - \mu}{\sigma} \right) - \sigma \phi \left( \frac{T - \mu}{\sigma} \right) + \sigma \phi \left( \frac{T_L - \mu}{\sigma} \right) \right] \tag{A4}$$

$$\int_T^{T_U} \left[ a + b \frac{T_U - x}{T_U - T} \right] f(x) dx$$

$$= \left( a + b \frac{T_U}{T_U - T} \right) \left[ \Phi \left( \frac{T_U - \mu}{\sigma} \right) - \Phi \left( \frac{T - \mu}{\sigma} \right) \right] - \frac{b}{T_U - T} \left[ \mu \Phi \left( \frac{T_U - \mu}{\sigma} \right) - \mu \Phi \left( \frac{T - \mu}{\sigma} \right) - \sigma \phi \left( \frac{T_U - \mu}{\sigma} \right) + \sigma \phi \left( \frac{T - \mu}{\sigma} \right) \right] \tag{A5}$$

Substituting Equations (A2)-(A5) into (A1), we have

$$C_{T_1}$$

$$= D_U \left[ 1 - \Phi \left( \frac{T_U - \mu}{\sigma} \right) \right] + D_L \Phi \left( \frac{T_L - \mu}{\sigma} \right) + k_1 \left\{ (\sigma^2 + \mu^2) \Phi \left( \frac{T - \mu}{\sigma} \right) - \sigma(T + \mu) \phi \left( \frac{T - \mu}{\sigma} \right) - (\sigma^2 + \mu^2) \Phi \left( \frac{T_L - \mu}{\sigma} \right) + \sigma(T_L + \mu) \phi \left( \frac{T_L - \mu}{\sigma} \right) - 2T \left[ -\sigma \phi \left( \frac{T - \mu}{\sigma} \right) + \mu \Phi \left( \frac{T - \mu}{\sigma} \right) + \sigma \phi \left( \frac{T_L - \mu}{\sigma} \right) - \mu \Phi \left( \frac{T_L - \mu}{\sigma} \right) \right] + T^2 \left[ \Phi \left( \frac{T - \mu}{\sigma} \right) - \Phi \left( \frac{T_L - \mu}{\sigma} \right) \right] \right\}$$

$$+ k_2 \left\{ (\sigma^2 + \mu^2) \Phi \left( \frac{T_U - \mu}{\sigma} \right) - \sigma(T_U + \mu) \phi \left( \frac{T_U - \mu}{\sigma} \right) - (\sigma^2 + \mu^2) \Phi \left( \frac{T - \mu}{\sigma} \right) + \sigma(T + \mu) \phi \left( \frac{T - \mu}{\sigma} \right) - 2T \left[ -\sigma \phi \left( \frac{T_U - \mu}{\sigma} \right) + \mu \Phi \left( \frac{T_U - \mu}{\sigma} \right) + \sigma \phi \left( \frac{T - \mu}{\sigma} \right) - \mu \Phi \left( \frac{T - \mu}{\sigma} \right) \right] + T^2 \left[ \Phi \left( \frac{T_U - \mu}{\sigma} \right) - \Phi \left( \frac{T - \mu}{\sigma} \right) \right] \right\}$$

$$+ a \left[ \Phi \left( \frac{T_L - \mu}{\sigma} \right) + 1 - \Phi \left( \frac{T_U - \mu}{\sigma} \right) \right] + \left( a - b \frac{T_L}{T - T_L} \right) \left[ \Phi \left( \frac{T - \mu}{\sigma} \right) - \Phi \left( \frac{T_L - \mu}{\sigma} \right) \right]$$

$$+ \frac{b}{T - T_L} \left[ \mu \Phi \left( \frac{T - \mu}{\sigma} \right) - \mu \Phi \left( \frac{T_L - \mu}{\sigma} \right) - \sigma \phi \left( \frac{T - \mu}{\sigma} \right) + \sigma \phi \left( \frac{T_L - \mu}{\sigma} \right) \right] +$$

$$\left( a + b \frac{T_U}{T_U - T} \right) \left[ \Phi \left( \frac{T_U - \mu}{\sigma} \right) - \Phi \left( \frac{T_U - \mu}{\sigma} \right) \right] - \frac{b}{T_U - T} \left[ \mu \Phi \left( \frac{T_U - \mu}{\sigma} \right) - \sigma \phi \left( \frac{T_U - \mu}{\sigma} \right) + \sigma \phi \left( \frac{T - \mu}{\sigma} \right) \right] \quad (A6)$$

**APPENDIX B: THE DETAIL DERIVATION OF EQUATION (7)**

$$\begin{aligned} C_{T_2} &= D_L \int_{-\infty}^{T_L} f(x) dx + \int_{T_L}^T k_1(T-x)f(x) dx + \int_T^{T_U} k_2(x-T)f(x) dx + D_U \int_{T_U}^{\infty} f(x) dx + \\ & a \int_{-\infty}^{T_L} f(x) dx + \int_{T_L}^T \left[ a + b \frac{x - T_L}{T - T_L} \right] f(x) dx + \int_T^{T_U} \left[ a + b \frac{T_U - x}{T_U - T} \right] f(x) dx + a \int_{T_U}^{\infty} f(x) dx \end{aligned} \quad (B1)$$

We have

$$\begin{aligned} & \int_{T_L}^T k_1(T-x)f(x) dx \\ &= k_1 T \left[ \Phi \left( \frac{T - \mu}{\sigma} \right) - \Phi \left( \frac{T_L - \mu}{\sigma} \right) \right] - k_1 \left[ -\sigma \phi \left( \frac{T - \mu}{\sigma} \right) + \mu \Phi \left( \frac{T - \mu}{\sigma} \right) \right] + \\ & \sigma \phi \left( \frac{T_L - \mu}{\sigma} \right) - \mu \Phi \left( \frac{T_L - \mu}{\sigma} \right) \end{aligned} \quad (B2)$$

$$\begin{aligned} & \int_T^{T_U} k_2(x-T)f(x) dx \\ &= -k_2 T \left[ \Phi \left( \frac{T_U - \mu}{\sigma} \right) - \Phi \left( \frac{T - \mu}{\sigma} \right) \right] + k_2 \left[ -\sigma \phi \left( \frac{T_U - \mu}{\sigma} \right) + \mu \Phi \left( \frac{T_U - \mu}{\sigma} \right) \right] \\ & + \sigma \phi \left( \frac{T - \mu}{\sigma} \right) - \mu \Phi \left( \frac{T - \mu}{\sigma} \right) \end{aligned} \quad (B3)$$

$$\begin{aligned} & \int_{T_L}^T \left[ a + b \frac{x - T_L}{T - T_L} \right] f(x) dx \\ &= \left( a - b \frac{T_L}{T - T_L} \right) \left[ \Phi \left( \frac{T - \mu}{\sigma} \right) - \Phi \left( \frac{T_L - \mu}{\sigma} \right) \right] + \frac{b}{T - T_L} \left[ \mu \Phi \left( \frac{T - \mu}{\sigma} \right) - \sigma \phi \left( \frac{T - \mu}{\sigma} \right) + \sigma \phi \left( \frac{T_L - \mu}{\sigma} \right) - \mu \Phi \left( \frac{T_L - \mu}{\sigma} \right) \right] \end{aligned}$$

$$\mu\Phi\left(\frac{T_L-\mu}{\sigma}\right)-\sigma\phi\left(\frac{T-\mu}{\sigma}\right)+\sigma\phi\left(\frac{T_L-\mu}{\sigma}\right) \tag{B4}$$

$$\int_T^{T_U} \left[ a+b\frac{T_U-x}{T_U-T} \right] f(x) dx$$

$$= \left( a+b\frac{T_U}{T_U-T} \right) \left[ \Phi\left(\frac{T_U-\mu}{\sigma}\right)-\Phi\left(\frac{T-\mu}{\sigma}\right) \right] - \frac{b}{T_U-T} \left[ \mu\Phi\left(\frac{T_U-\mu}{\sigma}\right) - \mu\Phi\left(\frac{T-\mu}{\sigma}\right) - \sigma\phi\left(\frac{T_U-\mu}{\sigma}\right) + \sigma\phi\left(\frac{T-\mu}{\sigma}\right) \right] \tag{B5}$$

Substituting Equations (B2)-(B5) into (B1), we have

$$C_{T_2}$$

$$= D_U \left[ 1-\Phi\left(\frac{T_U-\mu}{\sigma}\right) \right] + D_L \Phi\left(\frac{T_L-\mu}{\sigma}\right) + k_1 T \left[ \Phi\left(\frac{T-\mu}{\sigma}\right) - \Phi\left(\frac{T_L-\mu}{\sigma}\right) \right]$$

$$- k_1 \left[ -\sigma\phi\left(\frac{T-\mu}{\sigma}\right) + \mu\Phi\left(\frac{T-\mu}{\sigma}\right) \right] + \sigma\phi\left(\frac{T_L-\mu}{\sigma}\right) - \mu\Phi\left(\frac{T_L-\mu}{\sigma}\right)$$

$$- k_2 T \left[ \Phi\left(\frac{T_U-\mu}{\sigma}\right) - \Phi\left(\frac{T-\mu}{\sigma}\right) \right] + k_2 \left[ -\sigma\phi\left(\frac{T_U-\mu}{\sigma}\right) + \mu\Phi\left(\frac{T_U+\mu}{\sigma}\right) \right]$$

$$+ \sigma\phi\left(\frac{T-\mu}{\sigma}\right) - \mu\Phi\left(\frac{T-\mu}{\sigma}\right)$$

$$+ a \left[ \Phi\left(\frac{T_L-\mu}{\sigma}\right) + 1 - \Phi\left(\frac{T_U-\mu}{\sigma}\right) \right] + \left( a-b\frac{T_L}{T-T_L} \right) \left[ \Phi\left(\frac{T-\mu}{\sigma}\right) - \Phi\left(\frac{T_L-\mu}{\sigma}\right) \right]$$

$$+ \frac{b}{T-T_L} \left[ \mu\Phi\left(\frac{T-\mu}{\sigma}\right) - \mu\Phi\left(\frac{T_L-\mu}{\sigma}\right) - \sigma\phi\left(\frac{T-\mu}{\sigma}\right) + \sigma\phi\left(\frac{T_L-\mu}{\sigma}\right) \right] +$$

$$\left( a+b\frac{T_U}{T_U-T} \right) \left[ \Phi\left(\frac{T_U-\mu}{\sigma}\right) - \Phi\left(\frac{T-\mu}{\sigma}\right) \right] - \frac{b}{T_U-T} \left[ \mu\Phi\left(\frac{T_U-\mu}{\sigma}\right) - \mu\Phi\left(\frac{T-\mu}{\sigma}\right) - \sigma\phi\left(\frac{T_U-\mu}{\sigma}\right) + \sigma\phi\left(\frac{T-\mu}{\sigma}\right) \right] \tag{B6}$$

## A Method of Estimating the $p$ -adic Sizes of Common Zeros of Partial Derivative Polynomials Associated with a Seventh Degree Form

Siti Hasana Sapar, Kamel Ariffin Mohd Atan &  
Mohamad Rushdan Md Said

*Laboratory of Theoretical Mathematics, Institute for Mathematical Research  
Universiti Putra Malaysia, 43400 UPM, Serdang, Selangor, Malaysia*

Received: 28 July 2005

### ABSTRAK

Katakan  $x = (x_1, x_2, \dots, x_n)$  vektor dalam ruang  $Z^n$  dengan  $Z$  menandakan gelanggang integer dan  $q$  integer positif,  $f$  polinomial dalam  $x$  dengan pekali dalam  $Z$ . Hasil tambah eksponen yang disekutukan dengan  $f$  ditakrifkan sebagai  $S(f; q) = \sum \exp(2\pi i f(x)/q)$  yang dinilai bagi semua nilai  $x$  di dalam reja lengkap modulo  $q$ . Nilai  $S(f; q)$  adalah bersandar kepada penganggaran bilangan unsur  $|W|$ , yang terdapat dalam set  $V = \{x \pmod q \mid f_x \equiv 0 \pmod q\}$  dengan  $f_x$  menandakan polinomial-polinomial terbitan separa  $f$  terhadap  $x$ . Untuk menentukan kekardinalan bagi  $V$ , maklumat mengenai saiz  $p$ -adic pensifar sepunya perlu diperolehi. Makalah ini membincangkan suatu kaedah penentuan saiz  $p$ -adic bagi komponen  $(\xi, \eta)$  pensifar sepunya pembezaan separa  $f(x, y)$  dalam  $Z_p[x, y]$  berdarjah tujuh berasaskan teknik polihedron Newton yang disekutukan dengan polinomial terbitan. Polinomial berdarjah tujuh yang dipertimbangkan berbentuk  $f(x, y) = ax^7 + bx^6y + cx^5y^2 + sx + ty + k$ .

### ABSTRACT

Let  $x = (x_1, x_2, \dots, x_n)$  be a vector in a space  $Z^n$  with  $Z$  ring of integers and let  $q$  be a positive integer,  $f$  a polynomial in  $x$  with coefficients in  $Z$ . The exponential sum associated with  $f$  is defined as  $S(f; q) = \sum \exp(2\pi i f(x)/q)$  where the sum is taken over a complete set of residues modulo  $q$ . The value of  $S(f; q)$  has been shown to depend on the estimate of the cardinality  $|W|$ , the number of elements contained in the set  $V = \{x \pmod q \mid f_x \equiv 0 \pmod q\}$  where  $f_x$  is the partial derivative of  $f$  with respect to  $x$ . To determine the cardinality of  $V$ , the information on the  $p$ -adic sizes of common zeros of the partial derivatives polynomials need to be obtained. This paper discusses a method of determining the  $p$ -adic sizes of the components of  $(\xi, \eta)$  a common root of partial derivatives polynomial of  $f(x, y)$  in  $Z_p[x, y]$  of degree seven based on the  $p$ -adic Newton polyhedron technique associated with the polynomial. The seventh degree form considered is of the type  $f(x, y) = ax^7 + bx^6y + cx^5y^2 + sx + ty + k$ .

**Keywords:** Partial derivative polynomials, seventh degree form, Newton polyhedron technique

### INTRODUCTION

In our discussion, we use notation  $Z_p$ ,  $\Omega_p$  and  $\text{ord}_p x$  to respectively denote the ring of  $p$ -adic integers, completion of the algebraic closure of  $Q_p$  the field of rational  $p$ -adic numbers and the highest power of  $p$  which divides  $x$ . For each prime  $p$ , let  $f = (f_1, f_2, \dots, f_n)$  be an  $n$ -tuple polynomials in where  $Z_p[x]$  is the ring of  $p$ -adic integers and  $x = (x_1, x_2, \dots, x_n)$ .

The estimation of  $|W|$  has been the subject of many research in number theory one of which is in finding the best possible estimates to multiple exponential sums of the

form  $S(f; q) = \sum_{\text{mod } q} \exp\left(\frac{2\pi if}{q}\right)$  where  $f(x)$  is a polynomial in  $Z(x)$  and the sum taken over a complete set of residues  $x$  modulo a positive integer  $q$ .

Loxton and Vaughn (1985) are among the researchers who investigate  $S(f; q)$  where  $f$  is a non-linear polynomial in  $Z(x)$ . They find that the estimate of  $S(f; q)$  depends on the value of  $|V|$  the number of common zeros of the partial derivatives of  $f$  with respect to  $x$  modulo  $q$ . By using this result, the estimate of  $S(f; q)$  is found by other workers such as Mohd Atan (1986). He considered in particular the non-linear polynomial  $f(x, y) = ax^3 + bx^2y + cx^2y^2 + cx + dy + e$ . in which he found that the  $p$ -adic sizes for the zero  $(\xi, \eta)$  of this polynomial is  $\text{ord}_p \xi \geq \frac{1}{2}(\alpha - \delta)$  and  $\text{ord}_p \eta \geq \frac{1}{2}(\alpha - \delta)$  with  $\delta = \max\left\{\text{ord}_p 3a, \frac{3}{2}\text{ord}_p b\right\}$ .

Mohd Atan and Abdullah (1992) considered a cubic polynomial of the form  $f(x, y) = ax^3 + bx^2y + cxy^2 + dy^3 + kx + my + n$  and obtained the  $p$ -adic sizes for the root  $(\xi, \eta)$  of this polynomial as  $\text{ord}_p \xi \geq \frac{1}{2}(\alpha - \delta)$  and  $\text{ord}_p \eta \geq \frac{1}{2}(\alpha - \delta)$  with  $\delta = \max\{\text{ord}_p 3a, \text{ord}_p b, \text{ord}_p c, \text{ord}_p 3d\}$ .

In 1997 Chan and Mohd Atan investigated a polynomial of a higher degree than the one considered above in  $Z_p[x, y]$  of the form  $f(x, y) = ax^4 + bx^3y + cx^2y^2 + dxy^3 + ey^4 + mx + ny + k$  and showed that for  $(\xi, \eta)$  a root of  $f(x, y)$ ,  $\text{ord}_p \xi \geq \frac{1}{3}(\alpha - \delta)$  and  $\text{ord}_p \eta \geq \frac{1}{3}(\alpha - \delta)$  with  $\delta = \max\{\text{ord}_p a, \text{ord}_p b, \text{ord}_p c, \text{ord}_p d, \text{ord}_p e\}$ .

Heng and Mohd Atan (1999) determined the cardinality associated with the partial derivative functions of the cubic form  $f(x, y) = ax^3 + bx^2y + cx^2 + dy + e$ .

In their work, they attempt to find a better estimation by looking at the maximum number of common zeros associated with the partial derivatives  $f_x(x, y)$  and  $f_y(x, y)$ . A sharper result was obtained with  $\delta$  similar to the one considered by Mohd Atan (1986). However, the general result for polynomials of several variables is less complete.

In this paper, a method in determining the  $p$ -adic sizes of the component  $(\xi, \eta)$  a common root of partial polynomial of  $f(x, y)$  in  $Z_p(x, y)$  of degree seven. The polynomial that is considered in this paper is of the form  $f(x, y) = ax^7 + bx^6y + c^5y^2 + sx + ty + k$ .

We will arrive at the desired estimate by examining the combinations of the indicator diagrams associated with the Newton polyhedrons of  $f_x$  and  $f_y$ . The following section gives a brief description of the polyhedron as developed by Mohd Atan and Loxton (1986). It is an analogue of the  $p$ -adic Newton polygon developed by Koblitz (1977).

### NEWTON POLYHEDRON

#### Definition 2.1

Let  $p$  be a prime and  $f(x, y) = \sum a_{ij}x^i y^j$  a polynomial in  $Z_p[x, y]$ . We map the term  $T_{ij} = a_{ij}x^i y^j$  of  $f(x, y)$  to the points  $P_{ij} = (i, j, \text{ord}_p a_{ij})$  in the three dimensional Euclidean space and call this set of points Newton diagram of  $f(x, y)$ .

Below is an example of a Newton diagram for a lower degree polynomial.

#### Example 2.1:

**Definition 2.2**

Let  $p$  be a prime and  $f(x,y) = \sum a_{ij} x^i y^j$  a polynomial in  $\Omega_p[x,y]$ . The Newton polyhedron of

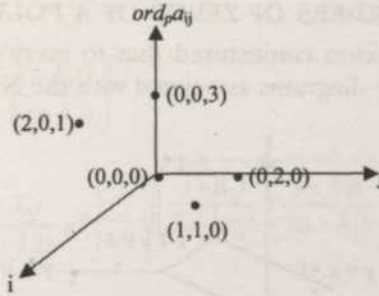


Fig. 1: Newton diagram of  $f(x,y) = 3x^2 + 2xy(y^2+27)$  with  $p = 3$

$f(x,y)$  is the lower convex hull of the Newton diagram of  $f(x,y)$ . It is the highest convex connected surface which passes through or below the point  $P_{ij}$  in the Newton diagram of  $f(x,y)$ . If  $a_{ij} = 0$  then the associated point is omitted since it lies at infinity above the  $i$ - $j$  plane.

Below is the Newton polyhedron associated with the polynomial in Example 2.1.

**Example 2.2:**

**Definition 2.3**

Let  $(\mu_r, \lambda_r, 1)$  be the normalized upward-pointing normal to the faces  $F_i$  of  $N_p$ , the Newton

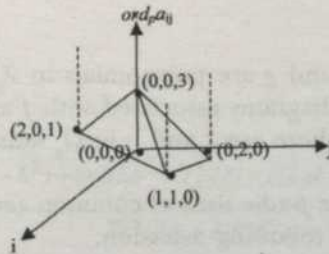


Fig. 2: The Newton polyhedron of  $f(x,y) = 3x^2 + 2xy(y^2+27)$  with  $p = 3$

polyhedron of a polynomial  $f(x,y)$  in  $\mathbb{Q}_p[x,y]$ . We map  $(\mu_r, \lambda_r, 1)$  to the points  $(\mu_r, \lambda_r)$  in the  $x$ - $y$  plane. If  $F_i$  and  $F_j$  are adjacent faces in  $N_p$  sharing a common edge, we construct the straight line joining  $(\mu_r, \lambda_r)$  and  $(\mu_s, \lambda_s)$ . If  $F_i$  has a common edge with the vertical face  $F$  say  $\alpha x + \beta y = \gamma$  in  $N_p$ , we construct the straight line segment joining  $(\mu_r, \lambda_r)$  and the appropriate point at infinity that corresponds to the normal of  $F$ , that is the segment along a line with slope  $-\alpha/\beta$ . We call the set of lines, therefore obtained the indicator diagram associated with the Newton polyhedron of  $f(x,y)$  (Mohd. Atan, 1986).

The indicator diagram associated with the Newton polyhedron in Example 2.2 is as shown in the following example.

Example 2.3 :

### P-ADIC ORDERS OF ZEROS OF A POLYNOMIAL

In 1986 Mohd Atan and Loxton conjectured that to every point of intersection of the combination of the indicator diagrams associated with the Newton polyhedrons of a pair

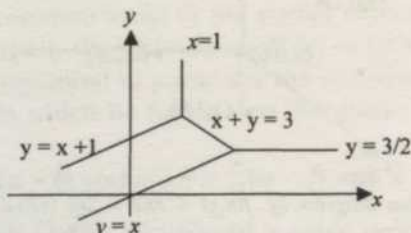


Fig. 3: Indicator diagram associated with the polynomial  $f(x,y) = 3x^2 + 2xy - y^2 + 27$  with  $p=3$

of polynomials in there exist common zeros of both polynomials whose  $p$ -adic orders correspond to this point. The conjecture is as follows :

*Conjecture*

Let  $p$  be a prime. Suppose  $f$  and  $g$  are polynomials in  $Z_p[x, y]$ . Let  $(\mu, \lambda)$  be a point of intersection of the indicator diagrams associated with  $f$  and  $g$ . Then there are  $\xi$  and  $\eta$  in  $\Omega_p$  satisfying  $f(\xi, \eta) = g(\xi, \eta) = 0$  and  $ord_p \xi = \mu, ord_p \eta = \lambda$ .

A special case of this conjecture was proven by Mohd Atan and Loxton (1986). Sapar and Mohd Atan (2002) improved this result and is written as follows:

*Theorem 3.1*

Let  $p$  be a prime. Suppose  $f$  and  $g$  are polynomials in  $Z_p[x, y]$ . Let  $(\mu, \lambda)$  be a point of intersection of the indicator diagrams associated with  $f$  and  $g$  at the vertices or simple points of intersections. Then there are  $\xi$  and  $\eta$  in  $\Omega_p$  satisfying  $f(\xi, \eta) = g(\xi, \eta) = 0$  and  $ord_p \xi = \mu, ord_p \eta = \lambda$ .

In Theorem 3.2 we give the  $p$ -adic sizes of common zeros of partial derivatives of the polynomial. First we have the following assertion:

*Lemma 3.1*

Let  $p > 7$  be an odd prime,  $a, b, c, s$  and  $t$  in  $Z_p$ .  $\lambda_1, \lambda_2$  be the zeros of  $k(x) = c^2x^2 - bcx - 9b^2 - 35ac$ . If  $U, V$  are in  $\Omega_p$  and  $ord_p U > ord_p V$  with

$$ord_p U = \frac{1}{2} ord_p \left( \frac{s + \lambda_1 t}{7a + \lambda_1 b} \right) \text{ and } ord_p V = \frac{1}{2} ord_p \left( \frac{s + \lambda_2 t}{7a + \lambda_2 b} \right)$$

then  $ord_p (U + V) = ord_p (U - V)$ .

Proof :

Let  $\lambda_1, \lambda_2$  be the zeros of  $k(x) = c^2x^2 + bcx + 9b^2 - 35ac$ , where

$$\lambda_1 = \frac{-b + \sqrt{140ac - 35b^2}}{2c}, \quad \lambda_2 = \frac{-b - \sqrt{140ac - 35b^2}}{2c}, \quad U = u \left( \frac{s + \lambda_1 t}{7a + \lambda_1 b} \right)^{1/2}$$

and  $V = v \left( \frac{s + \lambda_2 t}{7a + \lambda_2 b} \right)^{1/2}$ , where  $\text{ord}_p U = 0$ ,  $\text{ord}_p v = 0$

$$U + V = u \left( \frac{s + \lambda_1 t}{7a + \lambda_1 b} \right)^{1/2} + v \left( \frac{s + \lambda_2 t}{7a + \lambda_2 b} \right)^{1/2}$$

$$(U + V)^2 = \left[ \frac{s + \lambda_1 t}{7a + \lambda_1 b} u^2 + \frac{s + \lambda_2 t}{7a + \lambda_2 b} v^2 \right] + 2 \sqrt{\left( \frac{s + \lambda_1 t}{7a + \lambda_1 b} \right) \left( \frac{s + \lambda_2 t}{7a + \lambda_2 b} \right)} uv \tag{1}$$

Substituting  $\lambda_1, \lambda_2$  in (1) and simplifying, we have

$$(U + V)^2 = \left[ \frac{sc(14ac - b^2) + bt(18b^2 - 77ac) + c(7at - bs)\sqrt{140ac - 35b^2}}{2c^2(7a + \lambda_1 b)(7a + \lambda_2 b)} u^2 \right.$$

$$\left. + \frac{sc(14ac - b^2) + bt(18b^2 - 77ac) + c(bs - 7at)\sqrt{140ac - 35b^2}}{2c^2(7a + \lambda_1 b)(7a + \lambda_2 b)} v^2 \right]$$

$$+ 2 \sqrt{\left( \frac{s + \lambda_1 t}{7a + \lambda_1 b} \right) \left( \frac{s + \lambda_2 t}{7a + \lambda_2 b} \right)} uv.$$

Thus,

$$\text{ord}_p(U + V) = \frac{1}{2} \text{ord}_p \left[ \frac{sc(14ac - b^2) + bt(18b^2 - 77ac) + c(7at - bs)\sqrt{140ac - 35b^2}}{2c^2(7a + \lambda_1 b)(7a + \lambda_2 b)} u^2 \right.$$

$$\left. + \frac{sc(14ac - b^2) + bt(18b^2 - 77ac) + c(bs - 7at)\sqrt{140ac - 35b^2}}{2c^2(7a + \lambda_1 b)(7a + \lambda_2 b)} v^2 \right]$$

$$+ 2 \sqrt{\left( \frac{s + \lambda_1 t}{7a + \lambda_1 b} \right) \left( \frac{s + \lambda_2 t}{7a + \lambda_2 b} \right)} uv \tag{2}$$

Now consider,

$$\begin{aligned}
 U - V &= u \left( \frac{s + \lambda_1 t}{7a + \lambda_1 b} \right)^{\frac{1}{2}} - v \left( \frac{s + \lambda_2 t}{7a + \lambda_2 b} \right)^{\frac{1}{2}} \\
 (U + V)^2 &= \left[ \frac{s + \lambda_1 t}{7a + \lambda_1 b} u^2 + \frac{s + \lambda_2 t}{7a + \lambda_2 b} v^2 \right] - 2 \sqrt{\left( \frac{s + \lambda_1 t}{7a + \lambda_1 b} \right) \left( \frac{s + \lambda_2 t}{7a + \lambda_2 b} \right)} uv \\
 &= \left[ \frac{(s + \lambda_1 t)(7a + \lambda_2 b)u^2 + (s + \lambda_2 t)(7a + \lambda_1 b)v^2}{(7a + \lambda_1 b)(7a + \lambda_2 b)} \right] - 2 \sqrt{\left( \frac{s + \lambda_1 t}{7a + \lambda_1 b} \right) \left( \frac{s + \lambda_2 t}{7a + \lambda_2 b} \right)} uv \quad (3)
 \end{aligned}$$

Substituting  $\lambda_1, \lambda_2$  in (3) and simplifying, we have

$$\begin{aligned}
 (U - V)^2 &= - \left[ \frac{sc(b^2 - 14ac) + bt(77ac - 18b^2) + c(bs - 7at)\sqrt{140ac - 35b^2}}{2c^2(7a + \lambda_1 b)(7a + \lambda_2 b)} \right] u^2 \\
 &+ \left[ \frac{sc(b^2 - 14ac) + bt(77ac - 18b^2) + c(7at - bs)\sqrt{140ac - 35b^2}}{2c^2(7a + \lambda_1 b)(7a + \lambda_2 b)} \right] v^2 \\
 &- 2 \sqrt{\left( \frac{s + \lambda_1 t}{7a + \lambda_1 b} \right) \left( \frac{s + \lambda_2 t}{7a + \lambda_2 b} \right)} uv.
 \end{aligned}$$

Hence,

$$\begin{aligned}
 ord_p(U - V) &= \frac{1}{2} ord_p \left[ (-1) \left[ \frac{sc(b^2 - 14ac) + bt(77ac - 18b^2) + c(bs - 7at)\sqrt{140ac - 35b^2}}{2c^2(7a + \lambda_1 b)(7a + \lambda_2 b)} \right] u^2 \right. \\
 &+ \left. \left[ \frac{sc(b^2 - 14ac) + bt(77ac - 18b^2) + c(7at - bs)\sqrt{140ac - 35b^2}}{2c^2(7a + \lambda_1 b)(7a + \lambda_2 b)} \right] v^2 \right. \\
 &+ \left. 2 \sqrt{\left( \frac{s + \lambda_1 t}{7a + \lambda_1 b} \right) \left( \frac{s + \lambda_2 t}{7a + \lambda_2 b} \right)} uv \right]. \quad (4)
 \end{aligned}$$

By (2) and (4)  $ord_p(U + V) = ord_p(U - V)$ , since  $ord_p(14ac - b^2) = ord_p(b^2 - 14ac)$ ,  $ord_p(77ac - 18b^2) = ord_p(18b^2 + 77ac)$  and  $ord_p(7at - bs) = ord_p(bs - 7at)$ .

In the following lemma,  $U$  and  $V$  are as in Lemma 3.1.

Lemma 3.2

Let  $U, V$  be as above, and  $p > 7$  be an odd prime,  $a, b$  and  $c$  in  $Z_p$ ,  $\lambda_1, \lambda_2$  be the zeros of

$$k(x) = c^2x^2 + bcx + 9b^2 - 35ac \text{ and let}$$

$$\alpha_1 = \frac{3b + \lambda_1c}{7a + \lambda_1b} \text{ and } \alpha_2 = \frac{3b + \lambda_2c}{7a + \lambda_2b}.$$

If  $\text{ord}_p b^2 > \text{ord}_p ac$ , then

$$\text{ord}_p(\alpha_1 V - \alpha_2 U) = \text{ord}_p \frac{\sqrt{140ac - 35b^2}}{2c} [7ac - 3b^2](U+V) - \text{ord}_p(7a + \lambda_1b) - \text{ord}_p(7a + \lambda_2b).$$

Proof :

Let  $\alpha_1 = \frac{3b + \lambda_1c}{7a + \lambda_1b}$  and  $\alpha_2 = \frac{3b + \lambda_2c}{7a + \lambda_2b}$

with  $\lambda_1 = \frac{-b + \sqrt{140ac - 35b^2}}{2c}$  and  $\lambda_2 = \frac{-b - \sqrt{140ac - 35b^2}}{2c}$  the zeros of  $k(x) = c^2x^2 + bcx + 9b^2 - 35ac$ . Then

$$\begin{aligned} \text{ord}_p(\alpha_1 V - \alpha_2 U) &= \text{ord}_p \left( \frac{3b + \lambda_1c}{7a + \lambda_1b} V - \frac{3b + \lambda_2c}{7a + \lambda_2b} U \right) \\ &= \text{ord}_p [(3b + \lambda_1c)(7a + \lambda_2b)V - (3b + \lambda_2c)(7a + \lambda_1b)U]. \\ &\quad \text{ord}_p(7a + \lambda_1b) - \text{ord}_p(7a + \lambda_2b) \end{aligned} \tag{1}$$

Now,

$$\begin{aligned} &(3b + \lambda_1c)(7a + \lambda_2b)V - (3b + \lambda_2c)(7a + \lambda_1b)U \\ &= (21ab + 3b^2\lambda_2 + 7ac\lambda_1 + bc\lambda_1\lambda_2)V - (21ab + 3b^2\lambda_1 + 7ac\lambda_2 + bc\lambda_1\lambda_2)U \\ &= (21ab + bc\lambda_1\lambda_2)(V+U) + (b^2\lambda_2 + 7ac\lambda_1)V - (3b^2\lambda_1 + 7ac\lambda_2)U \end{aligned} \tag{2}$$

where  $\lambda_1, \lambda_2$  as above. That is,

$$\begin{aligned} &(3b + \lambda_1c)(7a + \lambda_2b)V - (3b + \lambda_2c)(7a + \lambda_1b)U \\ &= \left( 21ab + bc \left( \frac{-b + \sqrt{140ac - 35b^2}}{2c} \right) \left( \frac{-b - \sqrt{140ac - 35b^2}}{2c} \right) \right) (V - U) \\ &+ \left[ 3b^2 \left( \frac{-b + \sqrt{140ac - 35b^2}}{2c} \right) + 7ac \left( \frac{-b - \sqrt{140ac - 35b^2}}{2c} \right) \right] V \\ &- \left[ 3b^2 \left( \frac{-b + \sqrt{140ac - 35b^2}}{2c} \right) + 7ac \left( \frac{-b - \sqrt{140ac - 35b^2}}{2c} \right) \right] U \end{aligned} \tag{3}$$

Simplifying equation (3), we obtain,

$$(3b + \lambda_1 c)(7a + \lambda_2 b)V - (3b + \lambda_2 c)(7a + \lambda_1 b)U = \frac{b}{2c} [15b^2 - 35ac](V-U) + \frac{\sqrt{140ac - 35b^2}}{2c} [7ac - 3b^2](U + V).$$

Since  $p > 7$  and  $ord_p b^2 > ord_p ac$ , we have

$$ord_p \frac{b}{2c} [15b^2 - 35ac](V-U) = ord_p b + ord_p ac + ord_p (V-U) - ord_p c \tag{4}$$

and

$$ord_p \frac{\sqrt{140ac - 35b^2}}{2c} [7ac - 3b^2](U+V) = \frac{1}{2} ord_p ac + ord_p ac + ord_p (V+U) - ord_p c. \tag{5}$$

Since  $ord_p b > \frac{1}{2} ord_p ac$  and Lemma 3.1, we have from (4) and (5):

$$ord_p \frac{b}{2c} [15b^2 - 35ac](V-U) > ord_p \frac{\sqrt{140ac - 35b^2}}{2c} [7ac - 3b^2](U+V).$$

Thus,

$$ord_p [(3b + \lambda_1 c)(7a + \lambda_2 b)V - (3b + \lambda_2 c)(7a + \lambda_1 b)U] = ord_p \frac{\sqrt{140ac - 35b^2}}{2c} [7ac - 3b^2](U+V).$$

Therefore, from (1) we have

$$ord_p (\alpha_1 V - \alpha_2 U) = ord_p \frac{\sqrt{140ac - 35b^2}}{2c} [7ac - 3b^2](U+V) - ord_p (7a + \lambda_1 b) - ord_p (7a + \lambda_2 b).$$

Lemma 3.3

Let  $p > 7$  be an odd prime,  $a, b$  and  $c$  in  $Z_p$ .  $\lambda_1, \lambda_2$  be the zeros of  $k(x) = c^2 x^2 + bcx + 9b^2 - 35ac$  and let

$$\alpha_1 = \frac{3b + \lambda_1 c}{7a + \lambda_1 b} \text{ and } \alpha_2 = \frac{3b + \lambda_2 c}{7a + \lambda_2 b}.$$

If  $ord_p b^2 > ord_p ac$ , then  $ord_p \alpha_i = ord_p (\alpha_1 - \alpha_2) = \frac{1}{2} ord_p \frac{c}{a}$ , for  $i = 1, 2$ .

Proof :

The zeros of  $k(x) = c^2 x^2 + bcx + 9b^2 - 35ac$  are given by

$$\lambda_1 = \frac{-b + \sqrt{140ac - 35b^2}}{2c} \text{ and } \lambda_2 = \frac{-b - \sqrt{140ac - 35b^2}}{2c}.$$

Thus,

$$\lambda_1 c = \frac{-b + \sqrt{140ac - 35b^2}}{2c}$$

Since  $\text{ord}_p b^2 > \text{ord}_p ac$ ,  $p > 7$ , we have

$$\text{ord}_p \lambda_1 c = \text{ord}_p \left[ \frac{-b + \sqrt{140ac - 35b^2}}{2} \right] = \frac{1}{2} \text{ord}_p ac$$

Hence,  $\text{ord}_p \lambda_1 c = \frac{1}{2} \text{ord}_p ac < \text{ord}_p b$ .

Similarly it can be shown that  $\text{ord}_p \lambda_2 c = \frac{1}{2} \text{ord}_p ac < \text{ord}_p b$ .

Therefore,  $\text{ord}_p (3b + \lambda_1 c) = \text{ord}_p \lambda_1 c = \frac{1}{2} \text{ord}_p ac$ ,  $i = 1, 2$ . (1)

Now, consider

$$\lambda_1 b = b \left[ \frac{-b + \sqrt{140ac - 35b^2}}{2c} \right]$$

$$\text{ord}_p \lambda_1 b = \text{ord}_p b + \text{ord}_p \left[ \frac{-b + \sqrt{140ac - 35b^2}}{2} \right] - \text{ord}_p 2c$$

Since  $\text{ord}_p b > \frac{1}{2} \text{ord}_p ac$ ,

$$\begin{aligned} \text{ord}_p \lambda_1 c &= \text{ord}_p b + \frac{1}{2} \text{ord}_p ac - \text{ord}_p c \\ &= \text{ord}_p a. \end{aligned}$$

Thus,  $\text{ord}_p \lambda_1 c > \text{ord}_p a$ .

Similarly it can be shown that  $\text{ord}_p \lambda_2 c > \text{ord}_p a$ .

It follows that,  $\text{ord}_p (7a + \lambda_1 b) = \text{ord}_p a$ ,  $i = 1, 2$ . (2)

From (1) and (2), and since  $p > 7$ , we have

$$\text{ord}_p \alpha_i = \text{ord}_p \left( \frac{3b + \lambda_1 c}{7a + \lambda_1 b} \right), \quad i = 1, 2$$

That is

$$\begin{aligned} \text{ord}_p \alpha_i &= \frac{1}{2} \text{ord}_p ac - \text{ord}_p a \\ &= \frac{1}{2} \text{ord}_p \frac{c}{a}, \quad \text{for } i = 1, 2. \end{aligned} \quad (3)$$

It can be shown that

$$\alpha_1 - \alpha_2 = \frac{(\lambda_1 - \lambda_2)(7ac - 3b^2)}{(7a + \lambda_1 b)(7a + \lambda_2 b)}$$

where, 
$$\lambda_1 - \lambda_2 = \frac{\sqrt{140ac - 35b^2}}{c}.$$

Thus, 
$$\text{ord}_p(\alpha_1 - \alpha_2) = \text{ord}_p \sqrt{140ac - 35b^2} - \text{ord}_p c + \text{ord}_p(7ac - 3b^2) - \text{ord}_p(7a + \lambda_1 b) - \text{ord}_p(7a + \lambda_2 b).$$

Since  $p > 7$ ,  $\text{ord}_p b^2 > \text{ord}_p ac$  and by (2), we have

$$\begin{aligned} \text{ord}_p(\alpha_1 - \alpha_2) &= \frac{1}{2} \text{ord}_p ac - \text{ord}_p c + \text{ord}_p ac - 2 \text{ord}_p a \\ &= \frac{1}{2} (\text{ord}_p c - \text{ord}_p a). \end{aligned}$$

That is, 
$$\text{ord}_p(\alpha_1 - \alpha_2) = \frac{1}{2} \left( \text{ord}_p \frac{c}{a} \right). \tag{4}$$

From (3) and (4), we obtain

$$\text{ord}_p \alpha_i = \text{ord}_p(\alpha_1 - \alpha_2) = \frac{1}{2} \text{ord}_p \frac{c}{a}, \text{ for } i = 1, 2.$$

**Lemma 3.4**

Let  $p > 7$  be an odd prime,  $a, b, c, s$  and  $t$  in  $Z_p$ . Suppose that  $\alpha > 0$ ,  $\delta = \max\{\text{ord}_p a, \text{ord}_p b\}$ , and  $\text{ord}_p s, \text{ord}_p t \geq \alpha > \delta$ . Let  $\gamma, \beta$  be in  $\Omega_p$ ,  $\lambda_1$  and  $\lambda_2$  be the zeros of  $k(x) = c^2 x^2 + bcx + 9b^2 - 35ac$  and

$$U = \gamma^2 + \frac{3b + \lambda_1 c}{7a + \lambda_1 c} \gamma^2 \beta \text{ and } V = \gamma^2 + \frac{3b + \lambda_2 c}{7a + \lambda_2 c} \gamma^2 \beta.$$

If  $\text{ord}_p b^2 > \text{ord}_p ac$ ,  $\text{ord}_p a > \text{ord}_p c$  and  $\text{ord}_p U = \frac{1}{2} \text{ord}_p \frac{s + \lambda_1 t}{7a + \lambda_1 b}$ ,  $\text{ord}_p V = \frac{1}{2} \text{ord}_p \frac{s + \lambda_2 t}{7a + \lambda_2 b}$  then

$$\text{ord}_p \gamma \geq \frac{1}{6} (\alpha - \delta) \text{ and } \text{ord}_p \beta \geq \frac{1}{6} (\alpha - \delta).$$

Proof:

Let 
$$\alpha_1 = \frac{3b + \lambda_1 c}{7a + \lambda_1 b} \text{ and } \alpha_2 = \frac{3b + \lambda_2 c}{7a + \lambda_2 b}$$

with  $\lambda_1$  and  $\lambda_2$  zeros of  $k(x) = c^2 x^2 + bcx + 9b^2 - 35ac$ . The expressions for  $\lambda_1, \lambda_2$  are as given in the proof of Lemma 3.3. Then

$$U = \gamma^2 + \alpha_1 \gamma^2 \beta \tag{1}$$

$$V = \gamma^2 + \alpha_2 \gamma^2 \beta \tag{2}$$

By solving simultaneously (1) and (2), we obtain

$$\gamma^3 = \frac{\alpha_1 V - \alpha_2 U}{\alpha_1 - \alpha_2} \quad (3)$$

It follows that,

$$3 \text{ord}_p \gamma = \text{ord}_p (\alpha_1 V - \alpha_2 U) - \text{ord}_p (\alpha_1 - \alpha_2).$$

Suppose  $\min \{ \text{ord}_p \alpha_1 V, \text{ord}_p \alpha_2 U \} = \text{ord}_p \alpha_1 V$ . Then

$$\begin{aligned} 3 \text{ord}_p \gamma &\geq \text{ord}_p \alpha_1 V - \text{ord}_p (\alpha_1 - \alpha_2) \\ &= \text{ord}_p \alpha_1 + \text{ord}_p V - \text{ord}_p V - \text{ord}_p (\alpha_1 - \alpha_2). \end{aligned}$$

By Lemma 3.3,  $\text{ord}_p \alpha_1 = \text{ord}_p (\alpha_1 - \alpha_2)$  and by its proof  $\text{ord}_p (7a + \lambda_i b) = \text{ord}_p a$ ,  $i=1,2$ .

Therefore

$$3 \text{ord}_p \gamma \geq \text{ord}_p V.$$

That is,

$$\begin{aligned} 3 \text{ord}_p \gamma &\geq \frac{1}{2} \text{ord}_p \left( \frac{s + \lambda_2 t}{7a + \lambda_2 b} \right) \\ &= \frac{1}{2} [ \text{ord}_p (s + \lambda_2 t) - \text{ord}_p a ] \end{aligned} \quad (4)$$

where  $\text{ord}_p (s + \lambda_2 t) = \text{ord}_p [ 2cs + (-b - \sqrt{140ac - 35b^2})t ] - \text{ord}_p c$ .

That is,  $\text{ord}_p (s + \lambda_2 t) \geq \min \{ \text{ord}_p 2cs, \text{ord}_p (-b - \sqrt{140ac - 35b^2})t \} - \text{ord}_p c$ .

Suppose  $\min \{ \text{ord}_p 2cs, \text{ord}_p (-b - \sqrt{140ac - 35b^2})t \} = \text{ord}_p 2cs$ . Then,

$$\text{ord}_p (s + \lambda_2 t) \geq \text{ord}_p 2cs - \text{ord}_p c.$$

That is,  $\text{ord}_p (s + \lambda_2 t) \geq \text{ord}_p s$ . (5)

Hence, from (4) and (5).

$$3 \text{ord}_p \gamma \geq \frac{1}{2} (\text{ord}_p (s - \text{ord}_p a)).$$

Hence, by hypothesis,

$$\begin{aligned} \text{ord}_p \gamma &\geq \frac{1}{6} (\text{ord}_p (s - \text{ord}_p a)) \\ &\geq \frac{1}{6} (\alpha - \delta). \end{aligned}$$

Now, from (1) and (2), we will obtain

$$(2) \quad \beta = \frac{U-V}{(\alpha_1 - \alpha_2)\gamma^2}.$$

Therefore ,

$$\text{ord}_p \beta = \text{ord}_p(U-V) - \text{ord}_p(\alpha_1 - \alpha_2) - \text{ord}_p \gamma^2$$

with  $\text{ord}_p \gamma = \frac{1}{3} \text{ord}_p \frac{\alpha_1 V - \alpha_2 U}{\alpha_1 - \alpha_2}$  from (3). Then we have,

$$\text{ord}_p \beta = \text{ord}_p(U-V) - \frac{1}{3} \text{ord}_p(\alpha_1 - \alpha_2) - \frac{2}{3} \text{ord}_p(\alpha_1 V - \alpha_2 U).$$

By Lemma 3.2, we obtain

$$\begin{aligned} \text{ord}_p \beta &= \text{ord}_p(U-V) - \frac{1}{3} \text{ord}_p(\alpha_1 - \alpha_2) + \frac{2}{3} \text{ord}_p(7a + \lambda_1 b) + \frac{2}{3} \text{ord}_p(7a + \lambda_2 b) \\ &\quad - \frac{2}{3} \text{ord}_p \frac{\sqrt{140ac - 35b^2}}{2c} [7ac - 3b^2](U + V). \end{aligned}$$

Since  $\text{ord}_p b^2 > \text{ord}_p ac$ ,  $p > 7$  and from Lemma 3.1 and Lemma 3.3, we have

$$\begin{aligned} \text{ord}_p(U + V) - \frac{1}{3} \left( \frac{1}{2} \text{ord}_p \frac{c}{a} \right) + \frac{4}{3} \text{ord}_p a - \frac{2}{3} \left( \frac{1}{2} \text{ord}_p ac \right) \\ \geq \frac{2}{3} \text{ord}_p ac + \frac{2}{3} \text{ord}_p c \\ \geq \frac{1}{3} \min\{\text{ord}_p U, \text{ord}_p V\} + \frac{1}{2} \text{ord}_p a - \frac{1}{2} \text{ord}_p c. \end{aligned}$$

Suppose  $\min\{\text{ord}_p U, \text{ord}_p V\} = \text{ord}_p V$ , then

$$\begin{aligned} \text{ord}_p \beta &\geq \frac{1}{3} \text{ord}_p V + \frac{1}{2} \text{ord}_p a - \frac{1}{2} \text{ord}_p c \\ &= \frac{1}{6} [\text{ord}_p(s + \lambda_2 t) - \text{ord}_p(7a + \lambda_2 b) + \text{ord}_p a - 3 \text{ord}_p c]. \end{aligned}$$

By equation (2) in proof of Lemma 3.3 and (5), we obtain

$$\text{ord}_p \beta \geq \frac{1}{6} [\text{ord}_p s - \text{ord}_p a + 3 \text{ord}_p a - 3 \text{ord}_p c].$$

Since  $\text{ord}_p a > \text{ord}_p c$ , we have

$$\begin{aligned} \text{ord}_p \beta &\geq \frac{1}{6} [\text{ord}_p s - \text{ord}_p a] \\ &\geq \frac{1}{6} (\alpha - \delta). \end{aligned}$$

We will obtain the same result if

$$\min\{\text{ord}_p 2cs, \text{ord}_p (-b - \sqrt{140ac - 35b^2})t\} = \text{ord}_p (-b - \sqrt{140ac - 35b^2})t \text{ and ,}$$

$$\min\{\text{ord}_p U, \text{ord}_p V\} = \text{ord}_p U \text{ for } \text{ord}_p \gamma \text{ and } \text{ord}_p \beta.$$

$$\text{Therefore, } \text{ord}_p \gamma \geq \frac{1}{6} (\alpha - \delta) \text{ and } \text{ord}_p \beta \geq \frac{1}{6} (\alpha - \delta).$$

**Theorem 3.2**

Let  $f(x,y) = ax^7 + bx^6y + cx^5y^2 + sx + ty + k$  be a polynomial in  $Z_p[x,y]$  with  $p > 7$ . Let  $\alpha > 0$ ,  $\delta = \max\{\text{ord}_p a, \text{ord}_p b\}$ ,  $\text{ord}_p a > \text{ord}_p c$  and  $\text{ord}_p b^2 > \text{ord}_p ac$ . If  $\text{ord}_p f_x(0,0), \text{ord}_p f_y(0,0) \geq \alpha > \delta$  then there exists  $(\xi, \eta)$  such that  $f_x(\xi, \eta) = 0, f_y(\xi, \eta) = 0$  and

$$\text{ord}_p \xi \geq \frac{1}{6} (\alpha - \delta).$$

**Proof :**

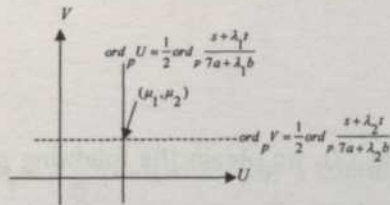


Fig. 4: The indicator diagrams of  $F(U,V) = (7a + \lambda_1 b)U^2 + s + \lambda_1 t$  and  $G(U,V) = (7a + \lambda_2 b)V^2 + \lambda_2 t$

Let  $g = f_x$  and  $h = f_y$  and  $\lambda$  be a constant.

Then,

$$(g + \lambda h)(x,y) = (7a + \lambda b)x^6 + (6b + 2\lambda c)x^5y + 5cx^4y^2 + s + \lambda t$$

and

$$\frac{(g + \lambda h)(x,y)}{7a + \lambda b} = x^6 + \left(\frac{6b + 2\lambda c}{7a + \lambda b}\right)x^5y + \left(\frac{5c}{7a + \lambda b}\right)x^4y^2 + \frac{s + \lambda t}{7a + \lambda b}. \tag{1}$$

By completing the square in equation (1), we obtain

$$\frac{(g + \lambda h)(x, y)}{7a + \lambda b} = \left( x^3 + \frac{3b + \lambda c}{7a + \lambda b} x^2 y \right) + \frac{s + \lambda t}{7a + \lambda b} \tag{2}$$

if

$$\frac{5c}{7a + \lambda b} - \left( \frac{3b + \lambda c}{7a + \lambda b} \right)^2 = 0.$$

That is  $c^2 x^2 + bcx + 9b^2 - 35ac = 0$ . (3)

From (3), we will obtain two values of  $\lambda$ , say  $\lambda_1, \lambda_2$  where

$$\lambda_1 = \frac{-b + \sqrt{35(4ac - b^2)}}{2c} \quad \text{and} \quad \lambda_2 = \frac{-b - \sqrt{35(4ac - b^2)}}{2c}.$$

Now, let

$$U = x^3 + \frac{3b + \lambda_1 c}{7a + \lambda_1 b} x^2 y, \tag{4}$$

$$V = x^3 + \frac{3b + \lambda_2 c}{7a + \lambda_2 b} x^2 y, \tag{5}$$

$$F(U, V) = (g + \lambda_1 h)(x, y) \tag{6}$$

and  $G(U, V) = (g + \lambda_2 h)(x, y)$ . (7)

By substitution of  $U$  and  $V$  in (2), we obtain the following polynomials in  $(U, V)$

$$F(U, V) = (7a + \lambda_1 b) U^2 + s + \lambda_1 t \tag{8}$$

$$G(U, V) = (7a + \lambda_2 b) V^2 + \lambda_2 t. \tag{9}$$

The combination of the indicator diagrams associated with the Newton polyhedron of (8) and (9) takes the form shown in the figure below:

From Figure 4 and Theorem 3.1 there exists  $(\hat{U}, \hat{V})$  such that  $F_1(\hat{U}, \hat{V}) = 0, G_1(\hat{U}, \hat{V}) =$

$0$  and  $ord_p \hat{U} = \mu_1, ord_p \hat{V} = \mu_2$  with  $\mu_1 = \frac{1}{2} ord_p \frac{s + \lambda_1 t}{7a + \lambda_1 b}$ . Also from (4) and (5) there exists  $(x_0, y_0)$  such that

$$\hat{U} = x_0^3 + \alpha_1 x_0^2 y_0 \quad \text{and} \quad \hat{V} = x_0^3 + \alpha_2 x_0^2 y_0$$

with  $\alpha_1 = \frac{3b + \lambda_1 c}{7a + \lambda_1 b}$ ,  $\alpha_2 = \frac{3b + \lambda_2 c}{7a + \lambda_2 b}$  in which  $\lambda_1, \lambda_2$  are zeros of

$$k(x) = c^2 x^2 + bcx + 9b^2 - 35ac.$$

In fact,  $x_0 = \left( \frac{\alpha_1 \hat{V} - \alpha_2 \hat{U}}{\alpha_1 - \alpha_2} \right)^{1/3}$  and  $y_0 = \frac{\hat{U} - \hat{V}}{(\alpha_1 - \alpha_2)^{1/3} (\alpha_1 V - \alpha_2 \hat{U})^{2/3}}$ , where from Lemma 3.2,

$\alpha_1 \hat{V} - \alpha_2 \hat{U} \neq 0$  and from Lemma 3.3,  $\alpha_1 - \alpha_2 \neq 0$ .

From Lemma 3.4 and hypothesis, we see that

$$\text{ord}_p x_0 \geq \frac{1}{6}(\alpha - \delta) \quad \text{and} \quad \text{ord}_p y_0 \geq \frac{1}{6}(\alpha - \delta).$$

We have, from (6) and (7),

$$F_1(\hat{U}, \hat{V}) = (g + \lambda_1 h)(x_0, y_0) \quad \text{and} \quad G_1(\hat{U}, \hat{V}) = (g + \lambda_2 h)(x_0, y_0).$$

Since  $F_1(\hat{U}, \hat{V}) = 0$ , it follows that  $g(x_0, y_0) + \lambda_1 h(x_0, y_0) = 0$ . (10)

Also since  $G_1(\hat{U}, \hat{V}) = 0$ ,  $g(x_0, y_0) + \lambda_2 h(x_0, y_0) = 0$ . (11)

From (10) and (11),  $(\lambda_1 - \lambda_2)h(x_0, y_0) = 0$ . Since  $\lambda_1 \neq \lambda_2$ , we have  $h(x_0, y_0) = 0$ . Similarly  $g(x_0, y_0) = 0$ .

Let  $\xi = x_0$  and  $\eta = y_0$ .

Thus  $\text{ord}_p \xi \geq \frac{1}{6}(\xi, \eta)$  and  $\text{ord}_p \eta \geq \frac{1}{6}(\alpha - \delta)$  with  $(\xi, \eta)$  a common zero of  $g$  and  $h$ .

### CONCLUSION

Our investigation finds that if  $p$  is an odd prime,  $p > 7$ ,

$f(x, y) = ax^7 + bx^6y + cx^5y^2 + sx + ty + k$  polynomial in  $Z_p[x, y]$  with  $\text{ord}_p b^2 > \text{ord}_p ac$  and  $\text{ord}_p a > \text{ord}_p c$ , then the  $p$ -adic sizes of common zeros of partial derivatives of this polynomial is  $\text{ord}_p \xi$

$\geq \frac{1}{6}(\alpha - \delta)$  and  $\text{ord}_p \eta \geq \frac{1}{6}(\alpha - \delta)$  with  $\alpha > \delta$  and  $\delta = \max\{\text{ord}_p a, \text{ord}_p b\}$ .

## REFERENCES

- CHAN, K.L. and MOHD. ATAN, K.A. (1997). On the estimate to solutions of congruence equations associated with a quartic form. *Journal of Physical Science*, 8, 21-34.
- HENG, S.H. and MOHD ATAN, K.A. (1999). An estimation of exponential sums associated with a cubic form. *Journal of Physical Science*, 10, 1-21.
- KOBLITZ, N. (1977). *p-adic Numbers, p-adic Analysis and Zeta Function*. New York: Springer-Verlag.
- LOXTON, J.H. and VAUGHN, R.C. (1985). The estimate of complete exponential sums. *Canad. Mth Bull*, 28(4), 440-454.
- MOHD. ATAN, K.A. (1986). Newton polyhedral method of determining p-adic orders of zeros common to two polynomials in. *Pertanika*, 9(3), 375-380. Universiti Pertanian Malaysia.
- MOHD. ATAN, K.A. and LOXTON, J.H. (1986). Newton polyhedral and solutions of congruences. In J.H. Loxton and A. Van der Poorten (Eds.), *Diophantine Analysis*. Cambridge: Cambridge University Press.
- MOHD ATAN, K.A. and ABDULLAH, I.B. (1992). Set of solution to congruences equations associated with cubic form. *Journal of Physical Science*, 3,1-6.
- SAPAR, S.H. and MOHD ATAN, K.A. (2002). Estimate for the cardinality of the set of solution to congruence equations (Malay). *Journal of Technology*, (36C), 13-40.

## Xanthenes and Xanthone Derivatives from *Garcinia nitida*

G. C. L. Ee\*, C. K. Lim, Y. H. Taufiq-Yap, M. A. Sukari & M. Rahmani

Department of Chemistry, Faculty of Science,  
Universiti Putra Malaysia, 43400, UPM,  
Serdang, Selangor, Malaysia

Received: 27 February 2006

### ABSTRAK

Satu kajian kimia terperinci ke atas kulit kayu *Garcinia nitida* telah menghasilkan lima xanton dan dua triterpenoid. Sebatian-sebatian ini adalah 1,3,7-trihidroksi-2,4-bis(3-metilbut-2-enil)xanthone; (1) osajaxanthone, (2) inophyllin B (3) 3-isomangostin, (4) rubraxanthone, (5) stigmasterol and stigmasterol acetate. Struktur sebatian-sebatian ini telah dikenalpasti dengan menggunakan spektroskopi RMN 1D and 2D. Tindak balas pengasitilan rubraxanthone telah menghasilkan dua sebatian baru rubraxanthone monoasitat (6) dan rubraxanthone diasitat (7) dan juga rubraxanthone triasitat (8).

### ABSTRACT

A detailed chemical study on the stem bark extracts of *Garcinia nitida* has led to the isolation of five xanthenes and two triterpenoids. They are 1,3,7-trihydroxy-2,4-bis(3-methylbut-2-enyl)xanthone (1) osajaxanthone, (2) inophyllin B, (3) 3-isomangostin, (4) rubraxanthone, (5) stigmasterol and stigmasterol acetate. The structures of these compounds were established using mainly 1D and 2D NMR spectroscopy. Acetylation of rubraxanthone resulted in two new compounds, rubraxanthone monoacetate (6) and rubraxanthone diacetate (7), along with rubraxanthone triacetate (8).

**Keywords:** *Garcinia nitida*, guttiferæ, xanthenes, triterpenoids

### INTRODUCTION

*Garcinia* species are widely distributed in Malaysia. Plants from this genus are known to have plenty of uses. Many species yield products that are useful to the native populations, while some have special economic importance (Heywood, 1982). The fruit of many species like *Garcinia mangostana*, *Garcinia xanthochymus* and *Garcinia multiflora* are edible and have a pleasant flavour. Some species like *Garcinia picrorrhiza* are used as medicament in curing diseases due to their medicinal properties (Burkill, 1966). Plants from the genus *Garcinia* have been reported to be rich in xanthenes and triterpenoids (Peres *et al.*, 2000; Nguyen and Harrison, 2000; Vieira *et al.*, 2004; Rukachaisirikul *et al.*, 2000; Merza *et al.*, 2004; Kosela *et al.*, 2000). In our continuing interest on the Malaysian *Garcinia* plants, we carried out detail chemical studies on the stem bark of *Garcinia nitida* which was collected from Sri Aman, Sarawak, Malaysia. This study has led to the isolation and identification of five xanthenes and two triterpenoids from the stem bark extracts of the species and the identification of three rubraxanthone derivatives from the acetylation of rubraxanthone. This paper reports the isolation and characterization of these compounds.

\* Corresponding Author:  
E-mail: gwen@fsas.upm.edu.my

## MATERIALS AND METHODS

*Plant Material* – The stem bark of *Garcinia nitida* was collected from Sri Aman Sarawak, Malaysia. The plant materials were identified by Miss Runi Sylvester from the Herbarium of Sarawak Forestry Department, Kuching, Sarawak, Malaysia.

*General* – Infrared spectra were measured in KBr/NaCl pellet on a Perkin-Elmer FTIR Spectrum BX spectrometer. EIMS were recorded on a Shimadzu GCMS-QP5050A spectrometer. NMR spectra were obtained using a Unity INOVA 500MHz NMR/ JEOL 400MHz FT NMR spectrometer using tetramethylsilane (TMS) as the internal standard. Ultra violet spectra were recorded in CHCl<sub>3</sub> on a Shimadzu UV-160A, UV-Visible Recording Spectrophotometer.

*Extraction and Isolation* – The air-dried and powdered stem bark of *Garcinia nitida* (2.0 kg) was extracted successively with hexane, chloroform and acetone at the room temperature. The extracts were evaporated to dryness under a reduced pressure to yield 102.0 g of crude hexane extract, 101.5 g of crude chloroform extract and 85.3 g of crude acetone extract. The crude hexane extract (20.0 g) was chromatographed on a silica gel column using a stepwise gradient system (hexane/CHCl<sub>3</sub>, CHCl<sub>3</sub>/Me<sub>2</sub>CO and Me<sub>2</sub>CO/MeOH) to give 25 fractions (*Frs.*). The *Frs.* 2-4 were combined and separated over a silica gel column (hexane/CHCl<sub>3</sub> and CHCl<sub>3</sub>/Me<sub>2</sub>CO gradient) to give stigmasterol acetate (8 mg). *Frs.* 8-10 were combined and subjected to column chromatography (CC) (SiO<sub>2</sub>; hexane/CHCl<sub>3</sub> and CHCl<sub>3</sub>/Me<sub>2</sub>CO gradient) to yield stigmasterol (10 mg). *Fr.* 11 was purified by repeated CC (SiO<sub>2</sub>; hexane/EtOAc and CHCl<sub>3</sub>/Me<sub>2</sub>CO gradient) to give inophyllin B (**3**) (8 mg). The crude chloroform extract (20.0 g) was fractionated by vacuum CC (SiO<sub>2</sub>; hexane-EtOAc and CHCl<sub>3</sub>-Me<sub>2</sub>CO gradient) to give 15 fractions. *Frs.* 2-3 were combined and purified by CC (SiO<sub>2</sub>; hexane/EtOAc and CHCl<sub>3</sub>/Me<sub>2</sub>CO gradient) to furnish the 5 subfractions. Subfractions 1-3 were combined and further purified by CC (SiO<sub>2</sub>; hexane/EtOAc and CHCl<sub>3</sub>/Me<sub>2</sub>CO gradient) and finally by CC (*Sephadex LH-20*; MeOH) to yield 1,3,7-trihydroxy-2,4-bis(3-methylbut-2-enyl)xanthone (**1**) (9 mg) and osajaxanthone (8 mg) (**2**). On the other hand, fractionation of the crude acetone extract (20.0 g) over a silica gel column (hexane-CHCl<sub>3</sub>, CHCl<sub>3</sub>-EtOAc and EtOAc-MeOH gradient) provided 25 fractions. *Frs.* 11 afforded rubraxanthone (**5**) (230 mg) and *Fr.* 8 was rechromatographed on a silica gel column (hexane-CHCl<sub>3</sub>, CHCl<sub>3</sub>-EtOAc and EtOAc-MeOH gradient) to give 20 subfractions. Subfraction 9 yielded 3-isomangostin (**4**) (10 mg).

*Acetylation of rubraxanthone (5)* – A solution of rubraxanthone (100 mg) in pyridine (15 ml) was added to 15 ml of acetic anhydride (Ac<sub>2</sub>O). The mixture was heated at 80°C for 2 hours and poured into ice water and left in the refrigerator overnight. The precipitate formed was filtered, washed with water and dried. The precipitate was then purified by column chromatography to yield rubraxanthone monoacetate (**6**) (8 mg), rubraxanthone diacetate (**7**) (20 mg) and rubraxanthone triacetate (**8**) (10 mg).

*1,3,7-Trihydroxy-2,4-bis(3-methylbut-2-enyl)xanthone (1)* – Yellow needles, mp 128-129°C. UV (EtOH)  $\lambda_{\max}$  nm (log e): 217.5 (0.85), 234.0 (1.14), 270.0 (1.23), 285.0 (1.07), 386.5 (0.23). IR  $\nu_{\max}$  cm<sup>-1</sup> (KBr): 3378, 1644, 1480, 1230. EI-MS m/z (rel. int.): 380 (39), 363 (34), 337 (22), 325 (31), 309 (68), 295 (18), 281 (62), 269 (100), 257 (9), 41 (11). <sup>1</sup>H NMR and <sup>13</sup>C NMR (see text).

*Osajaxanthone* (2) – Yellow needles, mp 247-248°C. UV (EtOH)  $\lambda_{\max}$  nm (log e): 237.5 (0.39), 285.5 (0.96), 339.0 (0.16), 381.0 (0.11). IR  $\nu_{\max}$   $\text{cm}^{-1}$  (KBr): 3446, 1650, 1478, 1232. EI-MS  $m/z$  (rel. int.): 310 (19), 295 (100), 155 (4), 147 (21), 93 (4), 77 (5), 65 (6), 53 (5).  $^1\text{H}$  NMR (400 MHz, acetone- $d_6$ ):  $\delta$  13.38 (1H, s, 1-OH), 8.99 (1H, s, 7-OH), 7.60 (1H, d,  $J = 2.8$  Hz, H-8), 7.49 (1H, d,  $J = 9.2$  Hz, H-5), 7.40 (1H, dd,  $J = 9.2, 2.8$  Hz, H-6), 6.72 (1H, d,  $J = 10.1$  Hz, H-4'), 6.38 (1H, s), 5.79 (1H, d,  $J = 10.1$  Hz, H-5'), 1.51 (3H, s, H-7''), 1.51 (3H, s, H-8').  $^{13}\text{C}$  NMR (100 MHz, acetone- $d_6$ ):  $\delta$  180.2 (C-9), 160.4 (C-3), 157.2 (C-1), 156.9 (C-4a), 153.7 (C-7), 149.5 (C-10a), 127.7 (C-5'), 124.1 (C-6), 120.6 (C-8a), 118.7 (C-5), 114.4 (C-4'), 108.1 (C-8), 103.8 (C-2), 102.8 (C-9a), 94.3 (C-4), 77.9 (C-6'), 27.3 (C-7'), 27.3 (C-8').

*Inophyllin B* (3) – Yellow needles, mp 174-175°C. UV (EtOH)  $\lambda_{\max}$  nm (log e): 213.0 (0.89), 241.0 (0.98), 281.0 (1.99), 336.5 (0.93). IR  $\nu_{\max}$   $\text{cm}^{-1}$  (KBr): 3444, 2968, 1632, 1464, 1290, 1264, 1186, 1128. EI-MS  $m/z$  (rel. int.): 394 (100), 380 (93), 365 (30), 353 (42), 339 (10), 325 (9), 309 (8), 182 (32), 168 (12), 162 (42), 153 (10), 139 (8), 115 (9), 53 (9), 41 (9).  $^1\text{H}$  NMR (400 MHz, acetone- $d_6$ ):  $\delta$  13.85 (1H, s, 1-OH), 7.50 (1H, d,  $J = 8.2$ , H-8), 6.79 (1H, d,  $J = 8.2$  Hz, H-7), 6.64 (1H, d,  $J = 10.1$  Hz, H-11), 6.52 (1H, dd,  $J = 18.3, 11.0$  Hz, H-19), 5.51 (1H, d,  $J = 10.1$  Hz, H-12), 5.04 (1H, d,  $J = 18.3$  Hz, H-20), 4.89 (1H, d,  $J = 11.0$  Hz, H-20), 1.56 (3H, s, H-17), 1.56 (3H, s, H-18), 1.39 (3H, s, H-14), 1.39 (3H, s, H-15).  $^{13}\text{C}$  NMR (100 MHz, acetone- $d_6$ ):  $\delta$  180.1 (C-9), 157.8 (C-3), 155.6 (C-1), 154.3 (C-4a), 151.0 (C-19), 150.1 (C-6), 145.0 (C-10a), 132.0 (C-5), 126.6 (C-12), 115.4 (C-8), 114.6 (C-11), 112.6 (C-2), 112.5 (C-8a), 112.0 (C-7), 105.6 (C-20), 103.9 (C-4), 101.9 (C-9a), 77.3 (C-13), 40.1 (C-16), 28.2 (C-17), 28.2 (C-18), 26.2 (C-14), 26.2 (C-15).

*3-Isomangostin* (4) – Yellow solid, mp 154-156°C. UV (EtOH)  $\lambda_{\max}$  nm (log e): 212.5 (1.10), 242.5 (1.04), 289.5 (1.42). IR  $\nu_{\max}$   $\text{cm}^{-1}$  (KBr): 3440, 1602, 1464, 1286. EI-MS  $m/z$  (rel. int.): 408 (43), 393 (100), 365 (53), 335 (27), 295 (18), 201 (11), 175 (20), 115 (26), 69 (10).  $^1\text{H}$  NMR (300 MHz,  $\text{CDCl}_3$ ):  $\delta$  13.72 (1H, s, 1-OH), 6.85 (1H, s, H-5), 6.75 (1H, d,  $J = 9.9$  Hz, H-4'), 6.26 (1H, s, H-4), 5.59 (1H, d,  $J = 9.9$  Hz, H-5'), 5.27 (1H, t,  $J = 5.1$  Hz, H-5''), 4.10 (2H, d,  $J = 5.1$  Hz, H-4''), 3.82 (3H, s, 7-OCH<sub>3</sub>), 1.85 (3H, s, H-7''), 1.71 (3H, s, H-8''), 1.49 (3H, s, H-7'), 1.49 (3H, s, H-8').  $^{13}\text{C}$  NMR (75 MHz,  $\text{CDCl}_3$ ):  $\delta$  181.2 (C-9), 159.9 (C-3), 157.9 (C-1), 156.3 (C-4a), 155.7 (C-10a), 154.6 (C-6), 142.6 (C-7), 137.0 (C-8), 132.2 (C-6''), 127.2 (C-5'), 123.1 (C-5''), 115.7 (C-4'), 112.1 (C-8a), 104.5 (C-2), 103.7 (C-9a), 101.7 (C-5), 94.2 (C-4), 77.9 (C-6'), 62.1 (7-OCH<sub>3</sub>), 28.3 (C-7'), 28.3 (C-8'), 26.5 (C-4''), 25.9 (C-8''), 18.3 (C-7'').

*Rubraxanthone* (5) – Orange crystals, mp 201-202°C. UV (EtOH)  $\lambda_{\max}$  nm (log e): 211.0 (0.97), 241.5 (1.12), 312.0 (0.76). IR  $\nu_{\max}$   $\text{cm}^{-1}$  (KBr): 3428, 1608, 1466, 1162. EI-MS  $m/z$  (rel. int.): 410 (16), 341 (100), 311 (24), 299 (30), 288 (14), 271 (10), 69 (29), 41 (39).  $^1\text{H}$  NMR (400 MHz, acetone- $d_6$ ):  $\delta$  13.48 (1H, s, 1-OH), 6.82 (1H, s, H-5), 6.28 (1H, d,  $J = 1.8$  Hz, H-4), 6.17 (1H, d,  $J = 1.8$  Hz, H-2), 5.26 (1H, t,  $J = 6.4$  Hz, H-12), 5.02 (1H, t,  $J = 6.9$  Hz, H-16), 4.09 (2H, d,  $J = 6.4$  Hz, H-11), 3.78 (3H, s, 7-OCH<sub>3</sub>), 2.03 (2H, m, H-15), 1.96 (2H, m, H-14), 1.81 (3H, s, H-18), 1.54 (3H, s, H-19), 1.50 (3H, s, H-20).  $^{13}\text{C}$  NMR (100 MHz, acetone- $d_6$ ):  $\delta$  182.7 (C-9), 165.3 (C-3), 164.8 (C-1), 157.9 (C-6), 157.5 (C-10a), 156.2 (C-4a), 144.5 (C-7), 138.2 (C-8), 135.1 (C-13), 131.5 (C-17), 125.1 (C-16), 124.7 (C-12), 111.9 (C-8a), 103.7 (C-9a), 102.8 (C-5), 98.7 (C-2), 93.8 (C-4), 61.4 (7-OCH<sub>3</sub>), 40.4 (C-14), 27.2 (C-11), 26.7 (C-15), 25.7 (C-19), 17.6 (C-20), 16.5 (C-18).

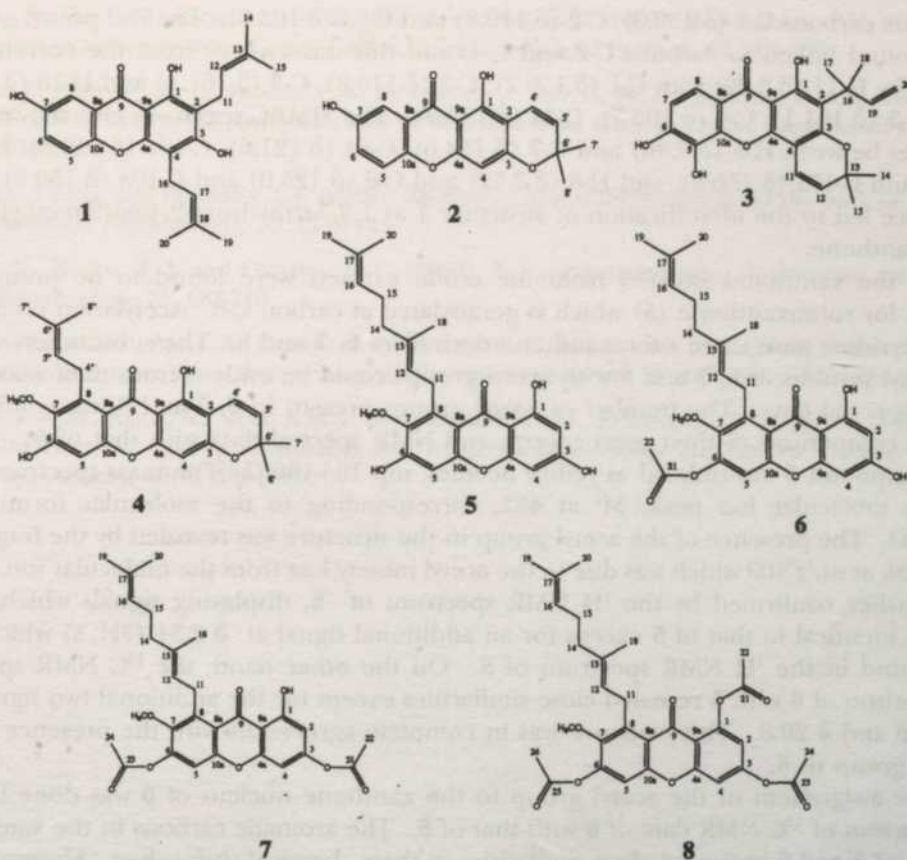
*Rubraxanthone monoacetate (6)* – Yellow crystals, mp 164-166°C. UV (EtOH)  $\lambda_{\max}$  nm (log e): 213.0 (0.98), 239.0 (1.51), 256.5 (1.36), 311.0 (0.87), 434.5 (0.05). IR  $\nu_{\max}$  cm<sup>-1</sup> (KBr): 3422, 2922, 1768, 1606, 1462, 1176. EI-MS m/z (rel. int.): 452 (7), 425 (5), 409 (7), 383 (35), 341 (100), 330 (11), 311 (19), 299 (25), 288 (13), 271 (9), 153 (6), 123 (7), 69 (27). <sup>1</sup>H NMR (400 MHz, acetone-*d*<sub>6</sub>):  $\delta$  13.17 (1H, s, 1-OH), 7.24 (1H, s, H-5), 6.32 (1H, d, *J* = 1.8 Hz, H-4), 6.20 (1H, d, *J* = 1.8 Hz, H-2), 5.22 (1H, t, *J* = 7.3 Hz, H-12), 4.99 (1H, t, *J* = 6.9 Hz, H-16), 4.11 (2H, d, *J* = 7.3 Hz, H-11), 3.76 (3H, s, 7-OCH<sub>3</sub>), 2.34 (3H, s, H-22), 2.03 (2H, m, H-15), 1.96 (2H, m, H-14), 1.79 (3H, s, H-18), 1.52 (3H, s, H-19), 1.48 (3H, s, H-20). <sup>13</sup>C NMR (100 MHz, acetone-*d*<sub>6</sub>):  $\delta$  182.9 (C-9), 168.6 (C-21), 166.0 (C-3), 164.9 (C-1), 158.1 (C-4a), 154.6 (C-6), 150.4 (C-10a), 147.9 (C-7), 139.2 (C-8), 135.6 (C-13), 131.6 (C-17), 125.1 (C-16), 124.2 (C-12), 117.3 (C-8a), 111.7 (C-5), 104.1 (C-9a), 99.0 (C-2), 94.0 (C-4), 62.0 (7-OCH<sub>3</sub>), 40.4 (C-14), 27.2 (C-15), 26.7 (C-11), 25.7 (C-19), 20.8 (C-22), 17.7 (C-20), 16.5 (C-18).

*Rubraxanthone diacetate (7)* – Yellow gum. UV (EtOH)  $\lambda_{\max}$  nm (log e): 210.5 (0.81), 236.0 (0.99), 256.5 (1.13), 292.0 (0.40), 361.5 (0.21). IR  $\nu_{\max}$  cm<sup>-1</sup> (KBr): 1776, 1600, 1460, 1188. EI-MS m/z (rel. int.): 494 (2), 451 (5), 425 (12), 383 (44), 341 (69), 311 (16), 299 (23), 285 (11), 123 (15), 69 (53), 41 (100). <sup>1</sup>H NMR (400 MHz, CDCl<sub>3</sub>):  $\delta$  13.09 (1H, s, 1-OH), 7.13 (1H, s, H-5), 6.64 (1H,  $\delta$ , *J* = 1.8 Hz, H-4), 6.50 (1H,  $\delta$ , *J* = 1.8 Hz, H-2), 5.18 (1H, t, *J* = 6.4 Hz, H-12), 5.01 (1H, t, *J* = 6.0 Hz, H-16), 4.11 (2H, d, *J* = 6.4 Hz, H-11), 3.75 (3H, s, 7-OCH<sub>3</sub>), 2.38<sup>a</sup> (3H, s, H-24), 2.30<sup>a</sup> (3H, s, H-22), 2.03 (2H, m, H-15), 1.98 (2H, m, H-14), 1.81 (3H, s, H-18), 1.59 (3H, s, H-19), 1.53 (3H, s, H-20). <sup>13</sup>C NMR (100 MHz, CDCl<sub>3</sub>):  $\delta$  182.6 (C-9), 168.2<sup>b</sup> (C-21), 167.9<sup>b</sup> (C-23), 163.2 (C-1), 156.6 (C-3), 155.9 (C-4a), 154.0 (C-6), 149.5 (C-10a), 146.9 (C-7), 139.2 (C-8), 135.9 (C-13), 131.3 (C-17), 124.2 (C-16), 122.5 (C-12), 116.9 (C-8a), 110.6 (C-5), 107.1 (C-9a), 104.4 (C-2), 100.0 (C-4), 61.6 (7-OCH<sub>3</sub>), 39.7 (C-14), 26.5 (C-15), 26.3 (C-11), 25.6 (C-19), 21.2<sup>c</sup> (C-22), 20.8<sup>c</sup> (C-24), 17.6 (C-20), 16.4 (C-18). <sup>a, b, c</sup> Interchangeable.

*Rubraxanthone triacetate (8)* – Yellow gum. UV (EtOH)  $\lambda_{\max}$  nm (log e): 211.5 (0.90), 240.0 (1.39), 271.0 (0.51), 341.0 (0.25). IR  $\nu_{\max}$  cm<sup>-1</sup> (KBr): 1760, 1610, 1450, 1186. EI-MS m/z (rel. int.): 536 (5), 493 (2), 467 (12), 451 (4), 425 (30), 383 (49), 341 (58), 311 (15), 299 (17), 284 (13), 69 (46), 43 (100). <sup>1</sup>H NMR (400 MHz, CDCl<sub>3</sub>):  $\delta$  7.14 (1H, d, *J* = 1.8 Hz, H-4), 7.10 (1H, s, H-5), 6.76 (1H, d, *J* = 1.8 Hz, H-2), 5.16 (1H, t, *J* = 6.4 Hz, H-12), 5.03 (1H, t, *J* = 6.0 Hz, H-16), 4.06 (2H, d, *J* = 6.4 Hz, H-11), 3.74 (3H, s, 7-OCH<sub>3</sub>), 2.42<sup>a</sup> (3H, s, H-22), 2.37<sup>a</sup> (3H, s, H-24), 2.32<sup>a</sup> (3H, s, H-26), 2.02 (2H, m, H-15), 1.95 (2H, m, H-14), 1.80 (3H, s, H-18), 1.59 (3H, s, H-19), 1.54 (3H, s, H-20). <sup>13</sup>C NMR (100 MHz, CDCl<sub>3</sub>):  $\delta$  175.8 (C-9), 169.4<sup>b</sup> (C-21), 168.1<sup>b</sup> (C-23), 168.0<sup>b</sup> (C-25), 156.7 (C-4a), 154.2 (C-1), 153.2 (C-6), 151.0 (C-3), 148.6 (C-10a), 146.9 (C-7), 139.2 (C-8), 135.4 (C-13), 131.2 (C-17), 124.4 (C-16), 122.8 (C-12), 118.9 (C-8a), 113.4 (C-9a), 112.5 (C-2), 110.3 (C-5), 108.1 (C-4), 61.6 (7-OCH<sub>3</sub>), 39.7 (C-14), 26.7 (C-15), 26.1 (C-11), 25.6 (C-19), 21.2<sup>c</sup> (C-24 & C-26), 20.9<sup>c</sup> (C-22), 17.7 (C-20), 16.4 (C-18). <sup>a, b, c</sup> Interchangeable.

## RESULTS AND DISCUSSIONS

Compound I was isolated as yellow needles, mp 128-129°C. This compound reacted positively with the methanolic ferric chloride test, indicating it to be a phenolic compound. The UV spectrum exhibited characteristic absorption bands of a hydroxylated xanthone at 217.5, 234.0, 270.0, 285.0, 386.5 nm. The IR spectrum exhibited strong



bands due to phenolic hydroxyls ( $3378\text{ cm}^{-1}$ ), a chelated carbonyl ( $1644\text{ cm}^{-1}$ ), conjugated  $\text{C}=\text{C}$  ( $1480\text{ cm}^{-1}$ ) and carbinol functionalities ( $1230\text{ cm}^{-1}$ ). The molecular formula was deduced to be  $\text{C}_{25}\text{H}_{24}\text{O}_5$  from its mass spectrum, which showed a molecular ion,  $\text{M}^+$  at  $m/z$  380.

The  $^1\text{H}$  NMR spectrum of **1** exhibited a downfield singlet at  $\delta$  13.25 for the chelated hydroxyl group attached to C-1. A group of signals consisting of a triplet at  $\delta$  5.20 (2H,  $J = 7.3\text{ Hz}$ ), two doublets at  $\delta$  3.53 (2H,  $J = 7.3\text{ Hz}$ ) and  $\delta$  3.39 (2H,  $J = 7.3\text{ Hz}$ ) and three singlets at  $\delta$  1.60 (6H, s),  $\delta$  1.74 (3H, s) and  $\delta$  1.83 (3H, s) indicated the presence of two 3-methylbut-2-enyl groups. A doublet of doublet at  $\delta$  7.29 (1H, dd,  $J = 9.2, 3.7\text{ Hz}$ ) was assigned to proton H-6 which was found to be *ortho*-coupled with proton H-5 [ $\delta$  7.40 (1H,  $\delta$ ,  $J = 9.2\text{ Hz}$ )] and *meta*-coupled with proton H-8 [ $\delta$  7.52 (1H,  $\delta$ ,  $J = 3.7\text{ Hz}$ )].

The  $^{13}\text{C}$  NMR spectrum of **1** showed signals for three protonated aromatic carbons, C-5 ( $\delta$  119.8), C-6 ( $\delta$  125.0) and C-8 ( $\delta$  109.2) as well as nine substituted aromatic carbons, C-1 ( $\delta$  159.2), C-2 ( $\delta$  110.8), C-3 ( $\delta$  161.1), C-4 ( $\delta$  106.7), C-4a ( $\delta$  153.9), C-7 ( $\delta$  154.6), C-8a ( $\delta$  121.6), C-9a ( $\delta$  103.6) and C-10a ( $\delta$  150.6). The chelated carbonyl carbon gave signals at  $\delta$  181.6 (C-9) and the existence of two 3-methylbut-2-enyl groups were revealed by the signals at  $\delta$  132.5 (C-13), 123.0 (C-12), 25.8 (C-14), 22.1 (C-11), 18.0 (C-15), and at  $\delta$  132.3 (C-18), 123.0 (C-17), 25.8 (C-19), 22.4 (C-16) and 18.1 (C-20).

The structure of **1** was further confirmed by the HMBC spectral data. In the HMBC spectrum, the chelated hydroxyl group ( $\delta$  13.25) was correlated to three quaternary

aromatic carbons C-1 ( $\delta$  159.2), C-2 ( $\delta$  110.8) and C-9a ( $\delta$  103.6). The two prenyl groups were found linked to carbons C-2 and C-4, and this was evident from the correlations shown by H-11 ( $\delta$  3.39) with C-1 ( $\delta$  159.2), C-2 ( $\delta$  110.8), C-3 ( $\delta$  161.1) and H-16 ( $\delta$  3.53) with C-3 ( $\delta$  161.1), C-4 ( $\delta$  106.7), C-4a ( $\delta$  153.9). The HMBC spectrum also showed the linkages between H-5 ( $\delta$  7.40) and C-7 ( $\delta$  154.6), C-8a ( $\delta$  121.6), C-10a ( $\delta$  150.8); H-6 ( $\delta$  7.29) and C-10a ( $\delta$  150.8), and H-8 ( $\delta$  7.52) and C-6 ( $\delta$  125.0) and C-10a ( $\delta$  150.8). This evidence led to the identification of structure **1** as 1,3,7-trihydroxy-2,4-bis(3-methylbut-2-enyl)xanthone.

All the xanthenes isolated from the crude extracts were found to be prenylated except for rubraxanthone (**5**) which is geranylated at carbon C-8. Acetylation on **5** with Ac<sub>2</sub>O-pyridine gave three rubraxanthone derivatives **6**, **7** and **8**. The substitution of the hydroxyl protons in **6**, **7** and **8** with acetyl groups could be evident from their mass and NMR spectral data. The number of acetyl groups present in **6**, **7** and **8** was confirmed by the comparison of their mass spectra and NMR spectral data with that of **5**.

Compound **6** was isolated as yellow needles, mp 164-166°C. The mass spectrum of **6** gave a molecular ion peak, M<sup>+</sup> at 452, corresponding to the molecular formula of C<sub>26</sub>H<sub>28</sub>O<sub>7</sub>. The presence of the acetyl group in the structure was revealed by the fragment ion peak at m/z 409 which was due to the acetyl moiety loss from the molecular ion. This was further confirmed by the <sup>1</sup>H NMR spectrum of **6**, displaying signals which were almost identical to that of **5** except for an additional signal at  $\delta$  2.34 (3H, s) which was not found in the <sup>1</sup>H NMR spectrum of **5**. On the other hand, the <sup>13</sup>C NMR spectral comparison of **6** with **5** revealed close similarities except for the additional two signals at  $\delta$  168.6 and  $\delta$  20.8. This evidence was in complete agreement with the presence of an acetyl group in **6**.

The assignment of the acetyl group to the xanthone nucleus of **6** was done by the comparison of <sup>13</sup>C NMR data of **6** with that of **5**. The aromatic carbons in the xanthone ring A of **5** and **6** indicated close similarities in their chemical shift values. However, for xanthone ring B, the aromatic carbons C-5, C-6 and C-7 gave signals at  $\delta$  102.8,  $\delta$  157.9 and  $\delta$  144.5, respectively for **5**, and  $\delta$  111.7,  $\delta$  154.6 and  $\delta$  147.9, respectively for **6**. The C-5 carbon signals of **5** and **6** were found to be significantly different by 8.9 ppm, indicating the presence of an acetoxyl group at carbon C-6, inducing a deshielding effect on the adjacent carbon C-5. Therefore, compound **6** was deduced to be rubraxanthone monoacetate that was monoacetylated at position C-6.

#### ACKNOWLEDGEMENTS

We gratefully acknowledge the financial support provided by the Malaysian Government IRPA programme and we are grateful to Mr Mohd Johadi Iskandar for recording the NMR spectra.

#### REFERENCES

- BURKILL, I. H. (1966). *Garcinia*. In W. Birtwistle, F.W. Foxworthy, J. B. Scrivenor, J. G. Watson, (Eds.), *A Dictionary of the Economic Products of the Malay Peninsula* (p. 1063-1074). Kuala Lumpur: Malaya Nature Society.
- HEYWOOD, V. H. (1982). In S.R. Chant (Eds.), *Popular Encyclopedia of Plants*. England: Press Syndicate of the University of Cambridge.

- KOSELA, S., HU, L. H., RACHMATIA, T., HANAFI, M. and SIM, K. Y. (2000). Dulxanthone F-H, three new pyranoxanthenes from *Garcinia dulcis*. *Journal of Natural Products*, 63, 406-407.
- MERZA, J., AUMOND, M. C., RONDEAU, D., DUMONTET, V., RAY, A. M. L., SERAPHIN, D. and RICHOMME, P. (2004). Prenylated xanthenes and tocotrienols from *Garcinia virgata*. *Phytochemistry*, 65(21), 2915-2920.
- NGUYEN, L.H.D. and HARRISON, L.J. (2000). Xanthenes and triterpenoids from the bark of *Garcinia vilersiana*. *Phytochemistry*, 53, 111-114.
- PERES, V., NAGEM, T. J. and OLIVEIRA, F. F. (2000). Tetraoxygenated natural occurring xanthenes. *Phytochemistry*, 55, 683-710.
- RUKACHAISIRIKUL, V., ADAIR, A., DAMPAWAN, P., TAYLOR, W. C. and TURNER, P. C. (2000). Lanostanes and friedolanostanes from the pericarp of *Garcinia hombroniana*. *Phytochemistry*, 55, 183-188.
- VIEIRA, L.M.M., KIJJOA, A., SILVA, A.M.S., MONDRANONDRA, I.O., KENGTHONG, S., GALES, L., DAMAS A.M. and HERZ, W. (2004). Lanostanes and friedolanostanes from the bark of *Garcinia speciosa*. *Phytochemistry*, 65(4), 393-398.

## INSTRUCTIONS TO AUTHORS

(Manuscript Preparation & Submission Guidelines)  
Revised May 2007

*We aim for excellence, sustained by a responsible and professional approach to journal publishing.  
We value and support our authors in the research community.*

Please read the guidelines and follow these instructions carefully; doing so will ensure that the publication of your manuscript is as rapid and efficient as possible. The Editorial Board reserves the right to return manuscripts that are not prepared in accordance with these guidelines.

### Guidelines for Authors

#### Publication policies

Pertanika policy prohibits an author from submitting the same manuscript for concurrent consideration by two or more publications. It prohibits as well publication of any manuscript that has already been published either in whole or substantial part elsewhere.

#### Editorial process

Authors are notified on receipt of a manuscript and upon the editorial decision regarding publication.

*Manuscript review:* Manuscripts deemed suitable for publication are sent to the Editorial Advisory Board members and/or other reviewers. We encourage authors to suggest the names of possible reviewers. Notification of the editorial decision is usually provided within to six weeks from the receipt of manuscript. Publication of solicited manuscripts is not guaranteed. In most cases, manuscripts are accepted conditionally, pending an author's revision of the material.

*Author approval:* Authors are responsible for all statements in articles, including changes made by editors. The liaison author must be available for consultation with an editor of The *Journal* to answer questions during the editorial process and to approve the edited copy. Authors receive edited typescript (not galley proofs) for final approval. Changes cannot be made to the copy after the edited version has been approved.

Please direct all inquiries, manuscripts, and related correspondence to:

Executive Editor  
Research Management Centre (RMC)  
4th Floor, Administration Building  
Universiti Putra Malaysia  
43400 UPM, Serdang, Selangor  
Malaysia  
Phone: + (603) 8946 6192  
Fax: + (603) 8947 2075  
[ndeeps@admin.upm.edu.my](mailto:ndeeps@admin.upm.edu.my)

#### Manuscript preparation

Pertanika accepts submission of mainly four types of manuscripts. Each manuscript is classified as **regular** or **original** articles, **short communications**, **reviews**, and proposals for **special issues**. Articles must be in **English** and they must be competently written and argued in clear and concise grammatical English. Acceptable English usage and syntax are expected. Do not use slang, jargon, or obscure abbreviations or phrasing. Metric measurement is preferred; equivalent English measurement may be included in parentheses. Always provide the complete form of an acronym/abbreviation the first time it is presented in the text. Contributors are strongly recommended to have the manuscript checked by a colleague with ample experience in writing English manuscripts or an English language editor. Lingually hopeless manuscripts will be rejected straightaway (e.g., when the language is so poor that one cannot be sure of what the authors really mean). This process, taken by authors before submission, will greatly facilitate reviewing, and thus publication if the content is acceptable.

The instructions for authors must be followed. Manuscripts not adhering to the instructions will be returned for revision without review. Authors should prepare manuscripts according to the guidelines of Pertanika.

#### 1. Regular article

*Definition:* Full-length original empirical investigations, consisting of introduction, materials and methods, results and discussion, conclusions. Original work must provide references and an explanation on research findings that contain new and significant findings.

*Size:* Should not exceed 5000 words or 8-10 printed pages (excluding the abstract, references, tables and/or figures). One printed page is roughly equivalent to 3 type-written pages.

#### 2. Short communications

*Definition:* Significant new information to readers of the Journal in a short but complete form. It is suitable for the publication of technical advance, bioinformatics or insightful findings of science and engineering development and function.

*Size:* Should not exceed 2000 words or 4 printed pages, is intended for rapid publication. They are not intended for publishing preliminary results or to be a reduced version of Regular Papers or Rapid Papers.

#### 3. Review article

*Definition:* Critical evaluation of materials about current research that had already been published by organizing, integrating, and evaluating previously published materials. Re-analyses as meta-analysis and systemic reviews are encouraged. Review articles should aim to provide systemic overviews, evaluations and interpretations of research in a given field.

*Size:* Should not exceed 4000 words or 7-8 printed pages.

#### 4. Special issues

*Definition:* Usually papers from research presented at a conference, seminar, congress or a symposium.

*Size:* Should not exceed 5000 words or 8-10 printed pages.

#### 5. Others

*Definition:* Brief reports, case studies, comments, Letters to the Editor, and replies on previously published articles may be considered.

*Size:* Should not exceed 2000 words or up to 4 printed pages.

With few exceptions, original manuscripts should not exceed the recommended length of 6 printed pages (about 18 typed pages, double-spaced and in 12-point font, tables and figures included). Printing is expensive, and, for the Journal, postage doubles when an issue exceeds 80 pages. You can understand then that there is little room for flexibility.

Long articles reduce the Journal's possibility to accept other high-quality contributions because of its 80-page restriction. We would like to publish as many good studies as possible, not only a few lengthy ones. (And, who reads overly long articles anyway?) Therefore, in our competition, short and concise manuscripts have a definite advantage.

#### Format

The paper should be formatted in one column format with the figures at the end. A maximum of eight keywords should be indicated below the abstract to describe the contents of the manuscript. Leave a blank line between each paragraph and between each entry in the list of bibliographic references. Tables should preferably be placed in the same electronic file as the text. Authors should consult a recent issue of the Journal for table layout. There is no need to spend time formatting your article so that the printout is visually attractive (e.g. by making headings bold or creating a page layout with figures), as most formatting instructions will be removed upon processing.

Manuscripts should be typewritten, typed on one side of the ISO A4 paper with at least 4cm margins and double spacing throughout. Every page of the manuscript, including the title page, references, tables, etc. should be numbered. However, no reference should be made to page numbers in the text; if necessary, one may refer to sections. Underline words that should be in italics, and do not underline any other words.

Authors are advised to use Times New Roman 12-point font. Be especially careful when you are inserting special characters, as those inserted in different fonts may be replaced by different characters when converted to PDF files. It is well known that 'µ' will be replaced by other characters when fonts such as 'Symbol' or 'Mincho' are used.

We recommend that authors prepare the text as a Microsoft Word file.

1. Manuscripts in general should be organised in the following order:
  - **Page 1: Running title.** Not to exceed 50 characters, counting letters and spaces.
  - **Corresponding author.** Street address, telephone number (including extension), fax number and e-mail address for editorial correspondence.
  - **Subject areas.** Most relevant to the study. Select one or two subject areas from (*refer to Referral Form A-attachment*).
  - **Number of black and white figures, colour figures and tables.** Figures submitted in color will be printed in colour at the authors' expense. See "6. Figures & Photographs" for details of cost.
  - \*Authors of Short Communications should state the total number of words (including the Abstract)
  - **Page 2: Authors.** Full names, institutions and addresses
  - **Abbreviations.** Define alphabetically, other than abbreviations that can be used without definition. Words or phrases that are abbreviated in the introduction and following text should be written out in full the first time that they appear in the text, with each abbreviated form in parenthesis.
  - **Footnotes.** Current addresses of authors if different from heading.
  - **Page 3: Abstract.** Less than 250 words for a Regular Paper, and up to 100 words for a Short Communication. For papers submitted to *Pertanika Journal of Tropical Agricultural Science (JTAS)* and *Pertanika Journal of Science and Technology (JST)*, submissions should be made in English. *Pertanika Journal of Social Sciences and Humanities (JSSH)* accepts submissions in both English and *Bahasa Melayu*. However, if the paper is submitted in *Bahasa Melayu*, an abstract in English should be provided by the author submitting the paper.
  - **Keywords.** Not more than eight in alphabetical order. Include the common name or scientific name, or both, of plant materials, etc.
  - **Page 4 and subsequent pages:** Text - Acknowledgments - References - Tables - Legends to figures - Figures.
2. **Authors' addresses.** Multiple authors with different addresses must indicate their respective addresses separately by superscript numbers:  
George Swan<sup>1</sup> and Nayan Kanwal<sup>2</sup>  
<sup>1</sup>Department of Biology, Faculty of Science, Duke University, Durham, North Carolina, USA.  
<sup>2</sup>Research Management Centre, Universiti Putra Malaysia, Serdang, Malaysia.
3. **Text.** Regular Papers should be prepared with the headings **Introduction, Materials and Methods, Results and Discussion, Conclusions** in this order. Short Communications should be prepared according to "9. Short Communications." below.
4. **Tables.** All tables should be prepared in a form consistent with recent issues of *Pertanika* and should be numbered consecutively with Arabic numerals. Explanatory material should be given in the table legends and footnotes. Each table should be prepared on a separate page. (Note that when a manuscript is accepted for publication, tables must be submitted as data - .doc, .rtf, Excel or PowerPoint file- because tables submitted as image data cannot be edited for publication.)
5. **Equations and Formulae.** These must be set up clearly and should be typed triple spaced. Numbers identifying equations should be in square brackets and placed on the right margin of the text.
6. **Figures & Photographs.** Submit an original figure or photograph. Line drawings must be clear, with high black and white contrast. Each figure or photograph should be prepared on a separate sheet and numbered consecutively with Arabic numerals. Appropriate sized numbers, letters and symbols should be used, no smaller than 2 mm in size after reduction to single column width (85 mm), 1.5-column width (120 mm) or full 2-column width (175 mm). Failure to comply with these specifications will require new figures and delay in publication. For electronic figures, create your figures using applications that are capable of

preparing high resolution TIFF files acceptable for publication. In general, we require 300 dpi or higher resolution for coloured and half-tone artwork and 1200 dpi or higher for line drawings. For review, you may attach low-resolution figures, which are still clear enough for reviewing, to keep the file of the manuscript under 5 MB. Illustrations will be produced at extra cost in colour at the discretion of the Publisher; the author will be charged Malaysian Ringgit 50 for each colour page.

7. **References.** Literature citations in the text should be made by name(s) of author(s) and year. For references with more than two authors, the name of the first author followed by 'et al.' should be used.

Swan and Kanwal (2007) reported that ...

The results have been interpreted (Kanwal et al. 2006).

- References should be listed in alphabetical order, by the authors' last names. For the same author, or for the same set of authors, references should be arranged chronologically. If there is more than one publication in the same year for the same author(s), the letters 'a', 'b', etc., should be added to the year.
- When the authors are more than 11, list 5 authors and then et al.
- Do not use indentations in typing References. Use one line of space to separate each reference. For example:
  - Jalaludin, S. (1997a). Metabolizable energy of some local feeding stuff. *Tumbuh*, 1, 21-24.
  - Jalaludin, S. (1997b). The use of different vegetable oil in chicken ration. *Mal. Agriculturist*, 11, 29-31.
  - Tan, S.G., Omar, M.Y., Mahani, K.W., Rahani, M., Selvaraj, O.S. (1994). Biochemical genetic studies on wild populations of three species of green leafhoppers *Nephotettix* from Peninsular Malaysia. *Biochemical Genetics*, 32, 415 - 422.
- In case of citing an author(s) who has published more than one paper in the same year, the papers should be distinguished by addition of a small letter as shown above, e.g. Jalaludin (1997a); Jalaludin (1997b).
- Unpublished data and personal communications should not be cited as literature citations, but given in the text in parentheses. 'In press' articles that have been accepted for publication may be cited in References. Include in the citation the journal in which the 'in press' article will appear and the publication date, if a date is available.

8. **Examples of other reference citations:**

**Monographs:** Turner, H.N. and Yong, S.S.Y. (2006). *Quantitative Genetics in Sheep Breeding*. Ithaca: Cornell University Press.

**Chapter in Book:** Kanwal, N.D.S. (1992). Role of plantation crops in Papua New Guinea economy. In Angela R. McLean (Eds.), *Introduction of livestock in the Enga province PNG* (p. 221-250). United Kingdom: Oxford Press.

**Proceedings:** Kanwal, N.D.S. (2001). Assessing the visual impact of degraded land management with landscape design software. In N.D.S. Kanwal and P. Lecoustre (Eds.), *International forum for Urban Landscape Technologies* (p. 117-127). Lullier, Geneva, Switzerland: CIRAD Press.

9. **Short Communications** should include **Introduction, Materials and Methods, Results and Discussion, Conclusions** in this order. Headings should only be inserted for Materials and Methods. The abstract should be up to 100 words, as stated above. Short Communications must be 5 printed pages or less, including all references, figures and tables. References should be less than 30. A 5 page paper is usually approximately 3000 words plus four figures or tables (if each figure or table is less than 1/4 page).

\*Authors should state the total number of words (including the Abstract) in the cover letter. Manuscripts that do not fulfill these criteria will be rejected as Short Communications without review.

## STYLE OF THE MANUSCRIPT

Manuscripts should follow the style of the latest version of the Publication Manual of the American Psychological Association (APA). The journal uses British spelling and authors should therefore follow the latest edition of the Oxford Advanced Learner's Dictionary.

## SUBMISSION OF MANUSCRIPTS

All articles submitted to the journal must comply with these instructions. Failure to do so will result in return of the manuscript and possible delay in publication.

The original manuscript and one copy, four copies of photographic figures, as well as a disk with the **electronic copy** (including text and figures) and a **declaration form and referral form A**, together with a **cover letter** need to be enclosed. They are available from the Pertanika's home page or from the Executive Editor's office. Please do not submit manuscripts directly to the editor-in-chief or to the UPM Press. All manuscripts should be submitted through the executive editor's office to be properly acknowledged and rapidly processed:

Dr. Nayan Kanwal  
Executive Editor  
Research Management Centre (RMC)  
4th Floor, Administration Building  
Universiti Putra Malaysia  
43400 UPM, Serdang, Selangor, Malaysia  
email: [ndeeps@admin.upm.edu.my](mailto:ndeeps@admin.upm.edu.my)  
tel: +603-8946 6192  
fax: +603 8947 2075.

Laser quality print is essential. Authors should retain copies of submitted manuscripts and correspondence, as materials can not be returned.

### Cover letter

All submissions must be accompanied by a cover letter detailing what you are submitting. Papers are accepted for publication in the journal on the understanding that the article is original and the content has not been published or submitted for publication elsewhere. This must be stated in the cover letter.

The cover letter must also contain an acknowledgement that all authors have contributed significantly, and that all authors are in agreement with the content of the manuscript.

The cover letter of the paper should contain (i) the title; (ii) the full names of the authors; (iii) the addresses of the institutions at which the work was carried out together with (iv) the full postal and email address, plus facsimile and telephone numbers of the author to whom correspondence about the manuscript should be sent. The present address of any author, if different from that where the work was carried out, should be supplied in a footnote.

As articles are double-blind reviewed, material that might identify authorship of the paper should be placed on a cover sheet.

**Note** When your manuscript is received at Pertanika it is considered to be in its final form. Therefore, you need to check your manuscript carefully before submitting it to the executive editor (see also **English language editing** below).

### Electronic copy

For preparation of manuscripts on disk, articles prepared using any one of the more popular word-processing packages are acceptable. Submissions should be made on a double-density or high-density 3.5" disk but a CD or DVD is preferable. The format, word-processor format, file name(s) and the title and authors of the article must be indicated on the disk/CD. The disk must always be accompanied by a hard-copy version of the article, and the content of the two must be identical. The disk text must be the same as that of the final refereed, revised manuscript. Disks formatted for IBM PC compatibles are preferred, though those formatted for Apple Macintosh are acceptable. The article must be saved in the native format of the word processor used, e.g. Microsoft Word (office version), etc. Although most popular word processor file formats are acceptable, we cannot guarantee the usability of all formats. If the electronic copy proves to be unusable, we will publish your article from the hard copy. Please do not send ASCII files, as relevant data may be lost. Leave a blank line between each paragraph and between each entry in the list of bibliographic references. Tables should be placed in the same electronic file as the text. Authors should consult a recent issue of the Journal for table layout.

### Peer review

In the peer-review process, three referees independently evaluate the scientific quality of the submitted manuscripts. The Journal uses a double-blind peer-review system. Authors are encouraged to indicate in **referral form A** the names of three potential reviewers, but the editors will make the final choice. The editors are not, however, bound by these suggestions.

Manuscripts should be written so that they are intelligible to the professional reader who is not a specialist in the particular field. They should be written in a clear, concise, direct style. Where contributions are judged as acceptable for publication on the basis of content, the Editor or the Publisher reserves the right to modify the typescripts to eliminate ambiguity and repetition and improve communication between author and reader. If extensive alterations are required, the manuscript will be returned to the author for revision.

### The editorial review process

What happens to a manuscript once it is submitted to *Pertanika*? Typically, there are seven steps to the editorial review process:

1. The executive editor and the editorial board examine the paper to determine whether it is appropriate for the journal and should be reviewed. If not appropriate, the manuscript is rejected outright.
2. The executive editor sends the article-identifying information having been removed to three reviewers. Typically, one of these is from the Journal's editorial board. Others are specialists in the subject matter represented by the article. The executive editor asks them to complete the review in three weeks and encloses two forms: (a) referral form B and (b) reviewer's comment form. Comments to authors are about the appropriateness and adequacy of the theoretical or conceptual framework, literature review, method, results and discussion, and conclusions. Reviewers often include suggestions for strengthening of the manuscript. Comments to the editor are in the nature of the significance of the work and its potential contribution to the literature.
3. The executive editor, in consultation with the editor-in-chief, examines the reviews and decides whether to reject the manuscript, invite the author(s) to revise and resubmit the manuscript, or seek additional reviews. Final acceptance or rejection rests with the Editorial Board, who reserves the right to refuse any material for publication. In rare instances, the manuscript is accepted with almost no revision. Almost without exception, reviewers' comments (to the author) are forwarded to the author. If a revision is indicated, the editor provides guidelines for attending to the reviewers' suggestions and perhaps additional advice about revising the manuscript.
4. The authors decide whether and how to address the reviewers' comments and criticisms and the editor's concerns. The authors submit a revised version of the paper to the executive editor along with specific information describing how they have answered the concerns of the reviewers and the editor.
5. The executive editor sends the revised paper out for review. Typically, at least one of the original reviewers will be asked to examine the article.
6. When the reviewers have completed their work, the executive editor and the editor-in-chief examine their comments and decide whether the paper is ready to be published, needs another round of revisions, or should be rejected.
7. If the decision is to accept, the paper is in press and the article should appear in print in approximately three to four months. The Publisher ensures that the paper adheres to the correct style (in-text citations, the reference list, and tables are typical areas of concern, clarity, and grammar). The authors are asked to respond to any queries by the Publisher. Following these corrections, page proofs are mailed to the corresponding authors for their final approval. At this point, only essential changes are accepted. Finally, the article appears in the pages of the Journal and is posted on-line.

### English language editing

Authors are responsible for the linguistic accuracy of their manuscripts. Authors not fully conversant with the English language should seek advice from subject specialists with a sound knowledge of English. The cost will be borne by the author, and a copy of the certificate issued by the service should be attached to the cover letter.

### Author material archive policy

Authors who require the return of any submitted material that is rejected for publication in the journal should indicate on the cover letter. If no indication is given, that author's material should be returned, the Editorial Office will dispose of all hardcopy and electronic material.

### Copyright

Authors publishing the Journal will be asked to sign a declaration form. In signing the form, it is assumed that authors have obtained permission to use any copyrighted or previously published material. All authors must read and agree to the conditions outlined in the form, and must sign the form or agree that the corresponding author can sign on their behalf. Articles cannot be published until a signed form has been received.

### Lag time

The elapsed time from submission to publication for the articles averages 6-8 months. A decision of acceptance of a manuscript is reached in 1 to 3 months (average 7 weeks).

### Back issues

Single issues from current and recent volumes are available at the current single issue price from UPM Press. Earlier issues may also be obtained from UPM Press at a special discounted price. Please contact UPM Press at [penerbit@putra.upm.edu.my](mailto:penerbit@putra.upm.edu.my) or you may write for further details at the following address:

UPM Press  
Universiti Putra Malaysia  
43400 UPM, Serdang  
Selangor Darul Ehsan  
Malaysia.

Pertanika Journal of SCIENCE & TECHNOLOGY  
VOLUME 15 NO. 1 • JANUARY 2007

Contents

Predicting Freezing Time for Keropok Lekor – M. Nordin Ibrahim, Sergei Y. Spotar & No Amaiza Mohd. Amin	1
Performance Evaluation of a Terrain-Accommodating Oil Palm Loose Fruit Collector – Rimfiel B. Janius & Abadanjumi Eskandar	15
Array Beampattern Using Goal – Farrukh Nagi & Wong Hung Way	25
Assessment of Public Exposure to Electromagnetic Fields by Overhead Power Transmission Lines: A Case Study – Law Puong Ling, Awangku Abdul Rahman, Azhaili Baharun & Ngu Lock Hei	35
Anthraquinones and Xanthones from <i>Cratoxylum glaucum</i> (Guttiferae) – G.C.L. Ee, A.S.M. Kua & M. Rahmani	43
Determining the Optimum Process Mean Based on Manufacturing Cost and Quality Loss – Chung-Ho Chen	49
A Method of Estimating the $p$ -adic Sizes of Common Zeros of Partial Derivative Polynomials Associated with a Seventh Degree Form – Siti Hasana Sapar, Kamel Ariffin Mohd Atan & Mohamad Rushdan Md Said	61
Xanthones and Xanthone Derivatives from <i>Garcinia nitida</i> – G.C.L. Ee, C.K. Lim, Y. H. Taufiq-Yap, M.A. Sukari & M. Rahmani	77



Research Management Centre (RMC)

4th Floor, Administration Building  
Universiti Putra Malaysia  
43400 UPM Serdang  
Selangor Darul Ehsan  
Malaysia

<http://www.rmc.upm.edu.my>

E-mail : [pertanika@rmc.upm.edu.my](mailto:pertanika@rmc.upm.edu.my)

Tel : +603 8946 6185/ 6192

Fax : +603 8947 2075

UPM Press

Universiti Putra Malaysia  
43400 UPM Serdang  
Selangor Darul Ehsan  
Malaysia

<http://penerbit.upm.edu.my>

E-mail : [penerbit@putra.upm.edu.my](mailto:penerbit@putra.upm.edu.my)

Tel : +603 8946 8855/8854

Fax : +603 8941 6172

ISSN 0128-7680

